NASA CONTRACTOR REPORT

NASA CR-332

DEVELOPMENT OF MACROSCOPIC WAVEGUIDE AND WAVEGUIDE COMPONENTS FOR OPTICAL SYSTEMS

by E. R. Schineller, H. M. Heinemann, D. W. Wilmot, and H. W. Redlien

Prepared under Contract No. NAS 12-2 *by*
WHEELER LABORATORIES, INC.
Great Neck, N. Y.
for Electronics Research Center

NATIONAL AERONAUTICS AND SPACE ADMINISTRATION • WASHINGTON, D. C. • JANUARY 1966

NASA CR-332

DEVELOPMENT OF MACROSCOPIC WAVEGUIDE AND WAVEGUIDE COMPONENTS FOR OPTICAL SYSTEMS

By E. R. Schineller, H. M. Heinemann,
D. W. Wilmot, and H. W. Redlien

Prepared under Contract No. NAS 12-2 by
WHEELER LABORATORIES, INC.
Great Neck, N. Y.
A subsidiary of Hazeltine Corporation

for The Space Optics Laboratory of the
ELECTRONICS RESEARCH CENTER

NATIONAL AERONAUTICS AND SPACE ADMINISTRATION

For sale by the Clearinghouse for Federal Scientific and Technical Information
Springfield, Virginia 22151 – Price $5.00

Foreword

This report covers an engineering study conducted by Wheeler Laboratories, Inc., a subsidiary of the Hazeltine Corporation, for the National Aeronautics and Space Administration during the period 1964 JAN 28 to 1964 NOV 28, under contract number NASw 888.

The study was initiated by a proposal to NASA presented in WL Report No. 1139, "Development of Macroscopic Waveguide and Waveguide Components for Optical Systems", 1963 APR.

An interim technical report was prepared and delivered to NASA in 1964 JUN; it was designated WL Report 1209, "A Macroscopic Waveguide Medium for Laser System Components" (see Appendix A).

In addition, a series of 8 monthly letters has been prepared to report on the detailed progress during each month of the contract period; these letters are listed with the references.

Summary

A theoretical and experimental study program has been conducted for the development of large size or "macroscopic" optical waveguide and components which operate in a single spatial mode. Such components are expected to be required for sophisticated laser systems. An all dielectric waveguide comprising a core and a cladding region of differing dielectric constants was chosen for detailed study. Each waveguide considered had a core dimension of the order of 100 wavelengths; the difference of dielectric constants between the core and cladding is about 0.0001, which permits propagation in this large size to be limited to a single mode.

The theoretical analysis of the waveguide medium has resulted in the formulation of mode cutoff conditions, field distributions and propagation characteristics. In addition, various methods for waveguide excitation have been evaluated. These properties have been verified experimentally by tests of a parallel-plate type glass-cladded, liquid-core waveguide, and a similar type bisected by a metal wall. In the practical embodiment of the bisected waveguide there were sufficient losses in the metal wall so that the modes of propagation were modified from those which would exist with a lossless wall.

Tests of additional waveguide configurations have been made as a first step in determining the feasibility of all-solid components. Preliminary tests included a variety of solid-core liquid-cladded types in both slab and circular rod geometries. Single-mode propagation was obtained in a slab waveguide fabricated from high optical quality fused quartz ground and polished to size. It was found that other optical materials, drawn and fire polished in either slab or circular rod shapes, had variations of dielectric constant which distorted or precluded single-mode propagation.

The study of components in macroscopic optical waveguide included theoretical design, performance analysis, and experimental evaluation. Study indicates directional couplers can be designed to provide equal power split in coupling lengths of less than 3 cm. For waveguide bends, study indicated a minimum radius of 50 cm,

unless reflecting plates are added. A somewhat larger minimum radius was indicated in experimental tests. Optical resonators in waveguide were found to have spatial characteristics fundamentally different from free-space types. The normal ambiguity between angle and frequency response is removed when resonant interference filters are made in optical waveguide. In addition the application of the waveguide resonator as a laser oscillator inherently provides an output in a single transverse mode. The common types of amplitude and frequency modulators can be constructed in waveguide; the possibility of operating with a very small volume of electro-optic material permits large bandwidth with low modulator power. A unique type of pulse modulator has been designed in which the modulation level is essentially independent of modulation voltage. Optical detectors fabricated in a single-mode waveguide have the property that, unlike conventional detectors which are sensitive to only the power in a signal, they are sensitive to the transverse distribution of both the amplitude and phase of a signal.

These studies and experiments have indicated that macroscopic optical waveguides and components are feasible in operation and construction and the concept offers promise of high performance components for sophisticated laser systems.

Contents

List of Figures

Contents (continued)

I. Introduction.

This final report covers a ten month program of theoretical and experimental investigation to demonstrate the feasibility of macroscopic optical waveguide and components. The long-term objective of this program is the development of single-mode optical waveguide and associated components which will operate in a manner similar to those currently available at microwave frequencies (Ref. 16).

It is believed that single-mode components are needed in any sophisticated information transfer system, and specifically at optical frequencies they are needed to realize the full potentialities of the coherent laser oscillator. It is recognized that in some arrangements a laser beam may be operated in a single transverse mode, such as the TEM-00 output of a gas laser, but it is also recognized that special care must be taken in the design of any transmission system to maintain the single-mode character. For example, a small scattering particle in a beam system introduces spurious components forming higher modes which may interfere with the intended operation of a system. On the other hand, a scattering particle in a system restricted to single-mode operation may introduce spurious signals, but these are damped or filtered by design so as not to be harmful.

Usually, single-mode operation implies waveguide dimensions comparable to the operating wavelength. For optical applications it is desirable to have a waveguide medium in a size large enough to permit component fabrication. Therefore, effort has been directed toward the development of macroscopic (large size) optical waveguide, waveguide of dimensions several orders of magnitude greater than the operating wavelength, which still may operate in a single mode. It is to be noted, however, that the waveguide is not intended for long range transmission, but rather for construction of components which probably will not exceed several centimeters in length.

The current study program has concentrated on dielectric waveguides with core regions of the order of 100 wavelengths in width and a cladding region somewhat wider; both slab and circular geometries have been investigated. The program has been divided into three main parts. The first part includes an analysis of field configurations

and propagation characteristics, and waveguide experiments to verify the theoretical results. The second part has concentrated on component studies and experiments. The third part includes a study of materials, fabrication techniques, and experimental measurements to develop a waveguide medium suitable for component implementation.

The results of the initial aspect of the investigation which included theoretical study and attendant experiments of waveguide characteristics have been previously reported to NASA in Wheeler Laboratories Report 1209, which is included in this report as Appendix A; it is summarized briefly in Section III, herein. The remaining parts of the program have been reported briefly in Ref. 30 and in greater detail in Sections IV to VIII, herein.

II. Symbols

The following list contains the symbols which are in addition to those listed in Appendix A, p. 8A.

l_c = length of coupling region.
l_1 = separation of interferometer plates.
l_m = length of modulation region.
B = radius of curvature.
B_1 = minimum radius of bend by "TIR" criterion.
B_2 = minimum radius of bend by "1/e" criterion.
b = separation of waveguide cores for evanescent-field coupler.
d_e = separation between electrodes in modulator.
R_r = "Rayleigh Range" = $d^2/2\lambda$.
g = ratio l_m/R_r.
I = intensity of wave transmitted through interferometer.
I_o = intensity of wave incident on interferometer.
P_{out} = optical power output of modulator.
P_{in} = optical power input to modulator.
s = power reflectivity.
θ_i = angle of incidence on interferometer.
θ_b = angle of incidence on dielectric interface within waveguide bend.

Φ = phase length of modulator section = $2\pi l_m/\lambda_g$.
Φ_o = free-space phase length of modulator section = $2\pi l_m/\lambda$.
Φ_m = maximum phase variation in modulator.
$\Delta\Phi$ = total phase shift between the first and second modes in coupling region.
λ_2 = wavelength of plane wave in the waveguide core dielectric.
q_e = propagation parameter for lowest order even mode.
q_o = propagation parameter for lowest order odd mode.
β = $2\pi/\lambda_g$ propagation constant in waveguide.
$\Delta\beta$ = difference between propagation constants of lowest order odd and even modes.
λ_{gm} = guide wavelength of m-th order mode.
v_p = phase velocity.
c = velocity of light in vacuum.
ω = radian frequency.
$\Delta\omega$ = bandwidth of modulation.

III. Optical Waveguide Theory.

This section briefly summarizes the material presented in Appendix A on the theoretical investigation and experimental evaluation of the propagation characteristics of macroscopic optical waveguide. The theoretical investigation analyzed modal characteristics, field distributions, propagation constants, attenuation and excitation; the experimental work comprised measurements of mode cutoff relations, field distributions and modal excitation. The objective of this initial investigation has been to verify that laboratory models of optical waveguides can be constructed which operate in accordance with the theory developed.

The waveguide studied herein is a dielectric type comprising a core surrounded by a cladding of slightly lower dielectric constant. A wave is guided in the core region by the process of total internal reflection from the core-cladding interfaces. A variation of the all-dielectric guide, where half the structure is imaged by a reflecting wall, has also been studied. In either type, operation can be restricted to only a single mode of propagation by proper choice

of waveguide parameters. The distinguishing feature between this guide and conventional optical waveguides is that operation is constrained to a single mode or a few controlled modes even though the size is large in terms of wavelength. This operation is achieved by maintaining a very small difference in dielectric constant between the core and cladding materials.

The specific requirements for maintaining single-mode propagation with large size have been formulated and a convenient means has been developed for representing these relationships on a mode chart. The requirement is that the product of the waveguide size in wavelengths together with the square root of the difference in dielectric constants be equal to some constant. For low-order modes, this product is of the order of unity; therefore, a one-hundred wavelength guide requires a difference of dielectric constants of the order of 0.0001. The mode charts which have been developed for both circular and slab configurations (Appendix A, Figs. 3, 4) graphically indicate the number of modes which will propagate in a waveguide of any size and difference of dielectric constants.

Expressions for the distribution of fields in the waveguide have been determined, and curves of the transverse field distribution of the first two lowest-order modes at typical operating conditions have been plotted (Appendix A, Figs. 7, 8). These results show that fields are present in both the core and cladding regions, and indicate the percentage of power in each region at different operating conditions.

The variation of propagation constant with frequency (dispersion) has been calculated for the slab waveguide. The results are presented by curves relating the normalized guide wavelength and waveguide size normalized to free-space wavelength (Appendix A, Fig. 9). The dispersion between the first two lowest-order modes can be determined from these curves for a few typical operating conditions. Such information is required for the design of directional couplers and certain other components.

The effects of lossy media on propagation have been investigated briefly. For waveguides composed of dielectric materials only, the attenuation is approximately equal to the free space attenuation of the core and cladding materials weighted by the ratio of power in each region. The attenuation of a typical guide is about 3 db per meter in the visible frequency band.

For a bisected slab waveguide having a metal wall as one of the reflecting surfaces, the dissipation of the metal affects not only the attenuation of individual modes, but the phase and amplitude of the propagation constant as well. The result is a departure from the usual imaging properties of an ideal conductor, and an alteration of the basic modal characteristics of the bisected slab configuration. The most significant effect of this mode alteration is that, unlike the case for an ideal (lossless) metal, the propagation characteristics for both TM and TE modes (parallel and perpendicular polarizations) are identical. It is estimated that the dissipation of the metal surface increases the attenuation to about 20 db per meter.

The excitation of the waveguide concerns the coupling of optical power from some external source to the guide. The two specific cases studied have been excitation of the waveguide by a plane wave and by focused radiation. To briefly summarize these studies, the direction, or angle of incident radiation affects the particular mode which is excited (in a multi-mode guide) for both plane wave and focused radiation. The lateral position of a focused spot on the end of the waveguide primarily affects the amplitude of the coupled signal. Formulas for the coupling efficiency for an arbitrary focused field are presented in Appendix A. It is shown that for optimum coupling efficiency, the field pattern of the incident signal should match the field pattern of the particular mode to be excited in the waveguide.

An experimental investigation of the propagation characteristics of macroscopic optical waveguides has been conducted to confirm agreement between experimental operation and the theory presented above. The experimental program involved the observation of various waveguide modes and measurement of the transverse field patterns in the waveguide. The waveguide employed for initial testing was a liquid-core, solid-cladding, dielectric-slab type. This configuration permits simple adjustment of the waveguide parameters so that their effect on propagation can be investigated. A complete description of the experimental waveguide and a discussion of the experimental procedures is presented in Appendix A, Section V.

To summarize these results, the experiments demonstrated close agreement with theory for the existence of propagating modes

at different operating conditions, as predicted by the mode chart. Measured field patterns were found to agree closely with the calculated patterns. For the bisected guide, the patterns of both polarizations were found to be identical and therefore, in agreement with the theory for a lossy metal.

The general conclusions derived from the initial investigation of optical waveguide are that single-mode and low-order mode propagation can be obtained experimentally in laboratory waveguide models, and the detailed propagation characteristics are closely described by the theory developed.

IV. Optical Waveguide Components.

This section presents the study and experimentation directed toward the development of components in a single-mode waveguide medium. Emphasis has been placed on the identification and understanding of the fundamental design parameters. Experimental evaluation of several components has been performed in order to demonstrate the feasibility of actually constructing these devices. Such demonstrations have been performed with experimental waveguides of the liquid-solid variety in slab and rod configurations. Ultimately, it is planned that these components will be fabricated in an all-solid single-mode waveguide medium as is currently being developed (Section V).

The components selected for study were mostly patterned after microwave devices and chosen primarily on the basis of their applicability to waveguide systems for optical communications and radar. In some cases the performance of these waveguide-type components is similar to that obtained with free-space-type components. However, in other cases the waveguide components have fundamental advantages which result from the single-mode nature of the waveguide medium.

A. Directional Couplers.

Directional couplers are found in all but the simplest optical systems. The conventional optical form of the directional coupler is a half-silvered mirror in an unbounded medium, as shown in the optical heterodyne system of Fig. 1(a). In a bounded propagation medium, such as the single-mode optical waveguide discussed in Section III and in Appendix A, the directional coupler may take the form of adjacent waveguides connected by coupling holes or slots as illustrated by the schematic drawing, in Fig. 1(b), of a balanced mixer for optical heterodyne detection.

A directional coupler is a junction of four transmission lines with selective coupling between particular terminals (ports) and isolation between others. In Fig. 2, power incident on port 1 is coupled in some ratio to ports 2 and 4 and isolated from port 3. Similarly, power incident on port 2 is coupled to ports 1 and 3 and decoupled from port 4. It has been shown that the impedance matching of all four ports is a necessary and sufficient condition for obtaining decoupling between the appropriate ports (Ref. 13).

In accordance with the stated objectives of this study, waveguide-type directional couplers for use at optical frequencies have been analyzed and design parameters have been evaluated. During this program, two directional coupler configurations, illustrated in Fig. 3, have been considered. The evanescent-field coupler [Fig. 3(a)] is formed by bringing two dielectric waveguides close so that they are coupled by the evanescent fields in the cladding. The slot coupler [Fig. 3(b)] is formed from two bisected, dielectric-slab waveguides arranged about a common metal wall which contains a coupling aperture in the form of a slot.

A number of techniques are available for analyzing coupled waveguide systems (Refs. 5, 7, 8, 9). An analysis, common in the microwave literature (Ref. 13), and based on the dispersion of the modes existing in the coupling region, is particularly applicable to the evanescent-field and slot couplers. In this analysis, it is assumed that an input to one port of a directional coupler results in the excitation of the lowest-order odd and even modes at the beginning of the coupling region. Since the phase velocities of these

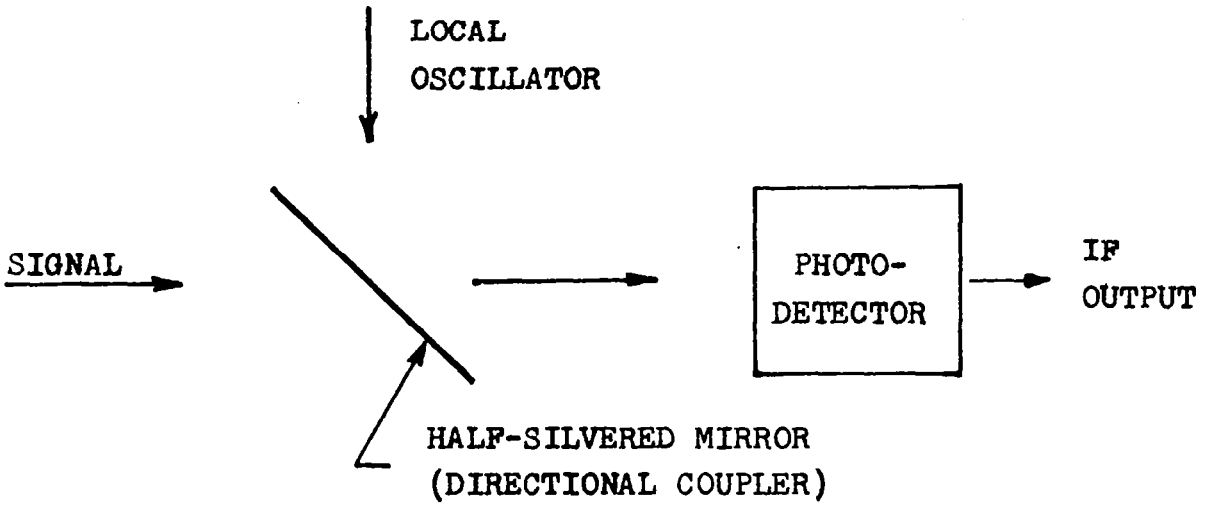

(a) Unbounded propagation medium (single mixer, schematic diagram).

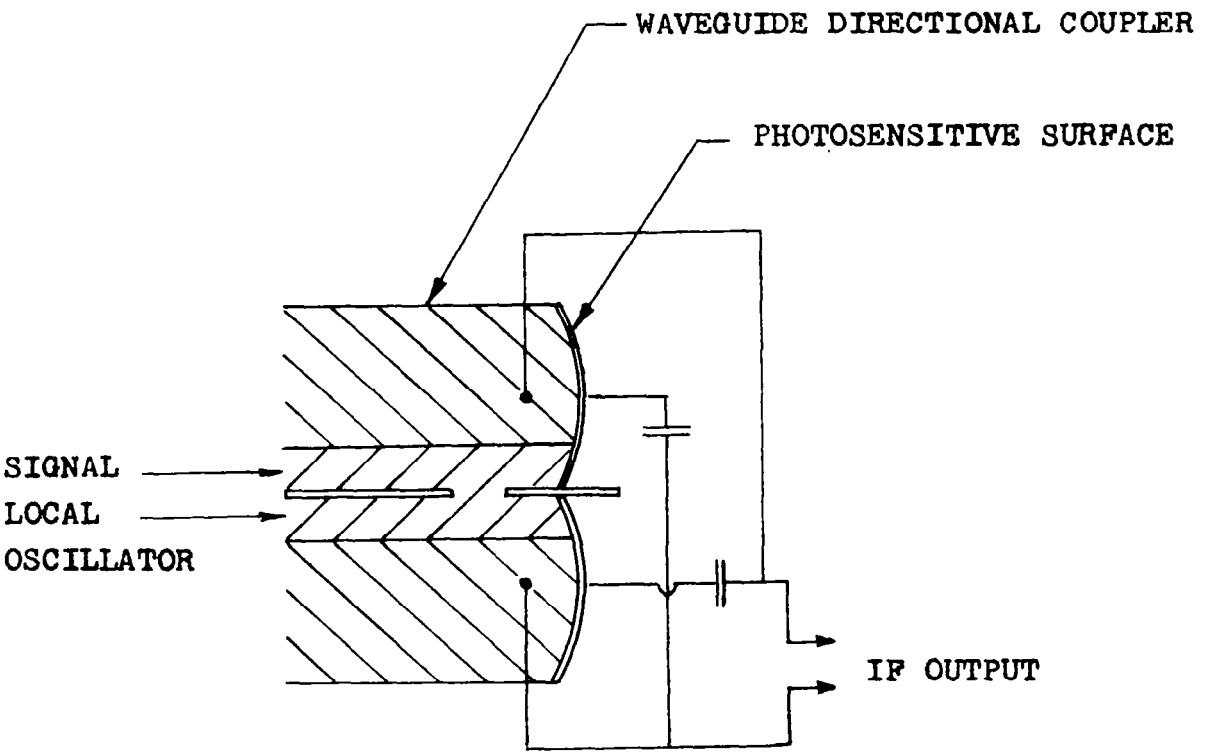

(b) Waveguide medium (balanced mixer, schematic diagram).

Fig. 1 - Applications of directional couplers to optical heterodyne detection.

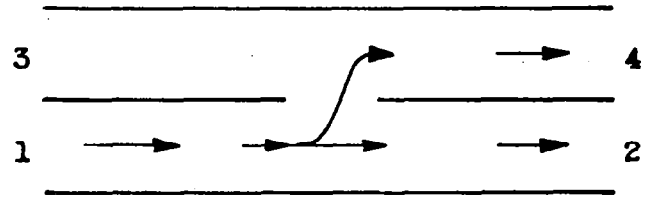

Fig. 2 - Schematic representation of a directional coupler.

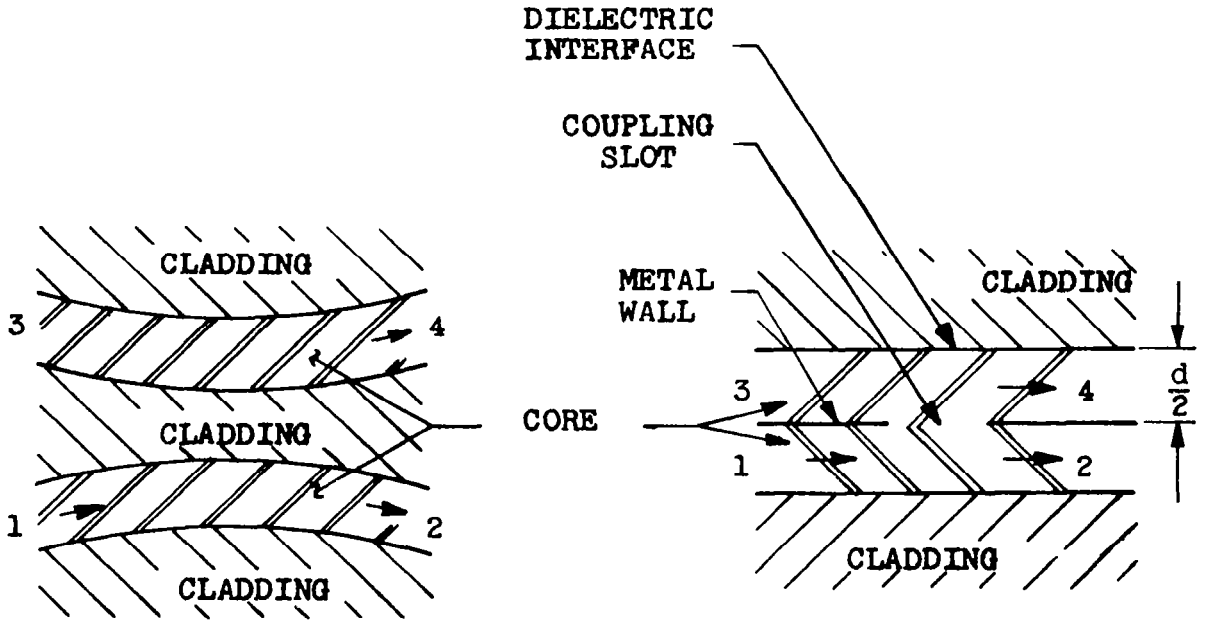

(a) Evanescent-field coupler (b) Slot coupler

Fig. 3 - Optical waveguide directional couplers.

modes will be different, their relative phase will change as they propagate through the coupling region. This relative phase shift is referred to as modal dispersion. If one mode advances π radians relative to the other, all of the power incident on port 1 will be coupled to port 4. Similarly, 2π radians of modal dispersion will couple all of the power to port 2. For intermediate amounts of dispersion, the coupling, which is defined as the ratio, in decibels, of power coupled to port 4 to power incident at port 1, is given by:

$$C = -20 \log_{10} (\sin \frac{\Delta\beta l_c}{2}); \qquad (1)$$

where $\Delta\beta l_c$ is the modal dispersion in radians, = $\Delta\Phi$. It may be seen that 3 db coupling (equal-power split) corresponds to $\pi/2$ radians of modal dispersion. The principal "electrical" parameter for the directional coupler is, therefore, the dispersion between the lowest order even and odd modes in the coupling region. It should be noted that the significance of the impedance matching of the ports is recognized. However, any further theoretical sophistication seems premature when many important practical parameters are still under study.

The calculation of modal dispersion in the coupling region of the evanescent-field coupler is outlined below. It should be noted that the equality of the phase velocities of TM and TE modes observed for the simple waveguide (p. 77A, Appendix A) does not necessarily hold for the more complicated structure in the coupling region. Therefore, the following analysis is restricted to TM modes as an example. However, similar results may be obtained for TE modes.

To analyze the dispersion, it has been assumed that the coupling region consists of two straight, parallel cores with separation b and length l_c in a common cladding as shown in Fig. 4(a). In a practical implementation proximity may be obtained by gently curving the waveguides as shown in Fig. 3. This results in a perturbation of the waveguide modes. However, if the bend radius is greater than the minimum bend radius discussed in part B of this section, the operational behavior is basically the same as the straight section analyzed below. It has been also assumed that the cores are bisected by ideal image planes as shown in Fig. 4(b) since this structure is

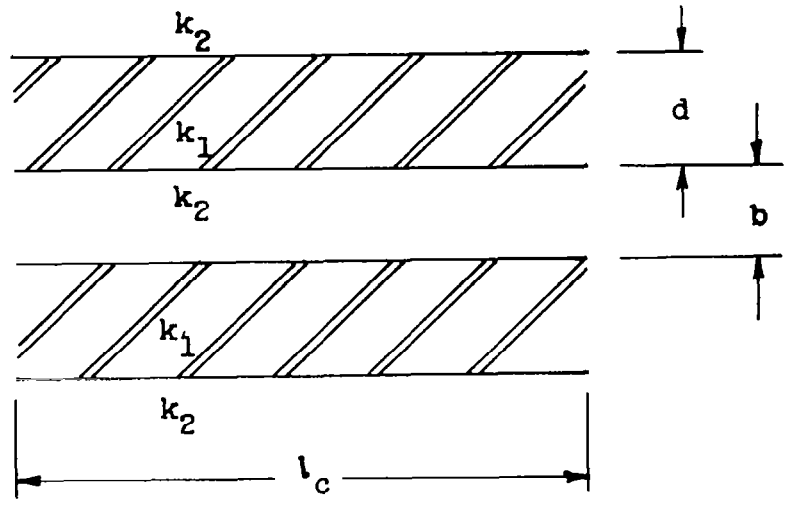

(a) Coupling region.

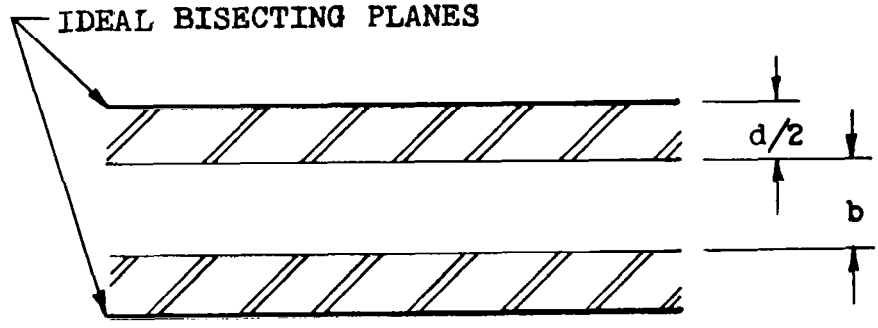

(b) Coupling region in bisected waveguide.

Fig. 4 - Coupling region in evanescent-field couplers.

more easily analyzed than the unbisected one. Therefore, the following analysis is exact for coupled, bisected slabs; however, it is also a good approximation for the case of weak coupling between unbisected waveguides. This coupler analysis will follow the analytic approach of "transverse resonance" developed, for simple waveguides, in Section III of Appendix A. As indicated there, the complete modal solution for a waveguide structure may be found by separately obtaining the solutions for the even and odd modes.

For the TM modes the characteristic equations obtained by the method of transverse resonance are:

$$\text{even:}\quad p \tan p = q \tanh q \left(\frac{b}{d} - 1\right) \quad (5a)$$

$$\text{odd:}\quad p \tan p = q \coth q \left(\frac{b}{d} - 1\right) \quad (5b) \qquad (2)$$

These equations may be solved graphically to obtain the p-q diagram of Fig. 5. The transverse fields in the coupling region are also shown in this figure. The relationship between the p-q curves and the guide wavelength is presented in Eq. 23 of Appendix A and from this it can be shown that the required coupling length is related to the desired dispersion $\Delta\Phi$, and the p-q curves by:

$$l_c = \frac{\Delta\Phi}{\Delta\beta} \; ; \qquad (3)$$

where

$$\Delta\beta = \frac{2\,(q_e^{\,2} - q_o^{\,2})}{\sqrt{k_2}\; K_o\; d^2} \qquad (4)$$

The value of q_e and q_o for a particular operating condition are determined by the intersection of the p-q curves with a circle of radius $K_o d \sqrt{\Delta k}\,/2$. In this manner, a design curve, useful for a typical waveguide configuration, has been obtained, and is plotted in Fig. 6 showing the coupling length for a 3 db coupler as a function of core separation. It may be seen from this curve that, with separations of the order of the core thickness, coupling lengths are quite reasonable; e.g., 3 db coupling may be obtained with a 10 micron

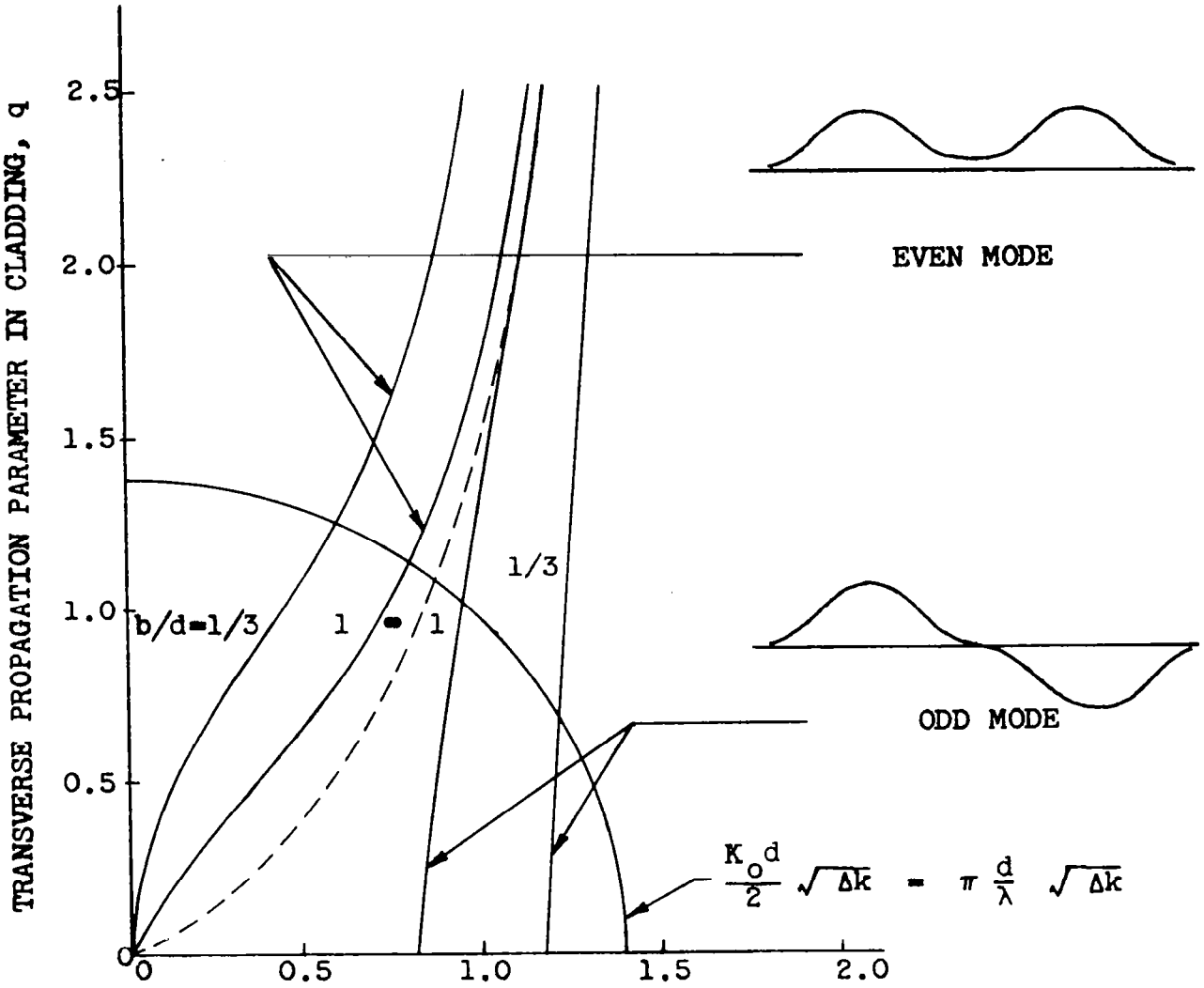

Fig. 5 - Characteristic p-q curves for the lowest order odd and even modes in an evanescent-field coupler.

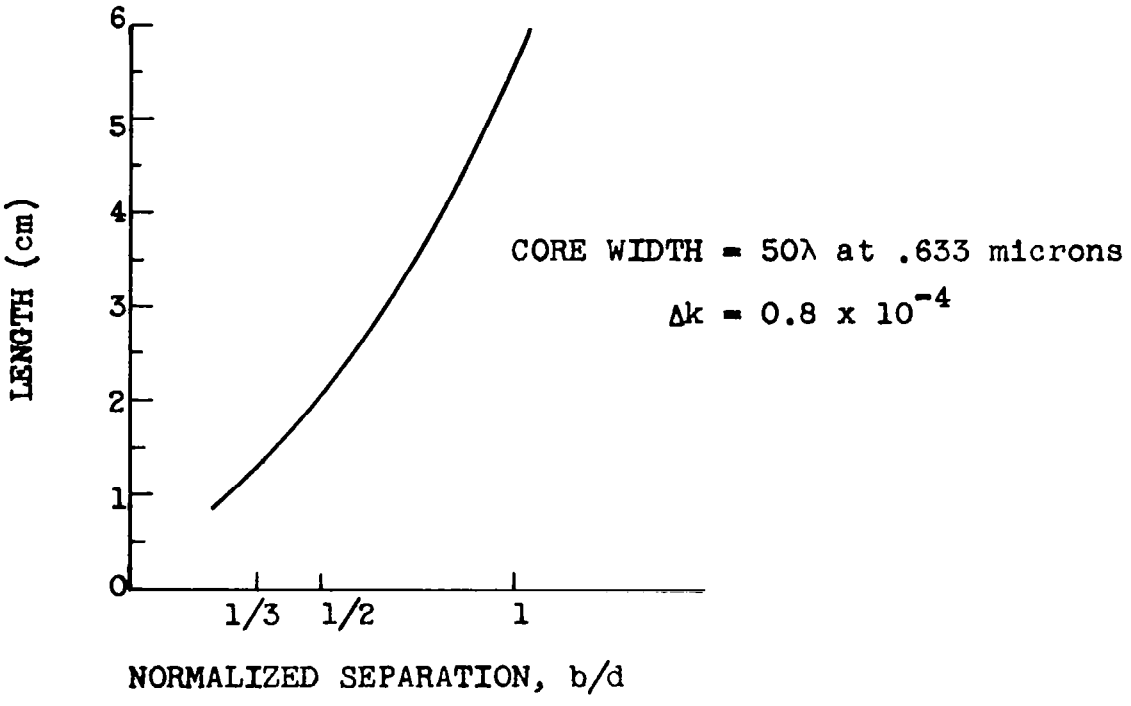

Fig. 6 - Length of coupling region for a 3 db evanescent-field coupler.

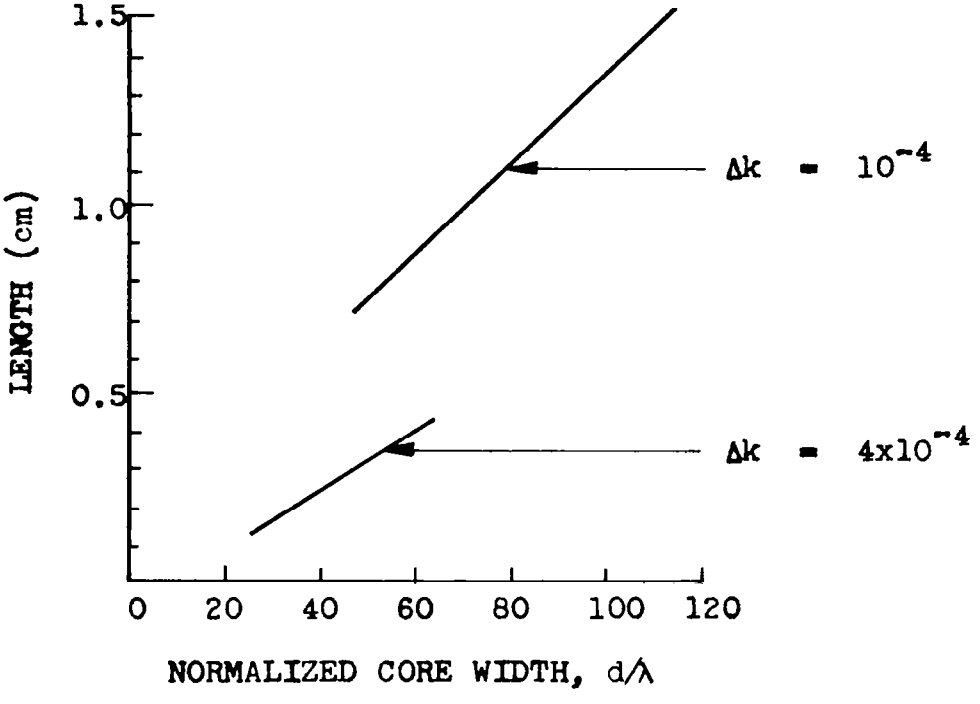

Fig. 7 - Length of coupling region for a 3 db slot coupler.

separation over a 1.25 cm coupling length. It should be noted that the theory is exact for weak coupling and that these numerical results are only approximate for 3 db coupling.

The dispersion between modes in the coupling region of a slot coupler may be readily determined. By inspection of Fig. 3(b) we see that this coupling region is simply the usual slab configuration of 2 times the core thickness of the individual waveguides. The coupling length is again given by Eq. 3. For this coupler, it is more appropriate to express the dispersive properties by:

$$\Delta\beta = \frac{2\pi}{\lambda} (A_0 - A_1), \tag{5}$$

where

$$A_m = \frac{\lambda}{\lambda_{g_m}} - \sqrt{k_2} \ . \tag{6}$$

Since A_m is easily obtained from Fig. 9 on page 25A of Appendix A, the coupling length as a function of waveguide parameters may be readily plotted as in Fig. 7. Again, the coupling lengths required are quite reasonable.

B. Bends.

Waveguide bends constitute an important class of optical waveguide components. The use of bends is necessary in complex waveguide circuits to obtain compact packaging of the various components. In addition, bends serve as an intermediate step in the fabrication of certain directional couplers as discussed in part A of this section.

It has been demonstrated with dielectric bends at microwave frequencies that there is a minimum allowable bend radius for dielectric waveguides; the amount of bending is limited by the amount of leakage from the bend, since such leakage contributes to transmission loss (Ref. 8 in Appendix A). The limitations differ from those for the metallic waveguide case, where reflections, rather than loss, are the main problem. Various criteria for determining the minimum bend

radius of dielectric-waveguide bends for negligible loss have been considered and an experimental program has been conducted.

A simple criterion for the determination of the minimum bend radius is the critical angle requirement for total internal reflection illustrated in Fig. 8. In this case, it is assumed that modal propagation is only slightly perturbed and negligible energy is radiated from the bend as long as the reflecting rays strike the interface at an angle greater than the critical angle. However, when the bend radius is decreased to the point where the angle of incidence within the bend is less than the critical angle, energy begins to leak from the waveguide and the mode becomes, effectively, a leaky mode. The angle of incidence within the bend, θ_b, is related to the bend radius, B_1 and the propagation angle, θ, by:

$$\sin \theta_b = \frac{B_1}{B_1+d} \sin \theta \tag{7}$$

Requiring that the angle of incidence in the bend be equal to, or less than, the critical angle ($\sin \theta_c < \sqrt{k_2/k_1}$) and expressing the result in terms of the guide wavelength in the straight section ($\lambda/\lambda_g = \sin \theta$), yields:

$$B_1 > \sqrt{k_2}\, d \left(\frac{\lambda}{\lambda_g} - \sqrt{k_2} \right)^{-1}, \tag{8}$$

as the minimum bend radius for no leakage.

A more rigorous solution to this problem is obtained from an analysis of the modes on a curved structure (Ref. 3). It can be shown that the fields near bends are evanescent in the vicinity of the core but become outward traveling waves at large distances from the structure. On this basis, a reasonable criteria is to assume that radiation is negligible as long as the fields at the onset of the traveling wave region are 1/e (-8.68 db) of their value at the core-cladding interface. The minimum bend radius according to this criterion is given by:

$$B_2 > \frac{1}{\sqrt{2}} \frac{\lambda}{2\pi} \left(\frac{\lambda}{\lambda_g} - \sqrt{k_2} \right)^{-3/2} \tag{9}$$

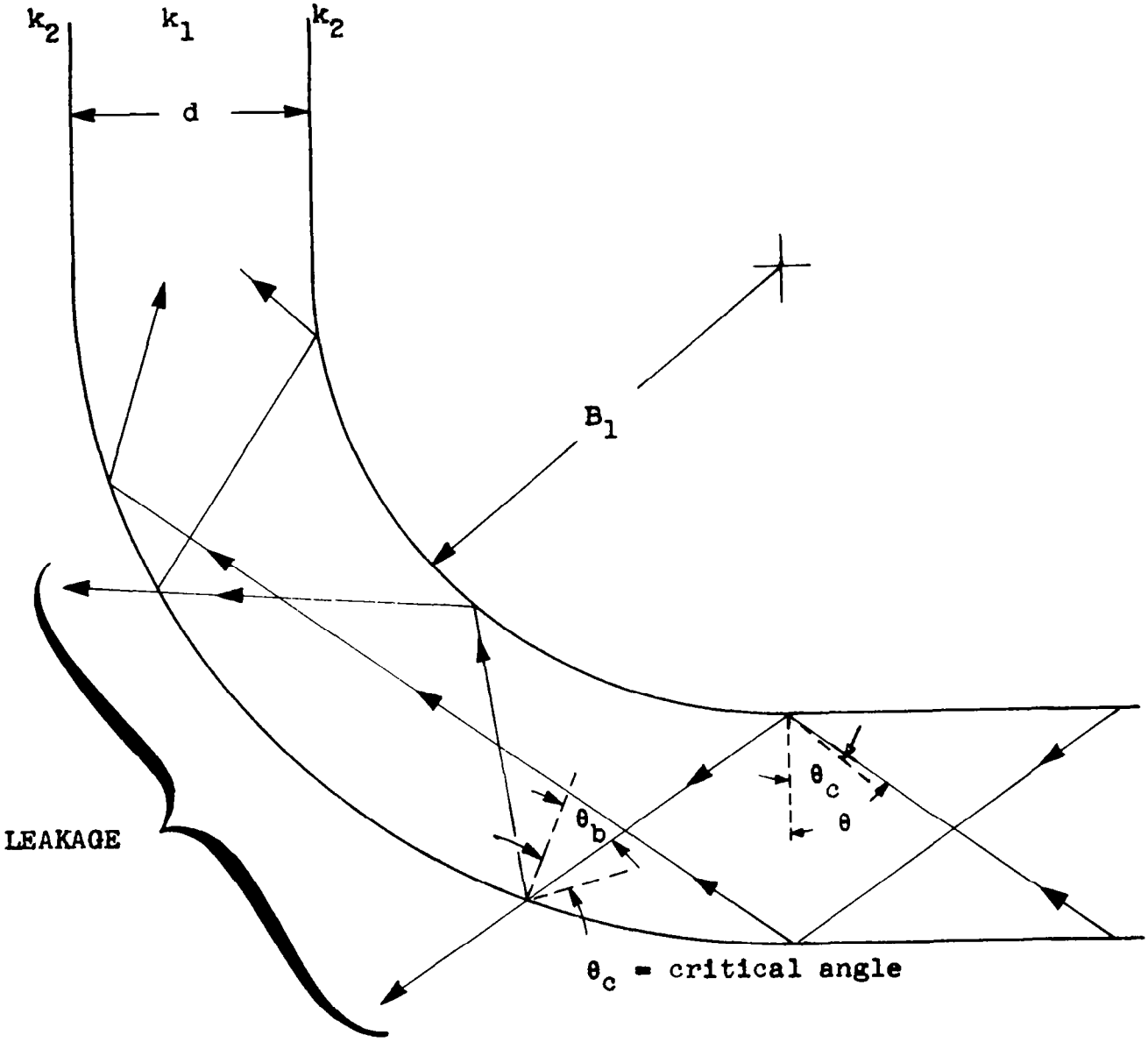

Fig. 8 - Illustration of critical angle criterion for determining minimum bend radius.

This expression is obviously different from that derived from the approximate approach (Eq. 8). It is instructive to take the ratio of the minimum bend radii and evaluate this quantity for the dominant mode when it is far from cut-off and the higher order m-th mode is just at cut-off. This process yields the simple relation,

$$B_2 = \frac{B_1}{m\pi}, \tag{10}$$

where the mode number, m, must be large to satisfy the "far from cut-off" requirement. The two rather different criteria lead to expressions which are functionally similar, differing by a factor of $1/m\pi$, with the exact solution indicating a smaller bend radius for multimode waveguides. For the case of interest, single-mode propagation, it may be shown that Eq. 10 is approximately correct and the ratio of the minimum bend radii differ in this case only by a factor of $1/\pi$. This discrepancy between the two approaches does not necessarily indicate that either approach is incorrect, but that they are based on fundamentally different criteria.

In addition to the theoretical analyses described above, the minimum bend radius has been experimentally evaluated. A 100λ wide, solid-core waveguide, 7.7 cm long, was mounted as shown in Fig. 9 so that the bend radius was easily adjustable. The output of the waveguide was monitored visually as a function of bend radius for various operating conditions, obtained by varying the difference in dielectric constants. The bend radius at which the waveguide output became visually undetectable (corresponding to about 20 db transmission loss) is plotted in Fig. 10. As the other extreme, the minimum bend radius for negligible loss, as calculated from Eq. 8 is also plotted on this figure. Obviously, the experimental data corresponding to 20 db transmission loss should correspond to greater bending (smaller bend radii) than the minimum bend radii (negligible radiation loss) calculated theoretically. However, as shown by Fig. 10, the measured performance indicated greater sensitivity to bending than the simple theoretical model predicted. It is significant that the experimental and theoretical curves differ by a constant scale factor. This indicates that the physical device exhibits the same functional dependence as the mathematical model. Further improvement

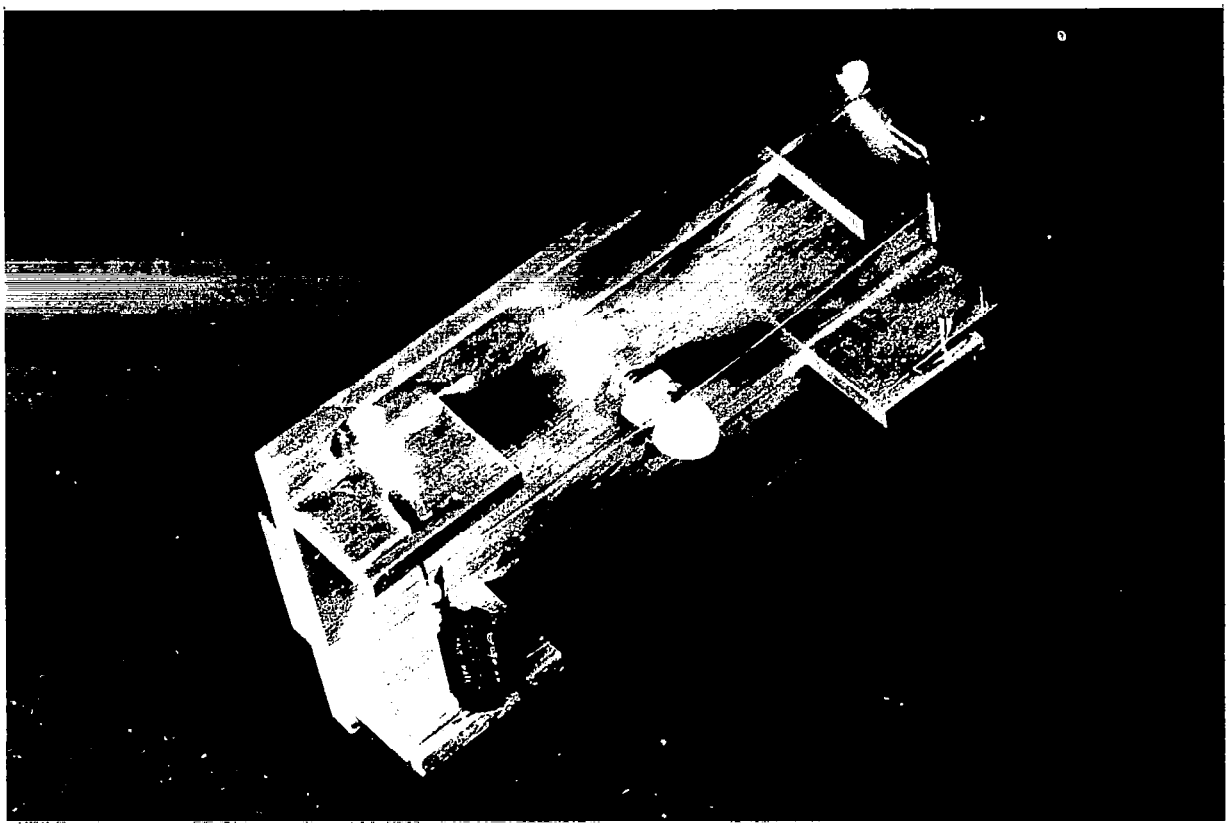

Fig. 9 - Experimental model of optical waveguide bend.

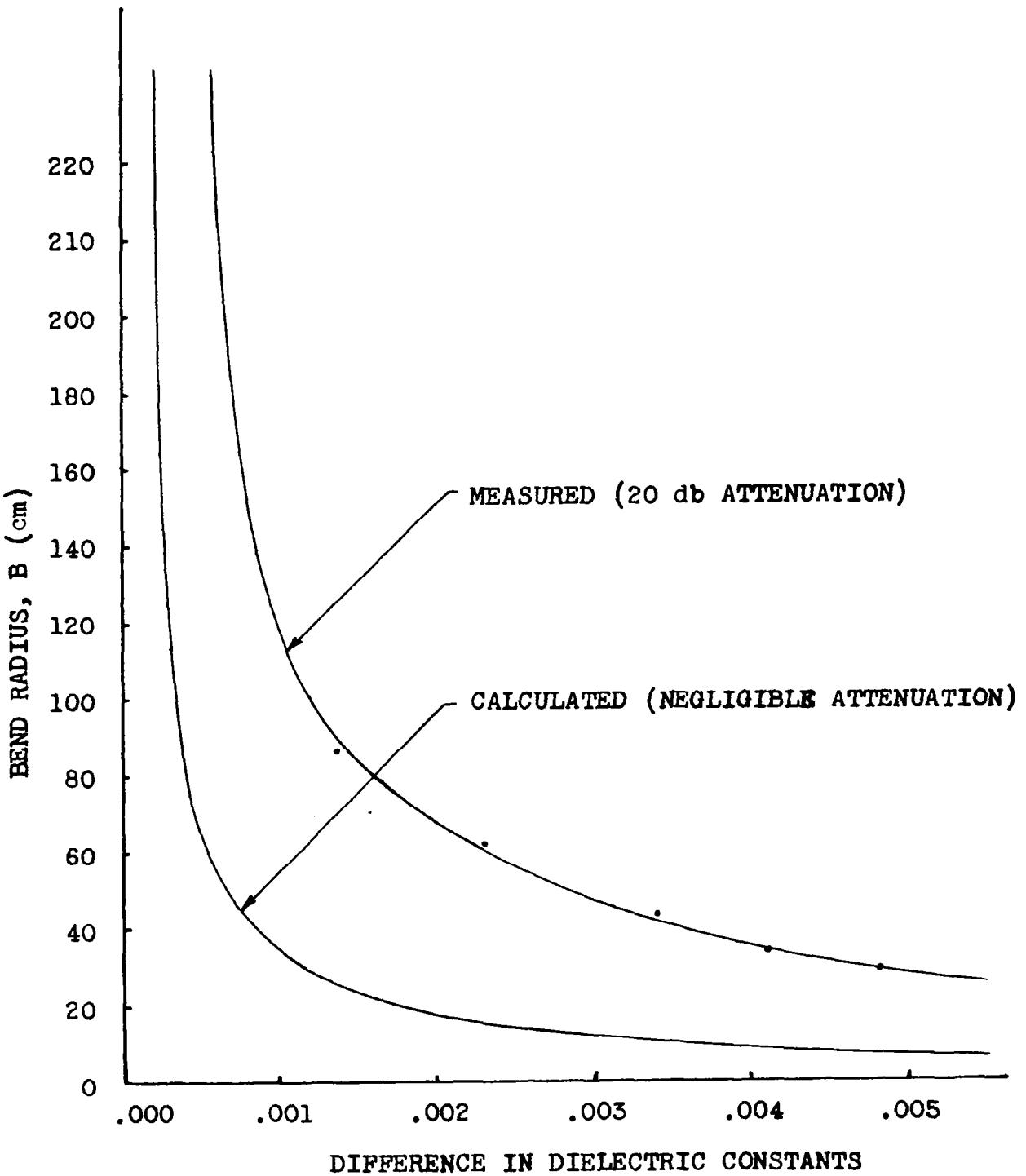

Fig. 10 - Dependence of bend radius on waveguide operating conditions.

of experimental technique and additional refinement of the theory to include such parameters as the gradient of dielectric constant caused by bending strain is expected to resolve the discrepancy between the theoretical and experimental data.

The above investigation indicates that optical waveguide bends, exhibiting negligible loss, may be fabricated with bend radii of the order of 4 meters. This is sufficient bending for application to directional-coupler fabrication, but it is not sufficient to obtain a right-angle bend within a reasonable length. To obtain larger amounts of bending, other techniques are being considered. These include: (1) increasing the difference in dielectric constants in the region of the bend to obtain tighter binding of the fields, and (2) utilization of bisected waveguide with the metal bisection on the outside of the bend as is done at microwave frequencies with dielectric image lines (Ref. 6).

C. Resonators.

Resonant cavities are important components in conventional optical systems; common examples are resonant laser cavities and multiple-layer interference filters. Since laser cavities and frequency filters will also be required within the proposed waveguide systems, an investigation of resonators in optical-waveguide has been conducted. The objective of this study has been the determination of resonator performance in terms of the waveguide design parameters. It has been considered sufficient to restrict the analysis to simple Fabry-Perot structures which are an integral part of the waveguide as illustrated in Fig. 11.

The transmitted intensity of a conventional free-space Fabry-Perot interferometer (Ref. 9 in Appendix A) is given by the expression:

$$\frac{I}{I_o} = \frac{1}{1 + \frac{4s}{(1-s)^2} \sin^2 \frac{\delta}{2}} , \qquad (11)$$

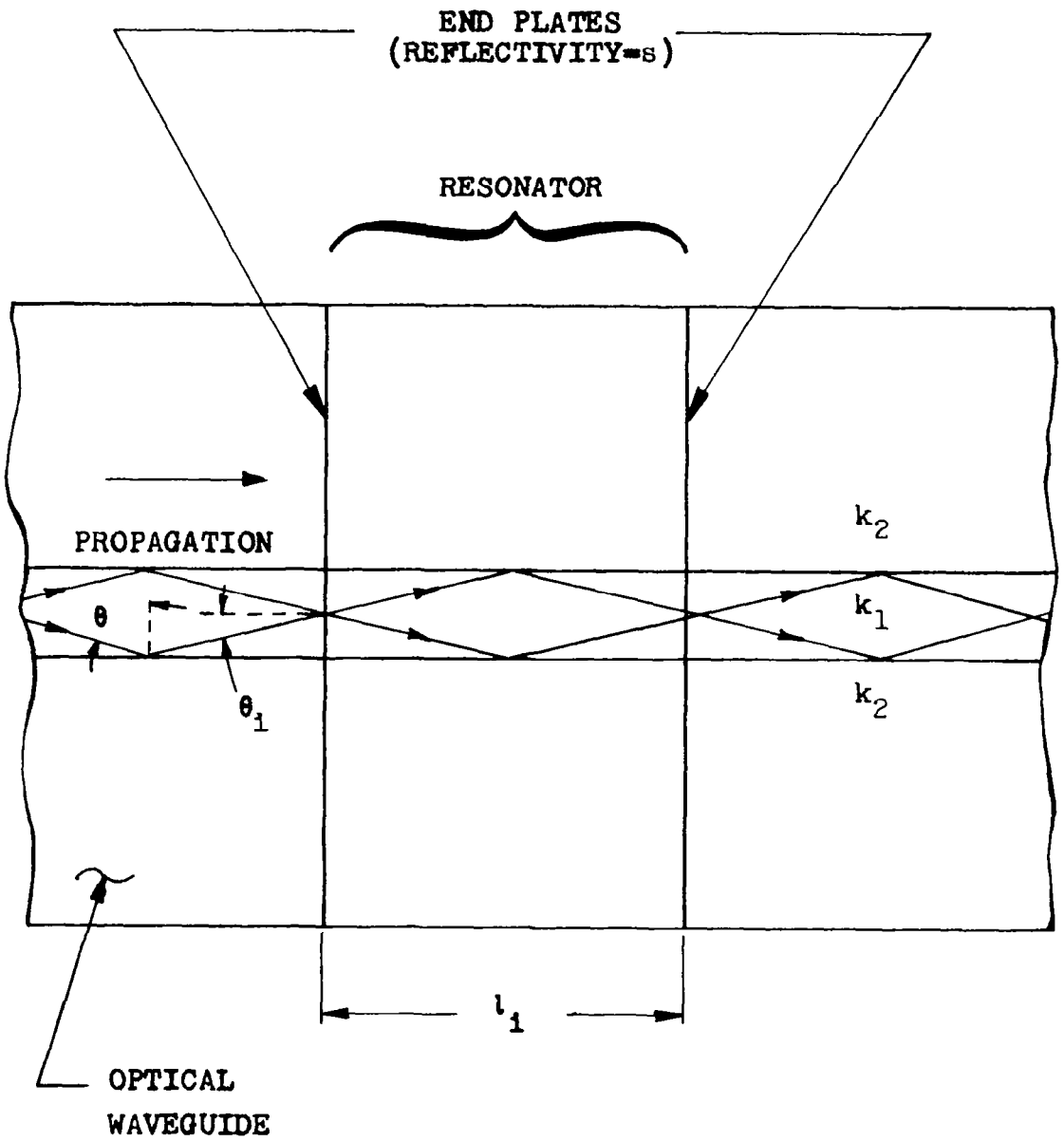

Fig. 11 - Optical-waveguide resonator.

where δ is given by:

$$\delta = \frac{4\pi}{\lambda} \sqrt{k}\, l_i \cos \theta_i , \qquad (12)$$

s is the reflectivity, and θ_i, the angle of incidence on the resonator, is an independent variable. These equations yield the familiar "comb filter" characteristics for both angle and frequency dependence.

It can be shown that Eqs. 11 and 12 apply for the dielectric waveguide medium as well as for free-space. However, in the waveguide case, θ_i, the angle of incidence on the resonator is a function of the waveguide parameters and the operating wavelength. The application of these equations to guided propagation is, in general, difficult. Fortunately, however, for a specific waveguide, θ_i is a function of wavelength only. Furthermore, over a typical laser bandwidth, this angle is essentially constant with frequency. Therefore, with cos θ_i regarded as a constant of the waveguide rather than as an independent variable, Eq. 11 and 12 may be applied directly.

The above discussion of the waveguide resonator has been concerned only with frequency response. It should be noted that the term "angle characteristic" has no meaning within a single-mode medium since the term "single-mode" implies that for a given frequency, propagation within the waveguide is constrained to a single angle; the only angle characteristic that may be associated with the waveguide resonator is the antenna reception pattern at the input to the waveguide system [Fig. 12(a)]. Therefore, it is possible, by working in a single-mode medium, to fabricate a Fabry-Perot resonator whose frequency response is independent of angle and determined by the resonator length and reflectivity in the conventional manner.

An example of the angle characteristic of a typical free-space Fabry-Perot resonator is shown in Fig. 12(b). For comparison the reception pattern of a 50 wavelength wide, single-mode waveguide containing a waveguide resonator is shown in Fig. 12(a). The frequency characteristics of the resonators were chosen with a half-power transmission width of about 80 Mc and the next order response separated about 1800 Mc from the first order response. Such a resonator, placed in front of a He-Ne gas laser 1 meter in length,

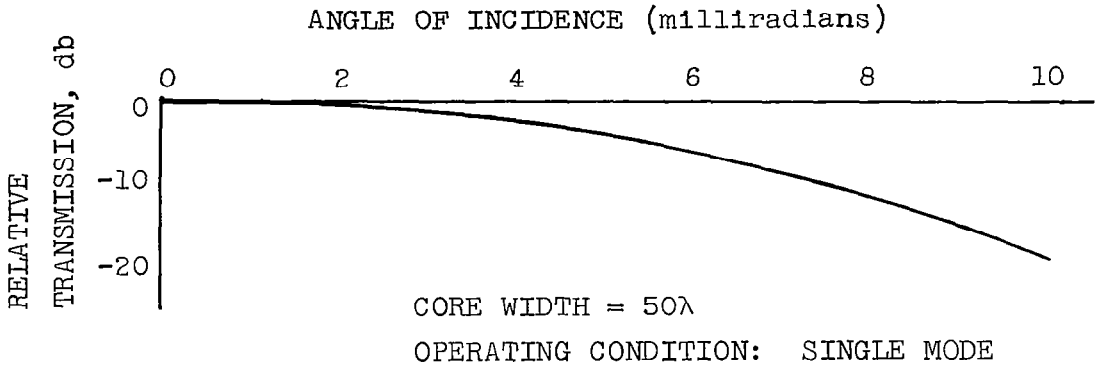

(a) Fabry-Perot filter in waveguide.

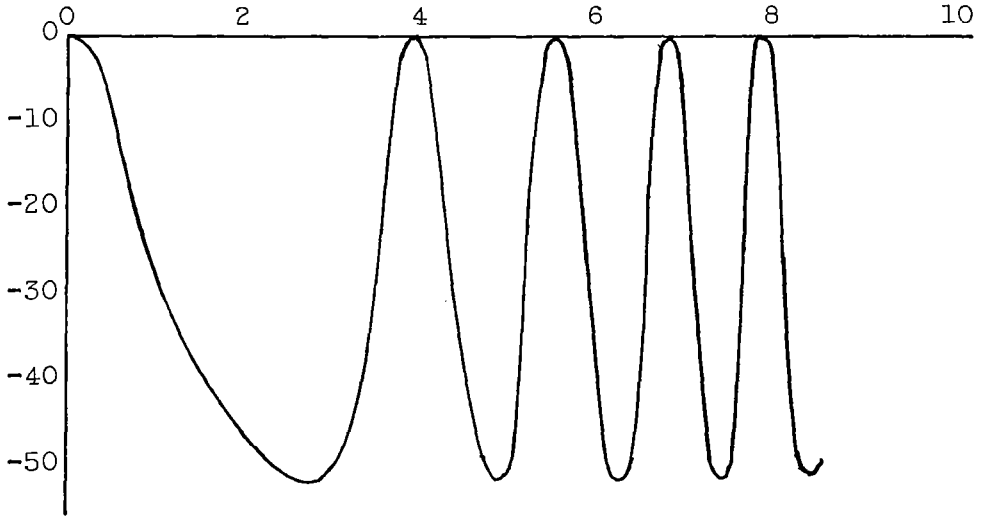

(b) Fabry-Perot filter in free space.

Fig. 12 - Computed angular dependence of optical resonators.

could pass one of the lines in the spectral output and reject all others which occur within the 900 Mc. Doppler-broadened width associated with the gas laser. It can be seen from the figure that such a frequency response results in a high degree of angle sensitivity for the free-space resonator, whereas, a waveguide resonator with the same frequency response has a much broader reception pattern.

It should be noted that the angular pass-bands occurring outside of the main reception pattern of the waveguide are eliminated only to the degree that the leaky waveguide modes are damped. Therefore, efficient leaky-mode damping is required for this component.

The waveguide resonator is somewhat unique among the waveguide components since it is easier to fabricate in an all-solid waveguide than in the liquid-solid experimental models presently available. Since an all solid waveguide is not presently available, a direct experimental evaluation of this component has not yet been carried out. However, a simple experiment has been conducted to demonstrate its unique angle independence. The experimental set-up is shown in Fig. 13. For the purposes of this experiment, the waveguide resonator was simulated by placing a 7.7 cm length of single-mode, quartz-rod, waveguide in front of a conventional Fabry-Perot resonator. The angle response of this system, with the angle of incidence on the waveguide as the variable, was measured as shown in Fig. 13(a). The waveguide was then removed so that the laser beam was directly incident on the Fabry-Perot as shown in Fig. 13(b) and the angle response was again determined. The results are plotted in Fig. 14. It can be seen that the waveguide did indeed convert the angle dependence of the resonator to the reception pattern of the waveguide.

The obvious application of the waveguide resonator is as a frequency filter. In this case, the design is based on Eqs. 11 and 12 as discussed above.

The use of the waveguide resonator as a laser cavity has also been considered. It is unique for this purpose in that it is inherently a single-mode structure; consequently, since no leaky modes will oscillate, all the power will occur in the lowest order transverse mode. A typical waveguide laser might consist of

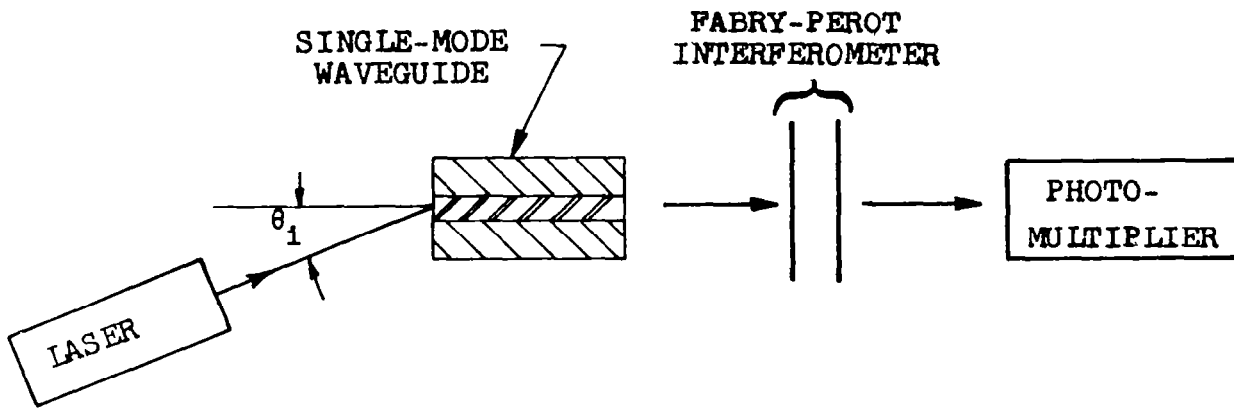

(a) Waveguide resonator.

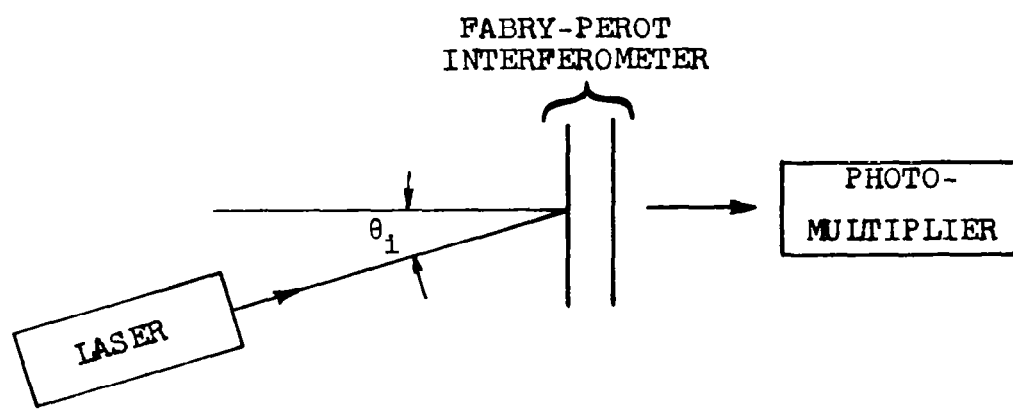

(b) Free-space resonator.

Fig. 13 - Block diagram of resonator demonstration.

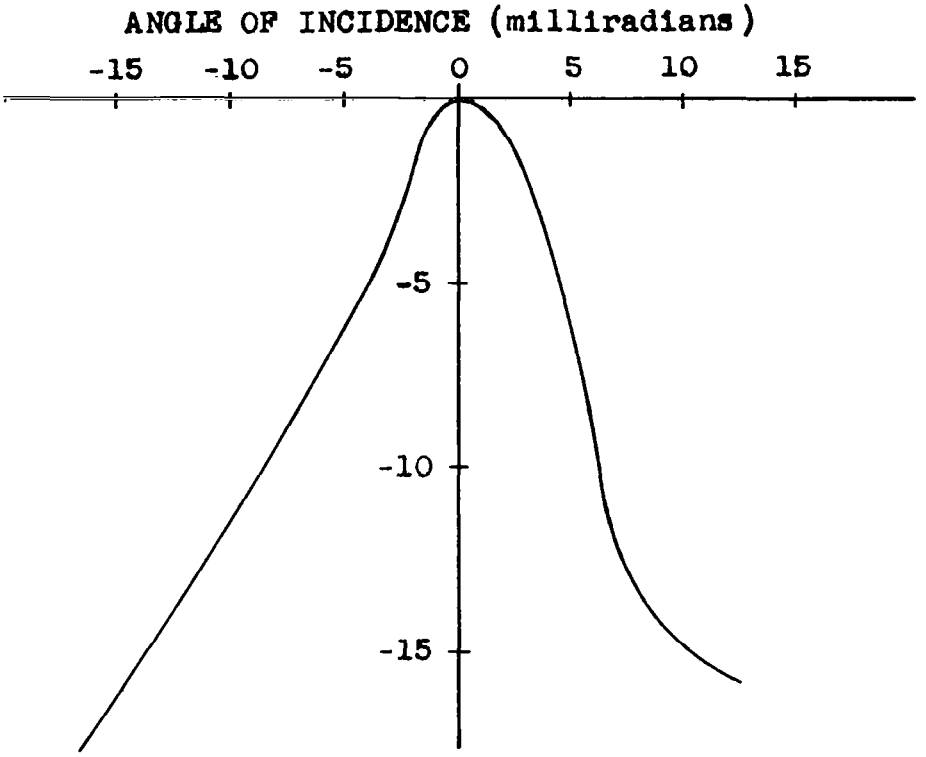

(a) Waveguide resonator.

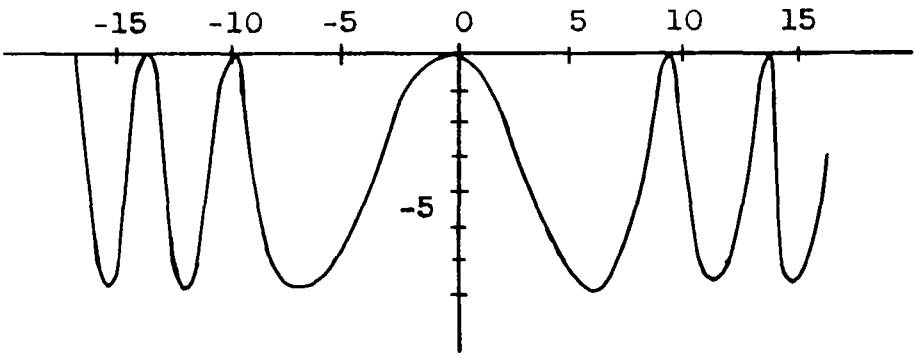

(b) Free-space resonator.

Fig. 14 - Measured angular dependence of optical resonators.

a core of doped glass surrounded by an undoped cladding. Optical pumping could be performed through the cladding, since it is transparent. For this application, the concept of macroscopic size is very significant. A laser fabricated in macroscopic single-mode waveguide ($\approx$50 microns) will have an active volume 2,500 times larger than can be obtained by simply reducing the dimensions of a conventional fiber laser (Ref. 21) to a size ($\approx$1 microns) where only a single mode oscillates.

The implementation of such a single-mode waveguide laser requires an extensive investigation of material parameters to determine the suitability of active laser materials for waveguide applications. However, it may be concluded that the waveguide resonator, in general, is well understood and its application as a frequency filter or laser cavity is considered feasible.

D. Modulators.

Modulation is essential to the useful functioning of any information-transfer system. Therefore, a practical optical waveguide system must contain some provision for modulation of the output signal. This section outlines the operating principles and design criteria for several waveguide modulators. In addition to their application within waveguide systems, waveguide-type modulators may find some application in more conventional optical systems. The utility of such modulators outside of the waveguide system derives from their potentially small volume relative to conventional modulators and the attendant reduction of modulation power which is directly proportional to the volume of the optical system (Ref. 10).

Modulation may be obtained within the waveguide medium by varying one or more of the waveguide parameters; electro-optic, magneto-optic, piezoelectric, mechanical, and thermal techniques are all adaptable to some extent for this purpose. All of the conventional types of modulation are possible. Three modulators, all based on the Kerr electro-optic effect have been analyzed during this study. One of these, a pulse modulator in which the effective presence or absence of the waveguide boundaries is the modulated parameter, was selected because of its novelty and its adaptability to the present

experimental waveguide configuration. The other modulators, a polarization modulator and a phase modulator, are directly analagous to previously reported free-space modulators (Ref. 14, 15) and have been chosen because preliminary experiments could be conducted in the same experimental configuration as the pulse modulator.

1. Pulse modulator.

A novel type of pulse modulation may be obtained within a waveguide system by inserting a section of waveguide which can be turned "on" and "off" by the modulating voltage. In the case considered, the "on" condition represents the usual guided propagation through this section. The "off" condition is obtained by setting the difference in dielectric constants at zero so that no waveguide propagation occurs; the modulator section is then equivalent to a free-space propagation path between the loosely coupled antennas formed by the open-ended waveguidesas shown in Fig. 15.

The modulation region of the pulse modulator for the "off" condition can be analyzed on the basis of coupled antenna theory already available in the literature (Ref. 22). Representing the waveguides at the input and output ports of the modulator by square antennas with cosine illumination in the bounded dimension and gaussian illumination in the unbounded dimension leads to a simple expression for coupled power.

$$\frac{P_{out}}{P_{in}} = \left(\frac{1}{g}\right)^2 \quad ; \tag{13}$$

where g is the antenna spacing normalized to the "Rayleigh" range (Ref. 22):

$$g = \frac{l_m}{R_r} = \frac{l_m^2 \lambda}{d^2} \tag{14}$$

The degree of modulation, which follows directly from Eq. 13 has been plotted in Fig. 16 as a function of the length of a typical modulator section. This curve indicates that 90% modulation may be obtained in the visible band with a modulation length of the

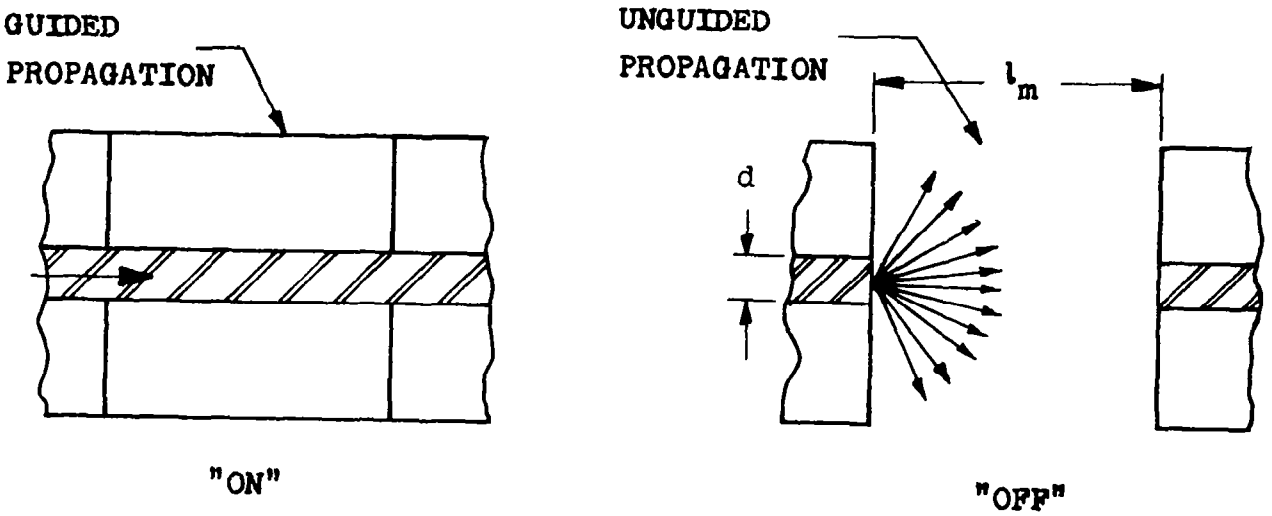

Fig. 15 - Operation of a pulse modulator.

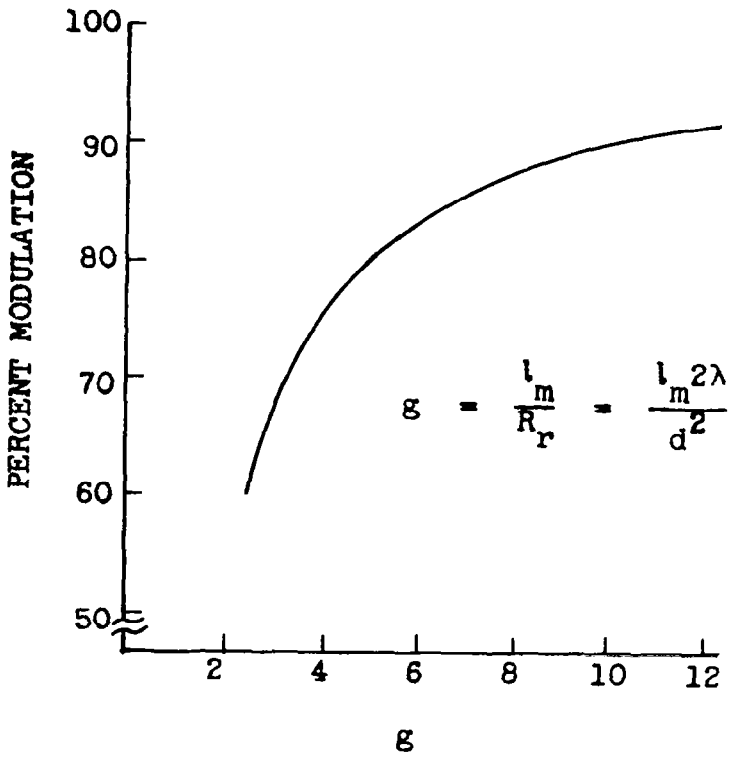

Fig. 16 - Performance of a pulse modulator as a function of length.

order of 0.5 cm for a waveguide with a 40 λ core. It should be noted that the modulation is determined mainly by the length of the coupling region; it is relatively independent of applied voltage. The function of the applied voltage is only to turn the waveguide "on" and "off"; in the idealized limit this can be done with an infinitesimal voltage change which increases the difference in dielectric constants either by decreasing the dielectric constant of the cladding or increasing the dielectric constant of the core.

The experimental evaluation of the pulse modulator has been conducted in the configuration shown in Fig. 17. Thick glass plates constitute the cladding medium while liquid nitrobenzene comprises the 0.025 mm core. An electric field is applied across the aluminum foil electrodes which are 0.025 mm thick and spaced 0.5 mm apart. The dielectric constant of the core is set equal to that of the cladding by adjusting the temperature of the liquid (p. 54, Appendix A). The waveguide is turned on by applying a voltage to the electrodes which, by means of the Kerr electro-optic effect, raises the dielectric constant of the nitrobenzene core. The propagation characteristics of such a waveguide may be obtained with reference to Fig. 18 in which the difference in dielectric constants, for waves with transverse magnetic polarization (TM modes) is plotted as a function of applied electrode voltage. A similar curve can be plotted for TE modes. For reliable modulation, the electrode voltage must be only high enough to achieve a difference of dielectric constant significantly greater than the inhomogeneity of the waveguide materials. There is an upper limit on modulation voltage so that single-mode operation is maintained.

In the pulse modulator waveguide configuration there may be an additional constraint on the propagation characteristics if the electrodes become an optical guiding surface. To avoid this situation, the modulator has been operated with an input beam diameter somewhat smaller than the electrode spacing. For this reason it is also necessary that the modulator length be less than the Rayleigh distance (Ref. 22) of the aperture formed by the electrodes at the input end, or more specifically, that:

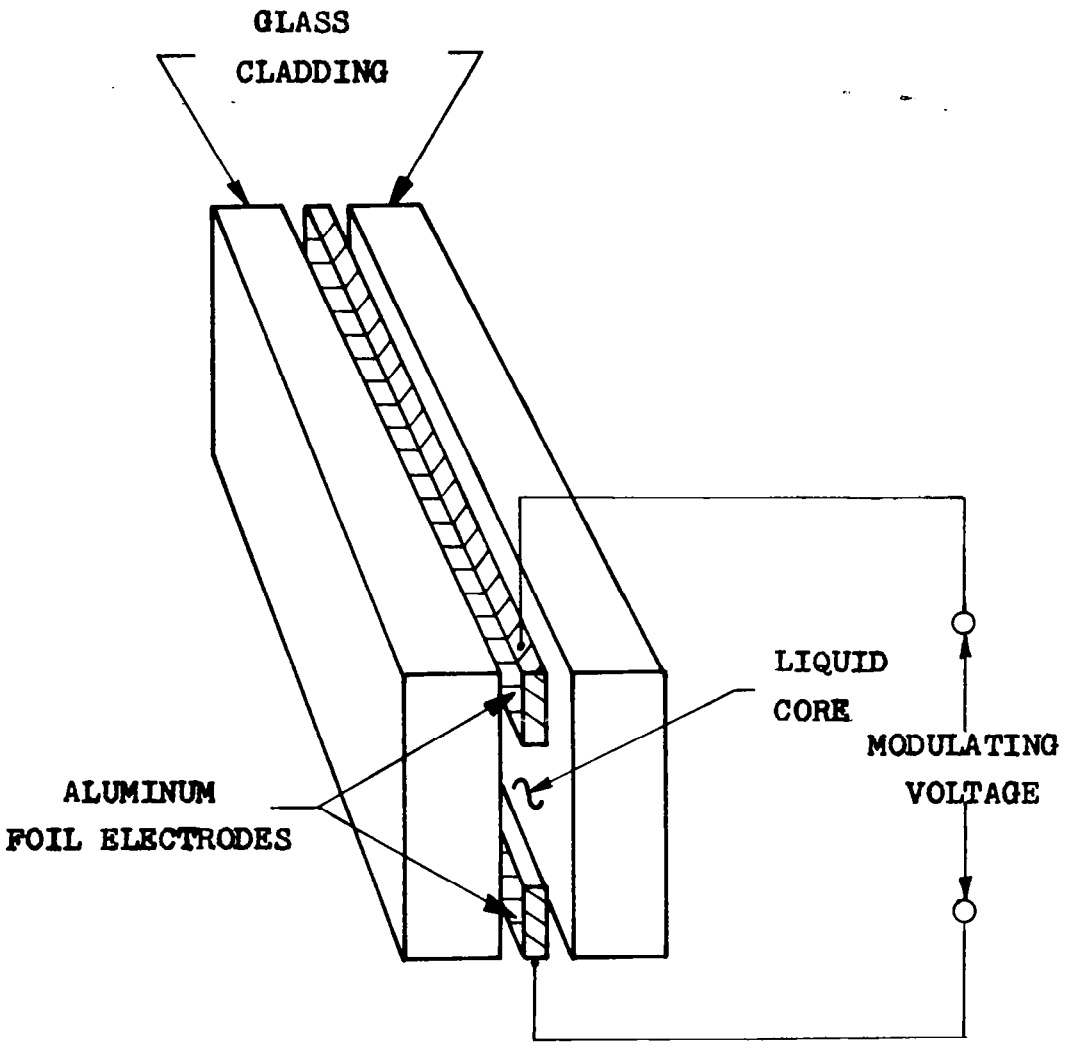

Fig. 17 - Experimental waveguide configuration for testing modulator concepts and design parameters.

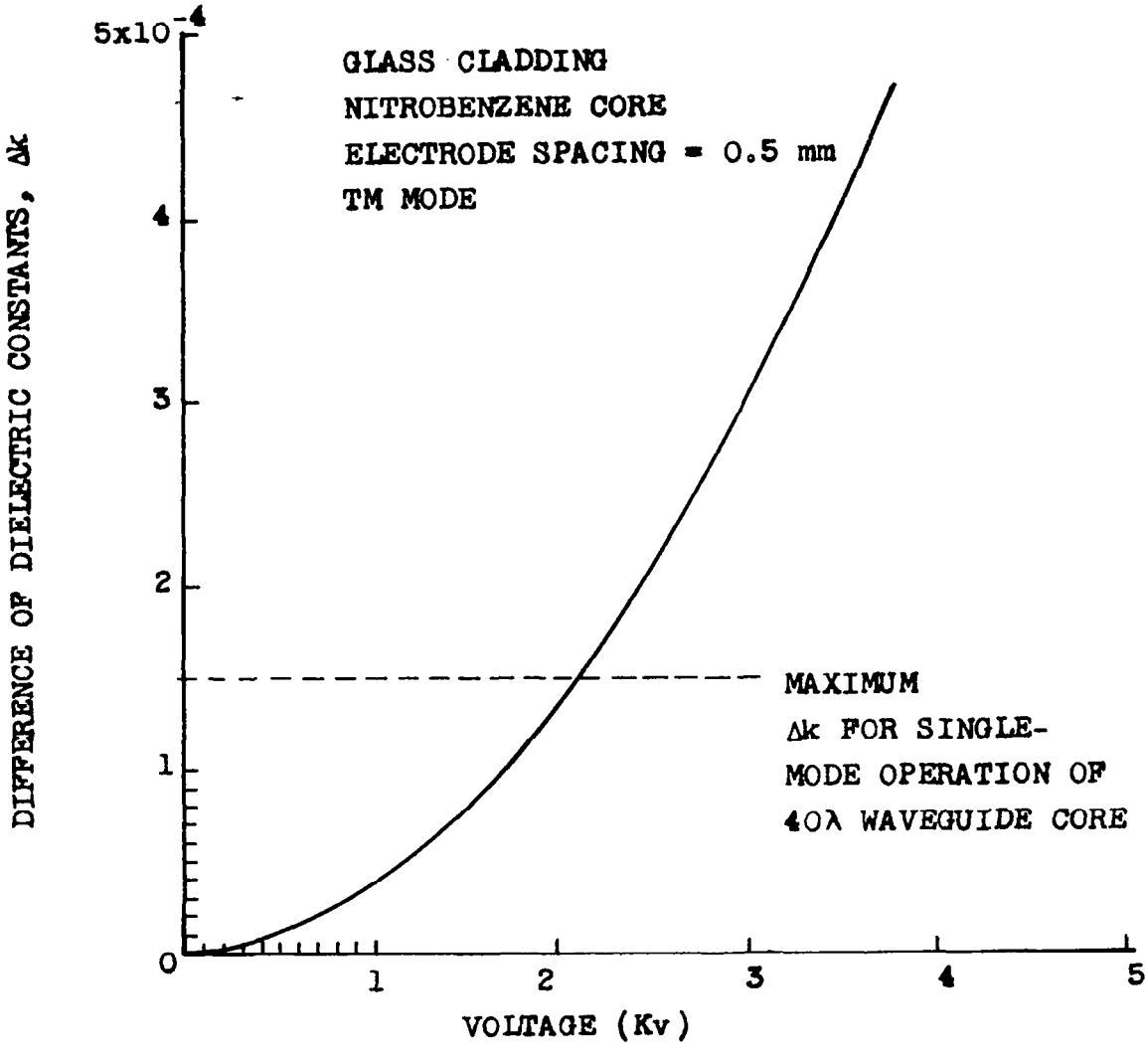

Fig. 18 - Difference in dielectric constant as a function of voltage for an experimental modulator.

$$l_m < \frac{d_e^2}{2\lambda}, \qquad (15)$$

where d_e is the electrode spacing.

The preliminary experimental program planned for this modulator included the measurement of output intensity as a function of applied voltage and a demonstration of pulse modulation at an audio rate. However, the operating temperature required to reduce the dielectric constant of the nitrobenzene (k = 2.40) to that of the glass (k = 2.29) is beyond the capabilities of the temperature control unit that was employed for the other waveguide experiments during this program. Therefore, it was not possible to implement a single-mode waveguide modulator during the present study, but an initial evaluation has been performed. The difference in dielectric constants of the waveguide was initially adjusted for highly multimode operation. The third mode was excited by a laser beam incident at the required angle and provision was made for raising the dielectric constant of the core by an applied voltage. Changes in the observed mode pattern were noted for applied voltages of the order of 100 volts and, when 500 volts was applied, propagation switched from the third to the second mode. This observation is consistent with theory, since the mode number corresponding to a particular propagation angle decreases as the difference in dielectric constants increases. This preliminary experiment indicates that field strengths of the order of 10 Kv/cm are sufficient to modulate the propagation characteristics.

2. Phase modulators.

Since phase modulation is often employed in communication systems, a preliminary feasibility study of a waveguide phase modulator has also been performed. Typical values for the important parameters have been computed, design curves have been plotted, and a simple experimental program is outlined.

Phase modulation within the optical-waveguide system may be obtained by modulating either the waveguide dimensions or the dielectric constants in such a way that the phase velocity is varied, thereby modulating the phase of the output signal. A phase modulator configuration identical to the pulse modulator of Fig. 17 has been

considered. For phase modulation, the difference in dielectric constants of the waveguide is adjusted for single-mode operation by temperature control and the application of a DC bias. The difference in dielectric constants is then varied electro-optically, thereby, modulating the phase length; the dependence of relative phase length on the difference in dielectric constants is shown in Fig. 19. It can be seen that the phase slope is greater for the unguided case ($d/\lambda = \infty$), but that the waveguide case approaches the unguided situation far from cut-off. Therefore, sensitivity of the waveguide modulator to the modulating voltage approaches, but does not exceed, that of the corresponding free-space modulator. The modulation index for phase modulation is equal to the maximum phase variation, Φ_m, which is related to the length of the modulation region by:

$$\frac{l_m}{\lambda} = \frac{\sqrt{k_1}}{\Delta k} \frac{\Phi_m}{\pi} \quad . \tag{16}$$

For visible He-Ne lasers and a waveguide 50 wavelengths wide, phase may be varied over a range of π radians by a single-mode modulator about 1 cm long. This modulator operates equally well in TM and TE modes and the equation given above applies to both.

A simple experimental arrangement for the observation of this phase modulation is illustrated in Fig. 20. The experimental setup consists of a conventional Michelson interferometer with the waveguide modulator in one arm. The zero-order fringe of the interference pattern goes from a maximum to a minimum for a phase change of $\pi/2$ radians in the modulator. Therefore, a photo cell and meter monitoring this intensity can be calibrated to indicate phase change directly. In this manner the phase modulation as a function of applied voltage may be measured.

3. Polarization Modulator.

The modulator configuration of Fig. 17 can also be employed for the preliminary evaluation of a polarization modulator. In this case, the waveguide is excited by a laser beam as shown in Fig. 21 so that both the TM and TE modes are excited. The dielectric constant of the core rises, creating the desired difference in

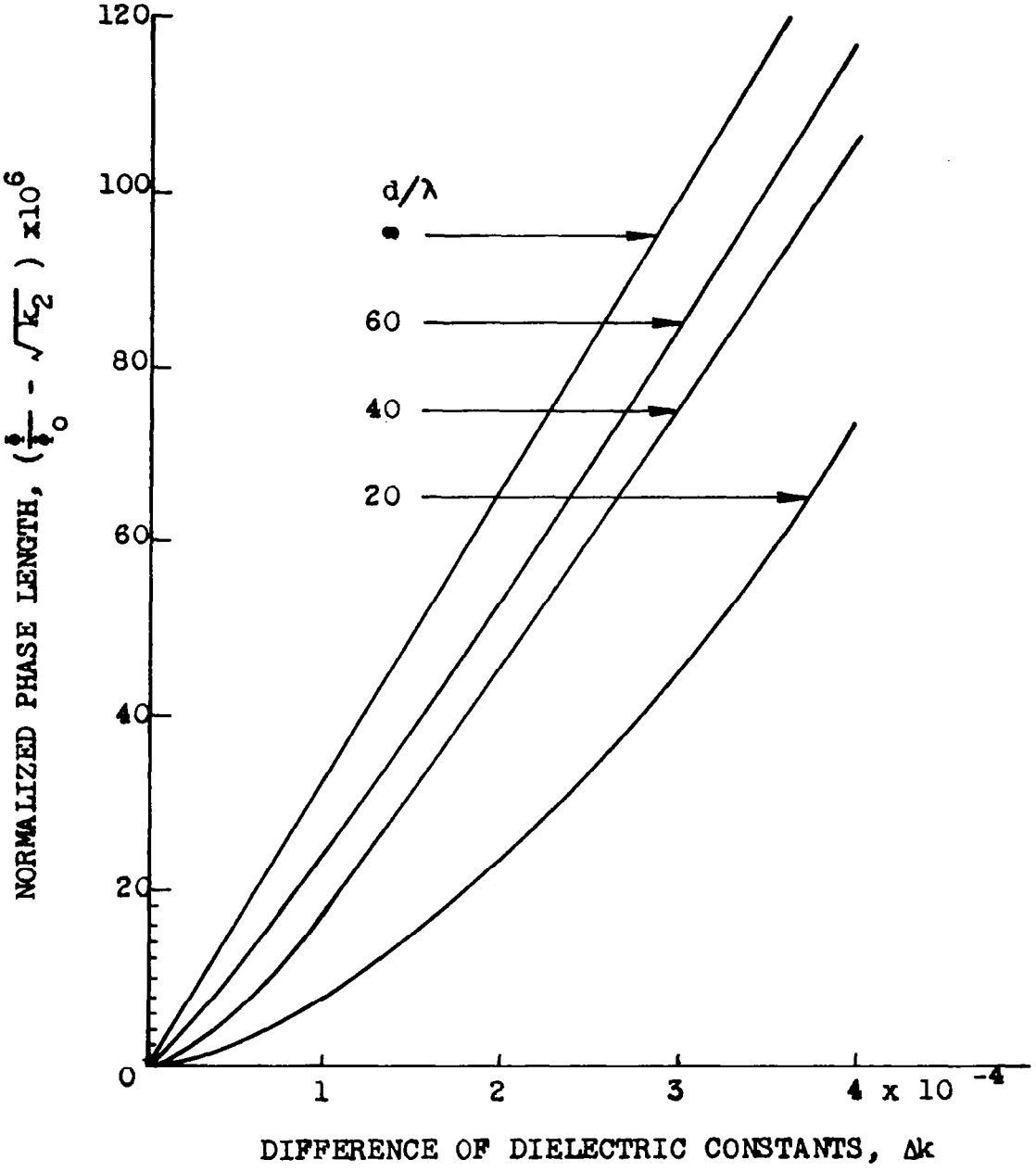

Fig. 19 - Dependence of normalized phase length on the difference in dielectric constants.

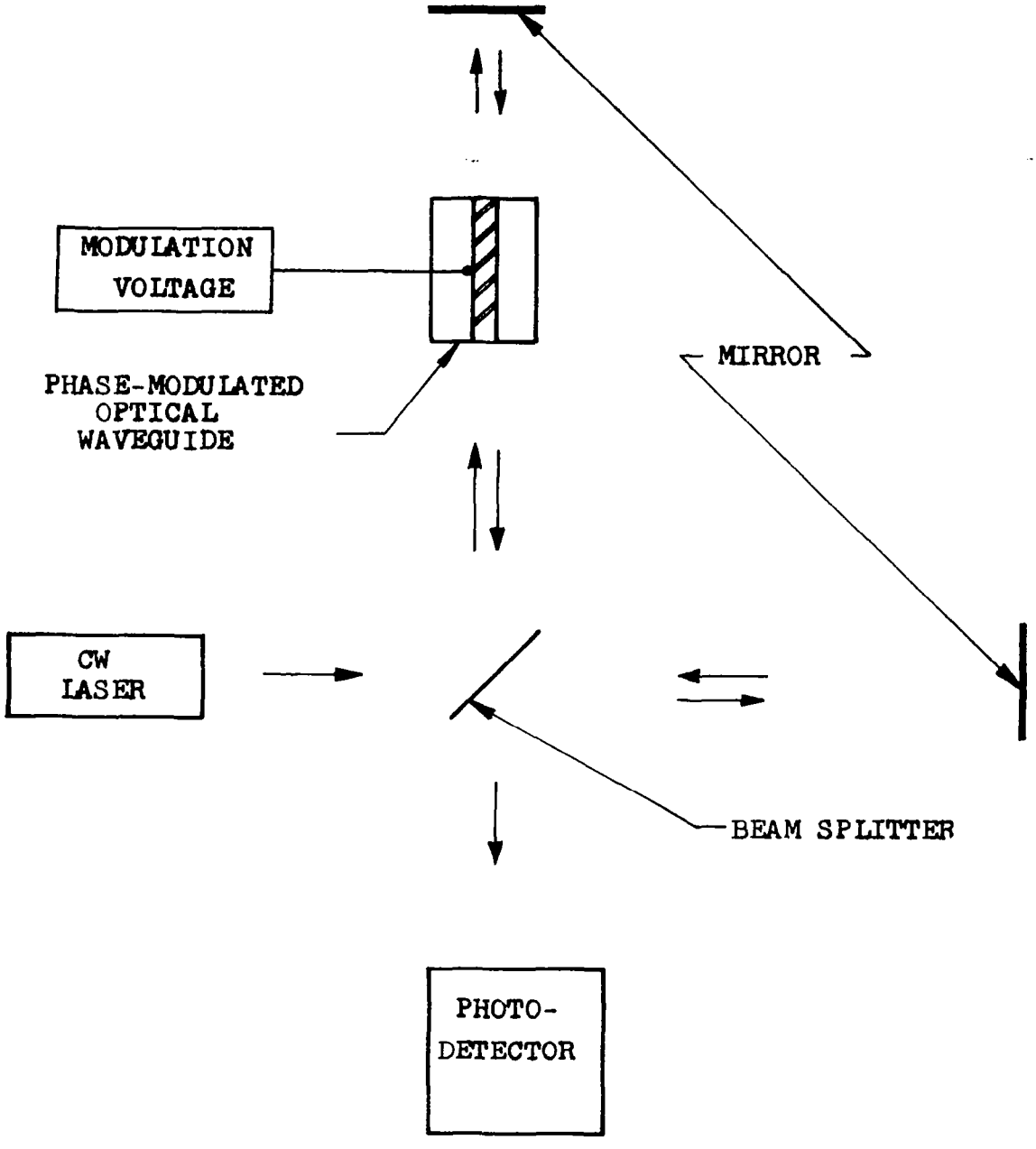

Fig. 20 - Block diagram of phase modulator experiment.

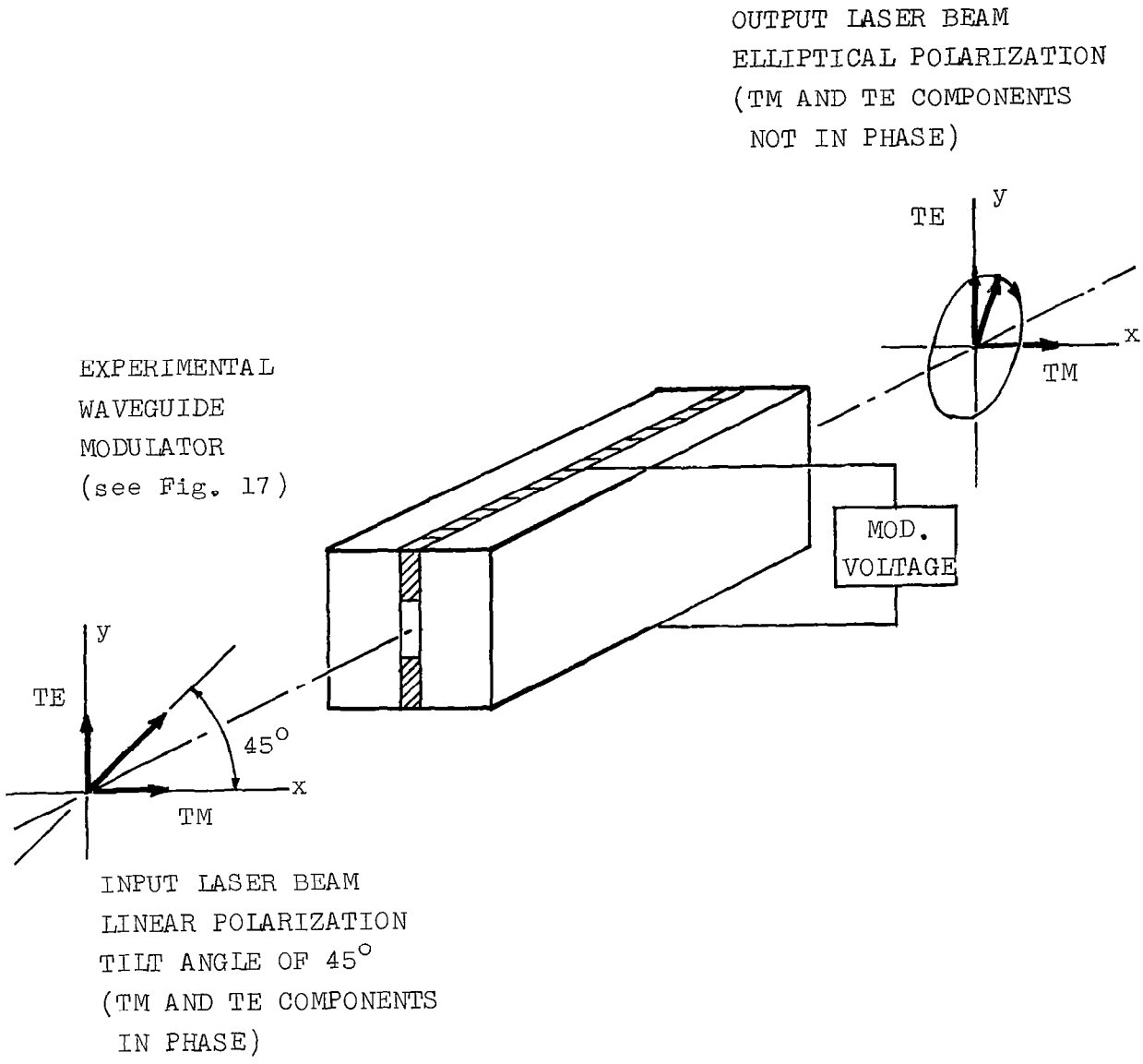

Fig. 21 - Schematic representation of polarization modulator.

dielectric constants. The Kerr effect, which causes the change in dielectric constant, results in different dielectric constants for different polarizations (Ref. 4). For this particular orientation of the electrodes, the difference in dielectric constants for TE modes is twice that for TM modes. This gives rise to a difference in phase velocity between these two cross-polarized modes and polarization modulation occurs in a manner exactly analagous to conventional Kerr-cell modulators (Ref. 1) and shutters (Ref. 4). When the modulator section is coupled directly to free-space, the output, as a function of voltage, will be essentially a plane wave of varying elliptical polarization. The modulation is preserved in subsequent waveguide sections because of the identical propagation characteristics of the TM and TE modes in the conventional waveguide.

Quantitative data on a polarization modulator may be obtained from Fig. 22 where relative phase length is plotted as a function of applied voltage for the modulator configuration of Fig. 17. The polarization of the output, as a function of the applied voltage may be found by using this curve to compute the phase difference between TM and TE modes and then applying the conventional theory of polarized waves (Ref. 2). For single-mode operation, the maximum applied voltage must not exceed the operating point for the next higher mode.

E. Detectors.

Detectors of various types are essential components in every optical system. A large variety of optical detectors are currently available including photomultipliers, bolometers, photodiodes, photoconductors, etc. In general, these devices have square-law responses and are inherently power sensitive relying either on the direct "counting" of photons by various processes such as the photoelectric effect or the indirect determination of optical power by measuring the temperature rise of an absorbing material.

Detection of the power within a waveguide system may be accomplished by placing any of the conventional detectors at the output of the waveguide. This has been the technique used in preliminary experimental work. However, in keeping with the ultimate

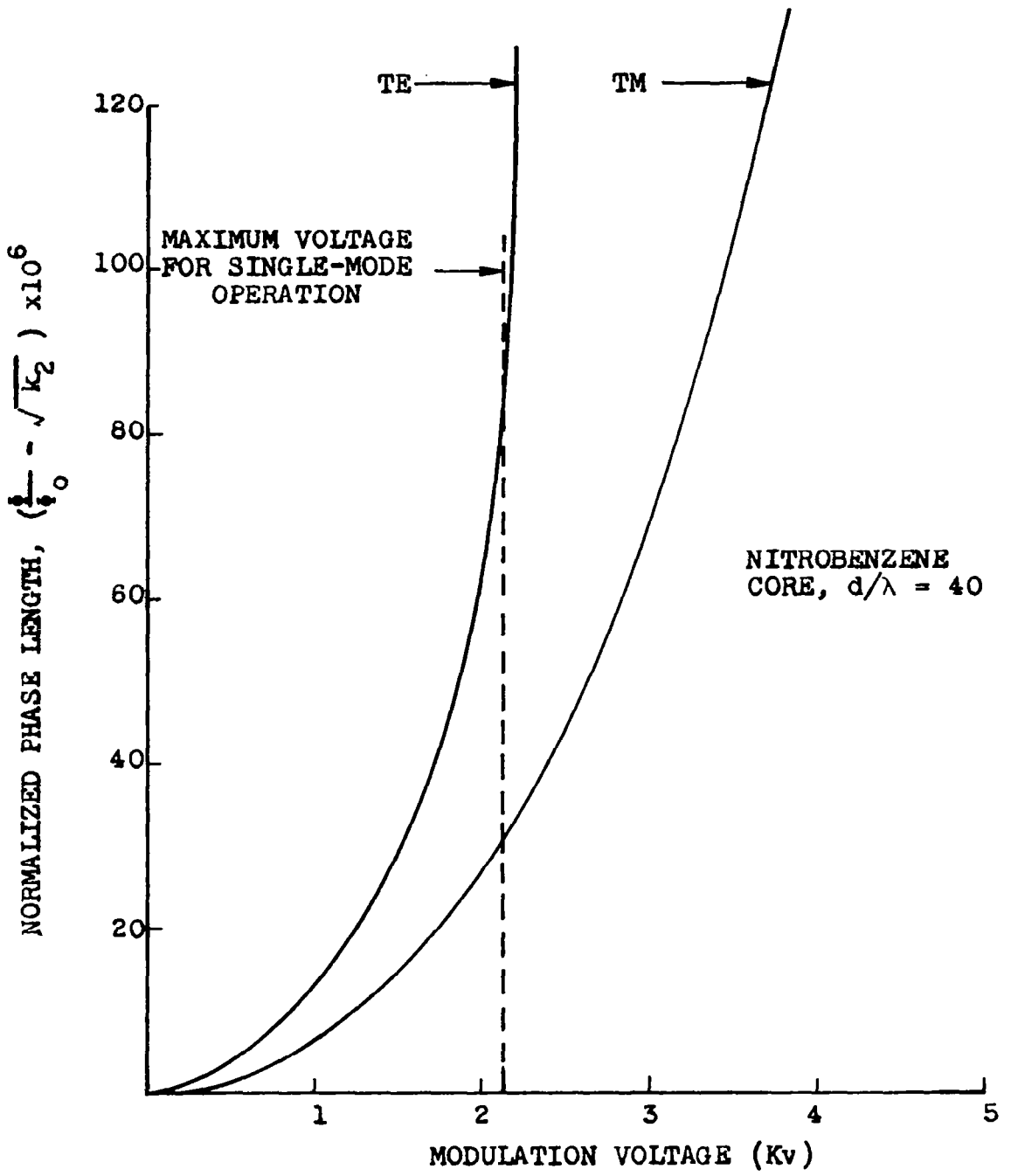

Fig. 22 - Dependence of normalized phase of orthogonal modes on voltage applied to polarization modulator.

objective of a compact, rigid, all-waveguide optical system, it is necessary to consider the fabrication of detectors within the waveguide medium.

In general, the solid-state devices such as photodiodes and photoconductors are more compatible with the waveguide medium than tube-type devices, such as the microwave phototube. The choice between photodiodes and photoconductors must be based on a detailed analysis of their behavior and compatibility with the overall waveguide system. Since such a study has not yet been performed, a definitive choice can not yet be made. However, on the basis of preliminary studies, it does appear that bulk photoconductors (Ref. 32) are particularly adaptable to the waveguide medium. As shown in Fig. 23, the bulk semiconductor can be easily mated with the waveguide.

Even though the design of waveguide detectors is presently in a preliminary stage, it is possible to conclude that such devices can be made and that their performance within a communication system will generally be similar to conventional devices.

During this brief study of waveguide detectors, it has been recognized that a detector comprising a short length of single-mode waveguide containing a photosensitive material has a rather unique optical property. Such a device is sensitive to both amplitude and phase in the transverse plane; i.e., it responds to phase variations in the plane of the waveguide aperture. This property makes the waveguide detector valuable as an optical probe.

Conventional optical detectors, with the exception of optical heterodyne systems, are power-sensitive devices. Such devices respond to the average incident power and are, therefore, insensitive to phase. However, a short length of single-mode waveguide containing a photodetector as shown in Fig. 23 performs the phase-sensitive detection of optical frequencies. Sensitivity of the detectors to phase variations across the aperture is the result of the waveguide reception characteristics. For a single-mode waveguide, Eq. 5 from Appendix A reduces to:

$$P_r \propto \left| \int_{-d/2}^{+d/2} f_i(x)\, f_r(x)\, dx \right|^2 , \qquad (17)$$

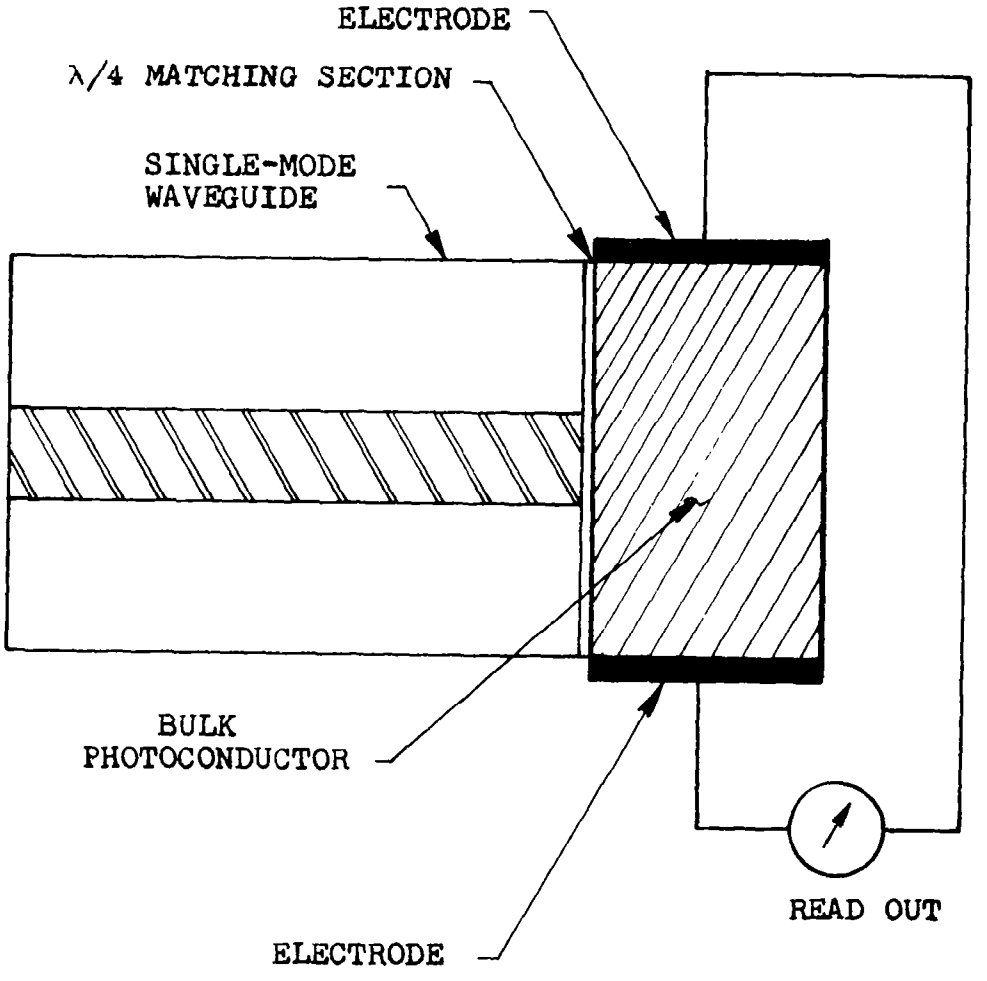

Fig. 23 - Schematic representation of a waveguide detector.

where $f_i(x)$ is the amplitude distribution of the field to be sampled, $f_r(x)$ is the aperture distribution of the waveguide, and P_r is the power coupled into the waveguide. Fig. 24 presents a graphical illustration of this relationship for a typical field distribution to be sampled. Fig. 24(a) shows this distribution to be a typical "probability slope" function (for instance, the second mode from a gas laser); the aperture distribution of a typical single-mode waveguide is shown in Fig. 24(b). The product of these curves is shown in Fig. 24(c). Since the product has odd symmetry about the center of the pattern, it is evident that the integral in Eq. 19 will equal zero and, therefore, the power indicated by the waveguide detector is identically zero. For comparison, a conventional power detector sampling this same pattern would indicate rather than a null some finite value, proportional to its aperture size.

The phase sensitive properties of the waveguide detector make this device particularly suitable as a probe of optical fields for coherence studies (Refs. 20, 29) and antenna scaling (Ref. 25). In a practical measurement it is desirable to have a large aperture in order to receive a large portion of the incident signal and keep the signal-to-noise ratio of the system high. With power-sensitive detectors there must be a design compromise between increasing the aperture size to improve the signal-to-noise ratio and decreasing the aperture size to improve the null resolution; the aperture of the waveguide detector may be increased without degrading null resolution so long as single mode propagation is maintained.

A waveguide detector has been simulated by placing a length of macroscopic optical waveguide in front of a conventional phototube, and a simple experiment has been performed to verify its operation and compare it with the conventional power detectors. In order to simplify the experiment, the phase-sensitive detection was achieved by operating the waveguide in a single mode condition, while for power detection, the same waveguide was operated in a highly multimode fashion. This latter condition is equivalent to no waveguide at all. A diffraction pattern was formed at a plane in space and scanned with both the waveguide and the power detectors. A comparison of the two measurements indicated that for the particular diffraction pattern studied, the measured peak to minimum ratio was 14 db with

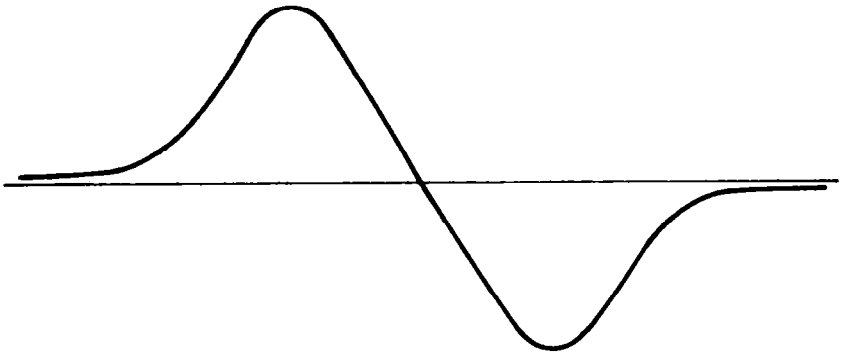

(a) amplitude distribution of field to be sampled, $f_i(x)$.

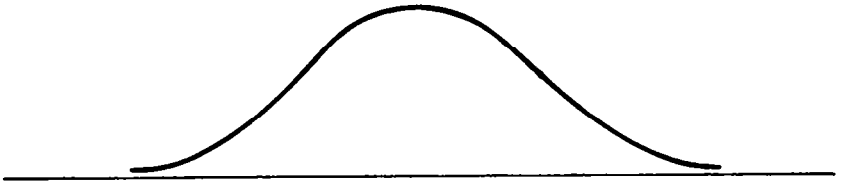

(b) aperture distribution of waveguide, $f_r(x)$.

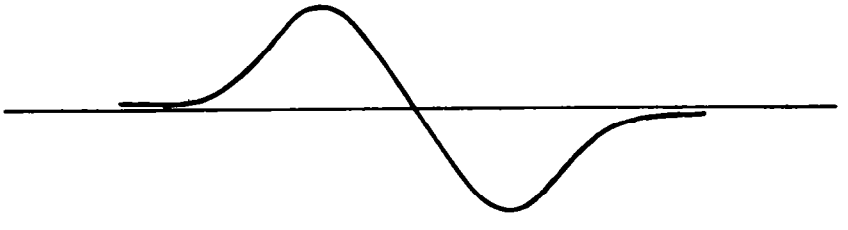

(c) $f_i(x)\ f_r(x)$

Fig. 24 - Waveforms involved in analysis of a waveguide detector.

the power detector and 21 db with the single-mode waveguide detector. The lower minimum signal observed with the waveguide illustrates the increased null resolution of the single-mode device.

V. Fabrication Study.

A study of materials and techniques for fabrication of macroscopic optical waveguides is presented in this section. The objective is to obtain waveguides which are suitable for the construction of various components, and are relatively stable and insensitive to environmental conditions.

The specific requirements for implementing the waveguide are: (1) a core dielectric of the required dimensions and with sufficient optical quality for single-mode operation, surrounded by a cladding dielectric of similar quality; (2) obtaining the required difference of dielectric constants between core and cladding and maintaining it over some range of environmental conditions. Since the environmental factor having the greatest effect on dielectric constant is temperature, an objective has been to utilize materials whose dielectric constant is least sensitive to temperature. In general, the dielectric constants of liquids change much more rapidly with temperature than solids; therefore, the long range objective has been construction of an all solid waveguide.

The investigation has included: (1) a survey of optical materials which are commercially available from various manufacturers; (2) theoretical and experimental evaluations of optical materials; and (3) consultation with specialists in the optical field on special materials and fabrication techniques. The results of this investigation, together with experimental results of tests performed on a number of different waveguide configurations, are presented below.

A. Configurations.

A variety of different types of waveguide have been considered. Sketches of experimental configurations are shown in Fig. 14

of Appendix A; the two basic ones are the slab and circular rod. Each of these may be fabricated with a liquid core and solid cladding or with a solid core and liquid cladding. The solid-core type is considered an intermediate step in the eventual development of a completely solid waveguide; it is more difficult to fabricate than the liquid-core type because high quality optical material is required in a very small size (about 0.05 mm thickness). Experimental testing of each of the configurations is discussed later in this section.

B. Materials.

A survey of various optical materials which may be suitable for the waveguide medium has been conducted. The most essential requirement for the waveguide medium is the optical homogeneity, which refers to the variation of dielectric constant throughout the material. For proper operation, this variation must be less than the difference in dielectric constants by some factor; for typical waveguides, this implies a variation of less than 10^{-5}. The other requirements of the waveguide material are a good optical surface finish and relatively low loss.

The first candidate for the waveguide medium is glass. Glass of sufficiently high optical homogeneity is generally available; however, it is difficult to obtain such glass in small fibers or slabs having cross-sectional dimensions of the order of 0.05 mm. Some sufficiently thin sheets of glass, such as Corning Microsheet, are commercially available; however, these sheets are fabricated by drawing and fire polishing and were determined to have insufficient homogeneity for use as a waveguide. Therefore it is expected that thin slabs will have to be fabricated from high quality glass by grinding and polishing techniques.

Quartz or fused silica is available in a variety of forms and in varying degrees of homogeneity, depending on the manufacturing process. Quartz rod and tubing is manufactured in small diameters by a drawing process. Thin slabs can be fabricated from very high quality quartz by grinding and polishing techniques. Both of these types have been tested and results are presented later in this section.

The many different types of plastics and the variety of forms in which they are available make them a logical choice for the waveguide medium. Most plastics are available in sheets or thin films in thicknesses as required for the waveguide. Many of these plastics have good optical transparency to light passing through a thin sheet or film; however, when light is transmitted through an appreciable length of these same plastics, a large amount of scattering is usually observed. This is caused by scattering centers and inhomogeneities which prohibit use as a waveguide medium. A list of plastics tested and their observed properties is given in Table 1. The only plastic which appears to have sufficient optical homogeneity is methyl methacrylate (lucite, plexiglas). This plastic is not commercially available in thin sheets, but it may be possible to obtain this form by special fabrication techniques.

C. Techniques for Control of Dielectric Constant.

One of the primary problems in fabricating macroscopic optical waveguide is obtaining the required difference of dielectric constants between core and cladding; a typical value is 10^{-4}. Although it is possible to obtain materials whose dielectric constant is homogeneous to an accuracy of 1 part in 10^4 or better, the absolute value of the dielectric constant cannot generally be specified to this accuracy prior to fabrication. Therefore it is not possible to purchase two pieces of glass, for example, whose dielectric constants differ by precisely 10^{-4}.

Consequently it is believed that the approach to obtaining solid materials with the required difference of dielectric constants is to start with two identical materials which were initially fabricated as a single unit, and then change one of the pieces slightly by some separate process. This processing might be used to either change the dielectric constant of one piece relative to the other or to change the dielectric constant of a limited region of a single piece. The latter technique may not result in a discrete interface between regions of different dielectric constant, but rather a gradient between the two. The two cases are illustrated in Fig. 25. The discrete interface corresponds to the configuration which has been studied in detail; the gradient guide has not been studied in detail,

PLASTIC MATERIAL	FORM	OBSERVED PROPERTIES	COMMENTS	APPLICATION
MYLAR	Thin film 0.02 mm to 0.2 mm	Excessive scattering	Films have poor surface quality.	----
LEXAN	Thin film 0.02 mm to 0.2 mm	Excessive scattering	Films have poor surface quality.	----
PLEXIGLAS	Sheet 1 mm to 20 mm	Low scattering; homogeneity specs. good.	Not available in thin sheets.	Completely solid waveguide
LUCITE	Sheet, rod 4 mm to 20 mm	Low scattering	Not available in thin sheets. Lucite resin for coating is available.	Solid-core or completely solid waveguide

Table 1. Summary of optical properties of plastics.

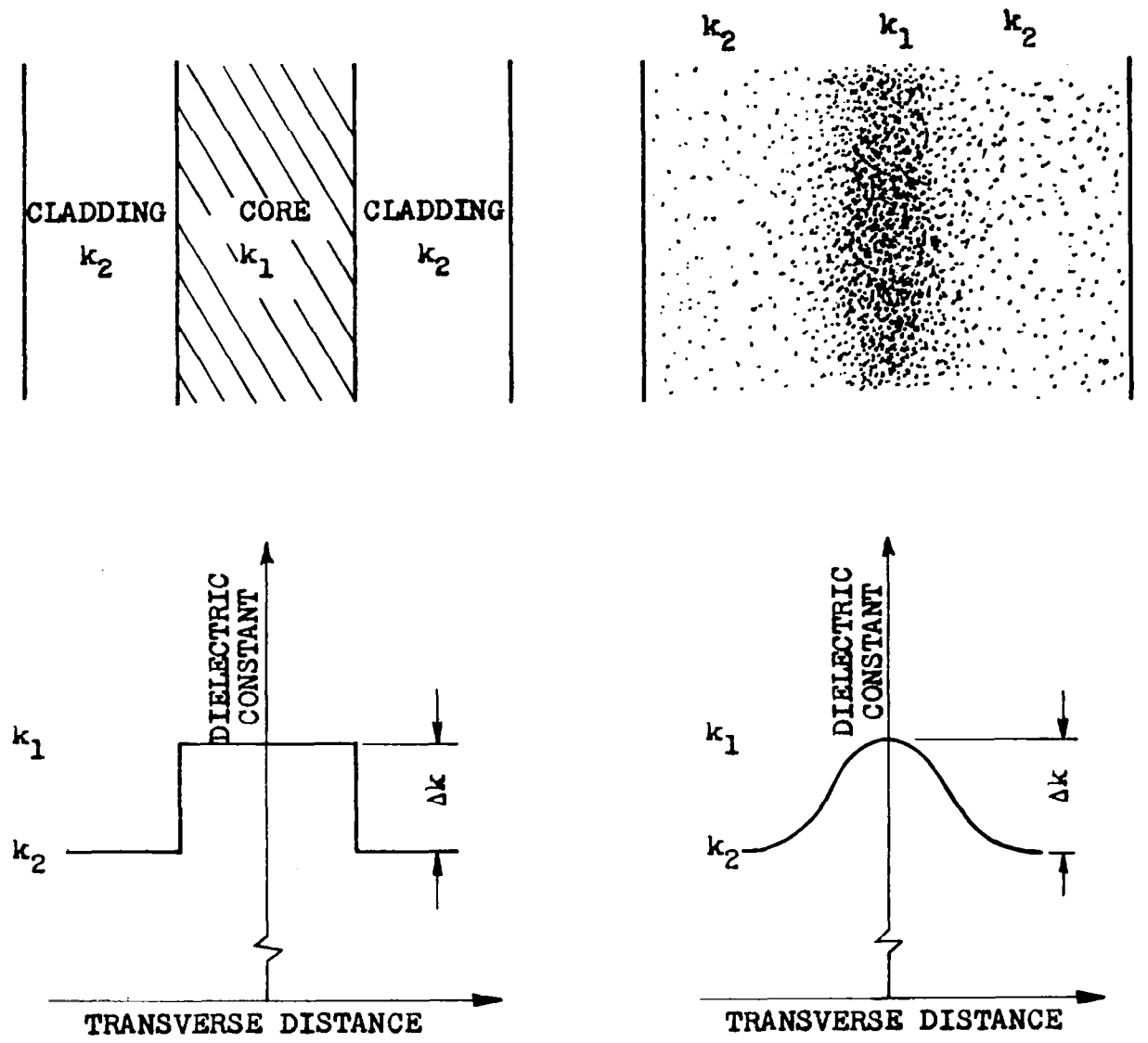

(a) Discrete interfaces

(b) k - gradient

Fig. 25 - Transverse configuration of optical waveguide.

but the propagation characteristics are basically the same as the discrete guide, and either type could be used as a waveguide medium for component construction.

A number of techniques for changing the dielectric constant of an optical medium have been considered. These can be divided into two types: (1) those which permanently change the material so that the effect remains after the processing is completed and (2) those where the dielectric constant is changed only during application of some external "force".

The first category includes techniques for chemically treating the material such as diffusion and leaching (Ref. 31). Only a preliminary investigation of these techniques has been performed; however, first indications show that the magnitude of change which is required is feasible. Another technique for permanently changing a material is radiation processing with either ultraviolet or atomic radiation. This technique appears attractive, but no actual estimates of the magnitude of the effects which can be obtained have been made.

The second category of techniques for controlling dielectric constant includes such phenomena as application of temperature gradients or electric fields to induce gradients of dielectric constant. These techniques are not as attractive as those described above, since the applied force must be continuous to maintain the gradient; however, they can be implemented at the present time. The technique of establishing a gradient by an electric field applied to an electro-optic material (Ref. 19) may be more useful for component fabrication or in specific applications where it is desirable to change the waveguide conditions during operation. This has been done for example in the modulator discussed in Section IV.

D. Experiments.

An experimental evaluation of a variety of different waveguide configurations and materials has been performed. The objective of these tests has been to investigate solid materials for their optical quality and ability to be fabricated in sizes suitable for

a waveguide core. The basic criterion used in evaluating these materials was to test for single-mode waveguide propagation. If a particular waveguide could be made to operate in a single fundamental (TE-0 or TM-0) mode, it was considered useful as a waveguide medium. The individual experiments performed are described briefly in the following paragraphs and results for each type of guide are summarized in Table 2 on page 64.

As a first attempt at operating a solid-core, slab waveguide, commercially available Corning Microsheet Glass slides were tested. A liquid cladding (chlorobenzene) was used so that the difference in dielectric constants could be easily adjusted by temperature control. The glass sheets were about 0.08 mm thick (120λ), fabricated of glass for which no homogeneity specifications were available. The sheets are manufactured by a drawing process and the surfaces then fire-polished. Experiments indicated it was not possible to achieve single-mode operation with these sheets. As the single-mode condition was approached, the sheet was observed to propagate as two separate waveguides near the glass surfaces, as shown by the photograph and pattern in Fig. 26. The effect observed indicates an apparent gradient in the dielectric constant of the glass which is maximum at the outside surfaces; it is believed this is caused by the fire polishing operation. Unfortunately, the gradient is not expected to be uniform or predictable enough to permit use as a dual waveguide.

Since the fire polishing process appears to induce gradients near the surface of a glass sheet, it appeared necessary to employ a grinding and polishing technique to obtain glass plates with the required thickness and optical homogeneity. Although it is difficult to grind and polish plates to a thickness of about 0.06 mm, it was possible to obtain them on special order. A series of such plates were fabricated from fused quartz by Dell Optics Co.; quartz was used because this company has experience in fabricating thin slabs of this material.

The first set of slabs tested were 0.13 mm wide, too thick for single mode operation; the large size (200λ) requires excessively high tolerances on homogeneity. The liquid cladding used with the quartz-core waveguides was Cineole, which has a dielectric constant closely

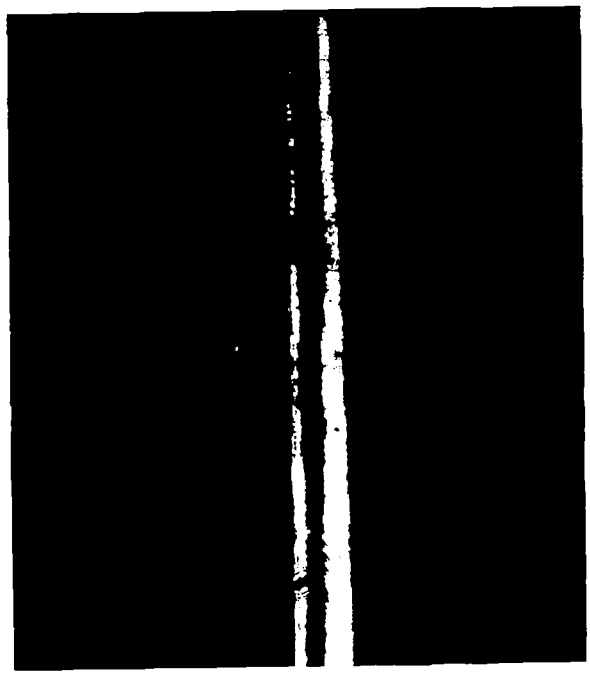

(a) photograph of aperture distribution (through microscope).

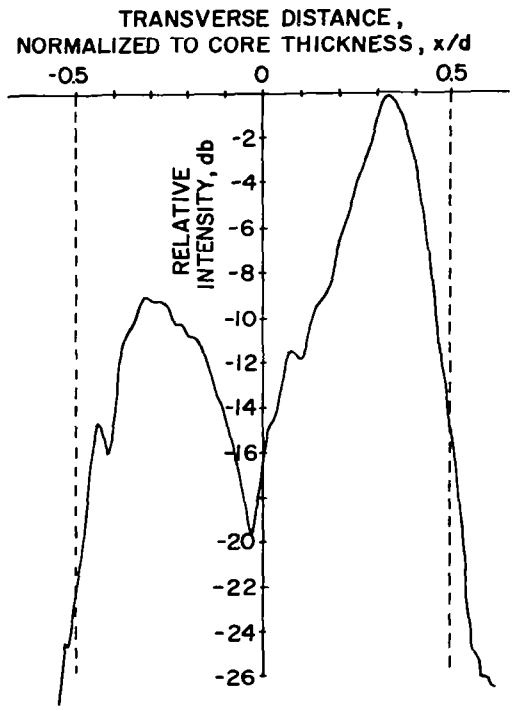

(b) aperture distribution.

Fig. 26 - Measured properties of Corning microsheet slab waveguide.

matching that of the quartz. A photograph of the waveguide aperture distribution and the corresponding field pattern of a high order (TE-3) mode is shown in Fig. 27. A second set of quartz slabs were obtained with a thickness of 0.06 mm. Although it was possible to achieve single-mode operation over limited regions of these slabs, the propagation characteristics were marginal, apparently due to small random inhomogeneities in the quartz.

Another set of slabs fabricated from a quartz with better homogeneity (Ultrasil) was then obtained, and experimental tests indicated good single-mode operation. A photograph of the aperture distribution of the fundamental (TE-0) mode in this waveguide is shown in Fig. 28(a) and the corresponding field pattern is shown in Fig. 28(b). These slabs were considered a successful demonstration of the feasibility of an all solid waveguide.

Waveguides have also been tested in the circular geometry. A liquid-core circular waveguide was fabricated from quartz tubing manufactured by General Electric, filled with the liquid, Cineole. This tubing has an inside diameter of 0.08 mm and outside diameter of 0.13 mm; the homogeneity was not accurately known but was believed to be better than 1 in 10^3. Marginal single-mode operation was achieved with this configuration; better performance was restricted by the tube walls. The outside wall of the tube is located where the field strength still has an appreciable value; therefore, the guide is not a simple circular guide but must be considered as a tubular waveguide. Since it was intended to restrict tests to the simple circular and slab waveguides, no further testing of the quartz tube waveguide was conducted.

A solid-core circular waveguide was fabricated from quartz rod manufactured by General Electric surrounded by Cineole cladding. The rod diameter was 0.08 mm and the homogeneity of the quartz was the same as the tubing described previously. Good multimode operation of this guide was achieved; however, when the difference in dielectric constants was reduced to the value required for single-mode operation, marginal single-mode operation was obtained. Upon further reduction in the difference of dielectric constants to negative values, the guide was observed to propagate as a single-mode guide limited to the center portion of the rod. This operation

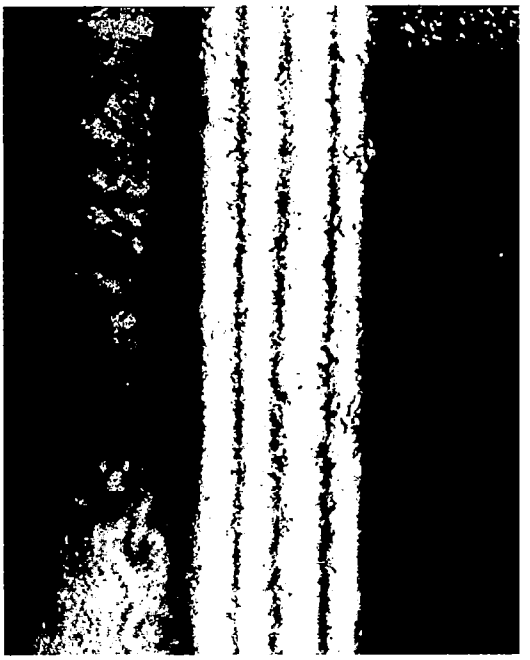

(a) photograph of aperture distribution (through microscope).

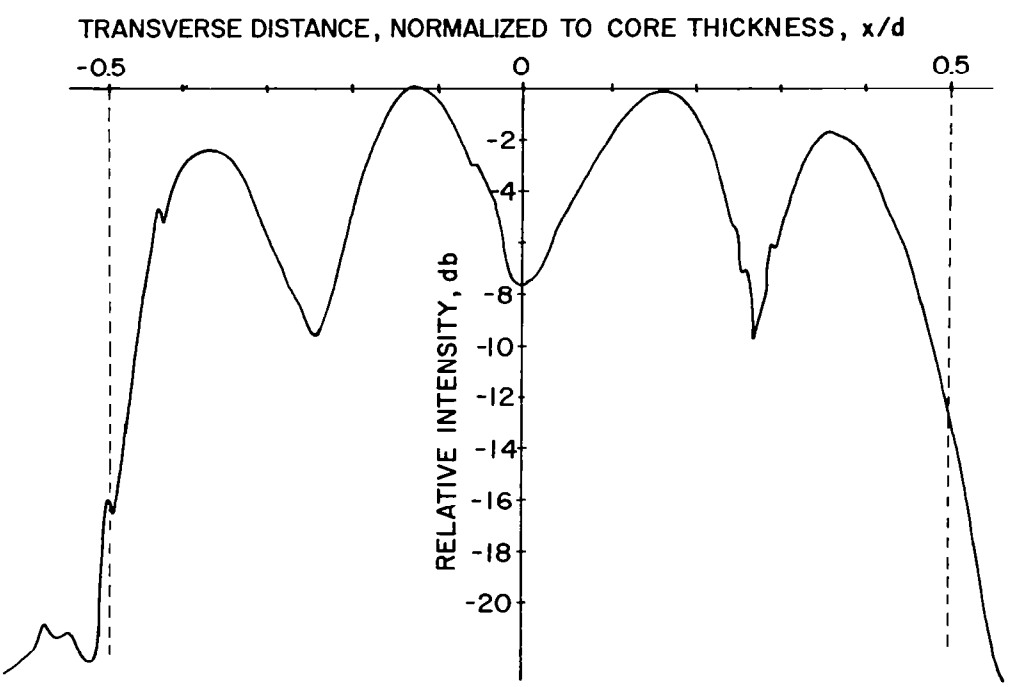

(b) aperture distribution.

Fig. 27 - Measured mode pattern of quartz slab waveguide (TE-03 mode).

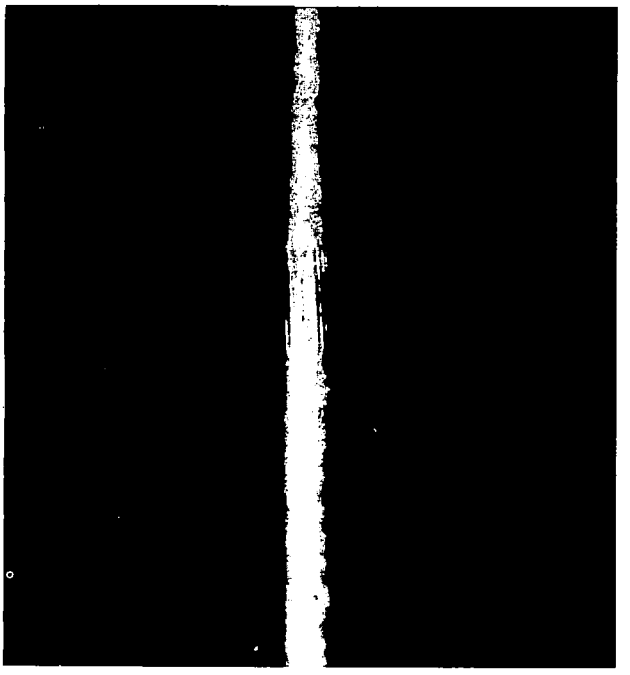

(a) photograph of aperture distribution (through microscope).

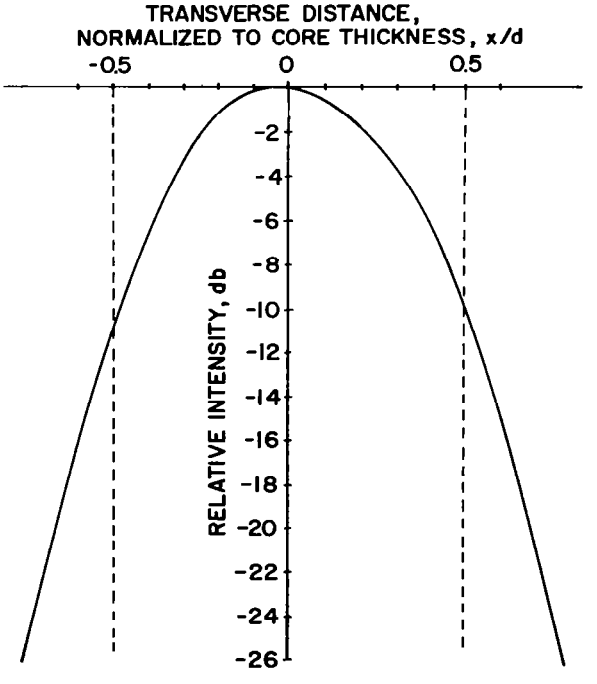

(b) aperture distribution.

Fig. 28 - Measured mode pattern of Ultrasil quartz slab waveguide (TE-0 mode).

is believed caused by a gradient in the dielectric constant in the cross-section of the rod which has a maximum value at the center. (See Fig. 25). Therefore, the rod acts as a natural waveguide without the presence of the outer interface and cladding. Photographs of the aperture distribution and radiation pattern of this guide are shown in Fig. 29(a), (b), and measured patterns are shown in Fig. 29 (c), (d). It can be seen that the radiation pattern is very similar to the aperture distribution, which indicates the pattern approximates a gaussian distribution. (The fringes present on the far-field pattern [Fig. 29(b)] are caused by spurious reflections and are not part of the actual pattern. Note they are absent in the pattern in Fig. 29(d)). Although exact calculations of the field distribution of a gradient guide have not been made (the exact nature of the gradient would have to be known), it would be approximately gaussian; therefore, the explanation agrees with theory. This type of gradient waveguide appears promising for certain applications. However, since the fields are restricted to the center of the rod, it is probably not immediately applicable to any component design which requires coupling to the fields in the cladding region.

A summary of the experimental results for all the different types of waveguide discussed above is presented in Table 2. In conclusion, the experimental evaluation of various waveguides has indicated that solid-core guides can be fabricated in both slab and circular geometries. The best approach for such fabrication is to start with a material having very good homogeneity and obtain the required waveguide dimensions by optical grinding and polishing techniques. The next step in obtaining a completely solid waveguide is to replace the liquid cladding by a solid material. The techniques for adjusting the dielectric constant of the cladding to the required value have not been experimentally evaluated, but preliminary studies indicate that several techniques appear feasible.

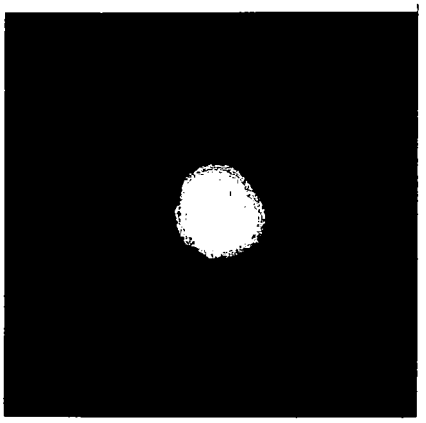

(a) photograph of aperture distribution (through microscope).

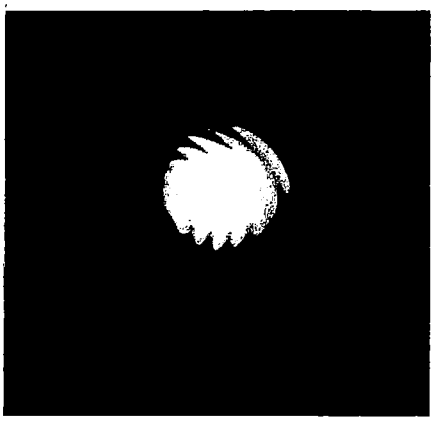

(b) far-field pattern (direct photograph).

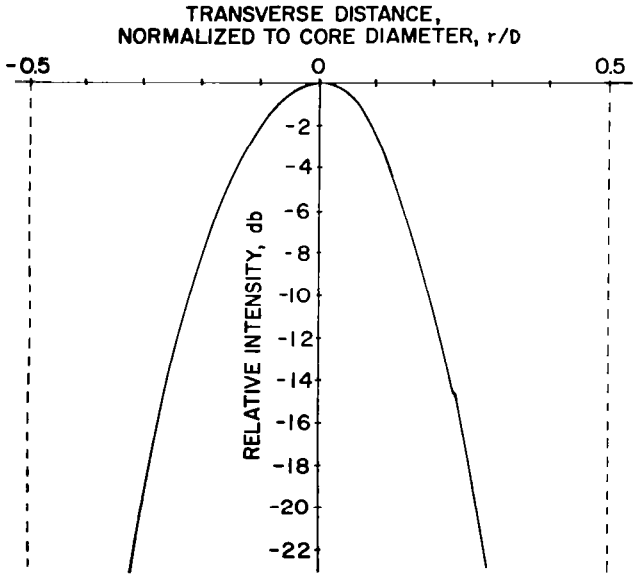

(c) aperture distribution.

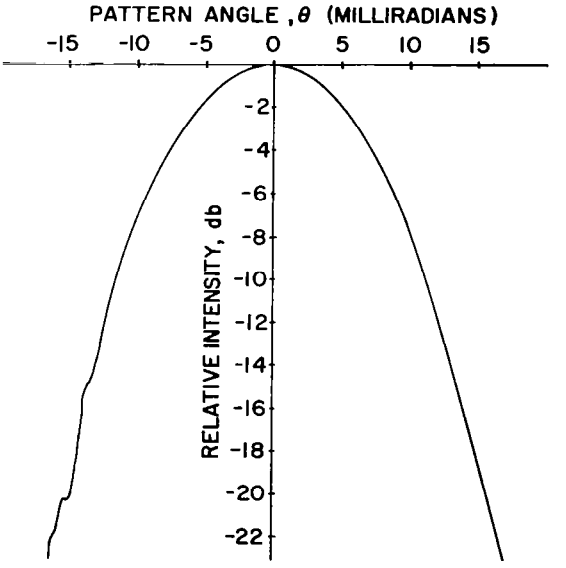

(d) far-field pattern.

Fig. 29 - Measured properties of quartz rod waveguide.

WAVEGUIDE TYPE	MATERIAL	PROPAGATION CHARACTERISTIC	MATERIAL PROPERTY	APPLICATION
SLAB, LIQUID-CORE	Chlorobenzene core, glass cladding	Good single and multimode operation	---	Waveguide studies
SLAB, SOLID-CORE	1)Microsheet glass	Multi-mode only	Poor homogeneity	- - -
	2)Quartz slab(0.13 mm)	Multi-mode only	Excessive size	- - -
	3) Quartz slab(0.06 mm)	Marginal single mode operation	Marginal homogeneity	- - -
	4)Ultrasil quartz (0.06 mm)	Good single and multi-mode operation	- -	General wave-guide components
CIRCULAR, LIQUID-CORE	Quartz tube (GE) 0.08 mm ID; 0.13 mm OD	Complex single and multi-mode operation	Wall thickness too small	None apparent
CIRCULAR SOLID-CORE	Quartz rod (GE) 0.08 mm dia.	Controlled multi-mode; fixed single mode	Gradient in dielectric constant	Specific waveguide components

Table 2. Summary of experimental waveguide configurations.

VI. Conclusions and Recommendations.

The results of a study for the development of single-mode optical waveguide and waveguide components are presented in this report. The theory of operation of this waveguide has been developed and the feasibility of constructing experimental models which operate according to the theory has been demonstrated. An analysis of optical components constructed in waveguide has shown that this concept provides significant advantages in performance over similar components operating in a free-space medium.

In the analysis of propagation in optical dielectric waveguides, various propagation characteristics have been calculated in detail for the macroscopic case. The requirements for maintaining single-mode propagation with large size have been calculated; the basic condition is that as the waveguide size is increased, the difference in dielectric constants between core and cladding must be decreased. A convenient means for representing these relationships on a mode chart has been developed. This chart indicates the number of modes which will propagate in a waveguide of any size and difference in dielectric constant. The distribution of fields within the waveguide has been calculated in general form, and specific results plotted for a few low-order modes at typical operating conditions. The field patterns have been measured experimentally using a liquid-core slab waveguide, and results are in good agreement with the calculated curves. The variation of propagation constant with frequency (dispersion) has been calculated for the slab waveguide. These dispersion curves have been utilized in the theoretical analysis of several components.

Theoretical evaluation and experimental testing of a bisected waveguide, with a metal wall as one of the reflecting surfaces has been made. Both theory and experiment show that the metal (aluminum) wall acts as a lossy dielectric at optical frequencies rather than as an ideal metal. A significant consequence of this fact is that the propagation characteristics of both polarizations (and hence both TM and TE modes) are identical.

A theoretical and experimental investigation of waveguide excitation has been performed using conventional antenna theory. For

plane wave excitation, the angle of incident radiation determines the particular mode which is excited (in a multi-mode guide); this behavior has been experimentally verified. For a focused input signal, the direction of radiation again determines primarily the mode which is excited, and the size and lateral position of the focused spot determine the efficiency of excitation. For maximum efficiency, the pattern of the focused fields should match the pattern of the mode to be excited.

The theory and experiments described above have shown sufficiently good agreement to verify that macroscopic optical waveguides can be fabricated in laboratory configurations which operate as the theory predicts.

A design and performance analaysis of various components constructed within the waveguide medium has been performed and experimental testing of some of these components has been made. The components which have received the greatest consideration are directional couplers, bends, filters, modulators and detectors.

In the study of waveguide directional couplers, an analysis of several configurations has been performed. The basic design problem is to relate the amount of coupling to the waveguide parameters. For a slot coupler consisting of two bisected waveguides separated by a thin metal wall with a slot, half-power coupling is obtained with a slot length of the order of one centimeter. For an evanescent-field coupler consisting of two waveguides separated by a distance of the order of one core width, half-power coupling is obtained for a coupling length of a few centimeters. Both types of couplers give practical sizes for construction.

In the study of bends, the maximum amount of curvature for which a guide will propagate with low attenuation has been determined. The basic relationship is that as the difference in dielectric constants is decreased, the radius of curvature of the bend must be increased. For a typical waveguide, the minimum radius is about 3 meters. Consequently, small amounts of bending such as are required for certain components are feasible by simply curving the waveguide; sharper bends will require a metal reflecting surface fabricated into the waveguide. Experimental testing of waveguide bends has indicated the same functional relationship between radius of curvature and

difference of dielectric constants as the theory; however, the amount of bending which could be obtained in these experiments was less than the theory predicted.

The properties of resonators or interference filters (such as Fabry-Perot) fabricated within the waveguide medium have been analyzed. Such resonators are useful as frequency filters and in the construction of laser oscillators. Construction in the waveguide provides a significant advantage over the free-space filters in that the interdependence between the angular and frequency responses (and hence ambiguity between spatial and frequency filtering) inherent in the free-space type is removed. The frequency characteristic of the waveguide filter is equal to that of the free-space filter operated at a fixed angle of incidence; the angular characteristic is determined by the radiation pattern of the waveguide. Therefore the frequency and angular characteristics can be independently controlled. The behavior described above has been experimentally verified by operating a free-space Fabry-Perot filter in tandem with a single-mode waveguide.

A number of different types of waveguide modulators utilizing the electro-optic and magneto-optic effects have been considered. In general, any of the common types of free-space modulators can be operated in the waveguide medium. In many cases, the volume of the modulating region can be made smaller in the waveguide case, and thus reduce the required modulator power or increase the modulation bandwidth. In addition to the usual techniques for obtaining amplitude, polarization, frequency and phase modulation, a type of pulse-amplitude modulation has been developed which is inherently dependent on the waveguide medium. This modulator operates by electro-optically switching the waveguide from a propagating to a non-propagating condition. This type of modulator has the characteristic that the degree of modulation is essentially dependent on the length of the modulator as opposed to the amount of the modulation voltage; this permits close to 100% modulation with very low voltages.

Construction of common optical detectors within the waveguide medium has been investigated briefly. The waveguide medium provides increased compactness and stability in many cases. A significant difference between detectors constructed in the waveguide and in free space, is that whereas conventional optical detectors are

sensitive to only the average power in a signal, the waveguide detector is sensitive to the transverse distribution of amplitude and phase. This sensitivity to the spatial phase of a signal increases the accuracy of certain specialized measurements such as the depth and location of minima in an interference pattern.

In concluding the analysis of waveguide components, it is expected that most conventional optical components can be constructed in the waveguide medium. In some cases, the performance is equivalent to that obtained in free-space types and in other cases the waveguide components have fundamental advantages which result directly from the waveguide medium.

In order to develop waveguides which are adaptable to component construction and practical for actual application in laser systems, a study of waveguide fabrication has been performed. The basic problem in fabrication is that of obtaining the small difference of dielectric constants between core and cladding with a core of the required size. The investigation of materials and techniques has been directed to the eventual development of an all-solid waveguide.

Preliminary to the development of the all-solid waveguide, a number of solid materials have been tested as waveguide cores. Solid-core guides have been successfully operated in both the circular and slab configurations. Apparently, the most promising fabrication technique is to grind and polish high quality glass or quartz to the required size. Polished glass or quartz slabs with a thickness of 0.06 mm are difficult to fabricate, but have been obtained on special order.

The final step to achieve a completely solid waveguide is to replace the liquid cladding by a solid material. It is not expected that solid materials can be fabricated with the dielectric constant pre-specified to the necessary degree of precision. Therefore, the cladding material will presumably be made by starting with material identical to the core and then changing the dielectric constant slightly. Techniques for doing this, such as chemical diffusion and leaching, and radiation processing appear feasible. It is believed the eventual development of a completely solid macroscopic optical waveguide is feasible and its development will proceed using the techniques described.

On the basis of the study program presented in this report, it is recommended that the development of macroscopic optical waveguide and waveguide components be continued. In particular, effort is recommended, as follows.

In order to construct operating waveguides which are relatively insensitive to environmental conditions, it is believed that completely solid waveguides are required. Therefore, it is recommended that the study of materials and fabrication techniques for development of solid waveguides and the study of techniques for control of dielectric constant be continued.

The analysis of waveguide components has indicated that in some cases significant advantages can be obtained by utilization of the waveguide medium. Therefore, further development of the components already studied including fabrication and experimental evaluation, as well as an investigation of additional conventional or non-conventional optical components is recommended.

In addition to the specific areas of study, it is recommended that the application of macroscopic waveguide and waveguide components to laser systems be studied.

VII. Acknowledgements.

The work described in this report has been performed during the period of 1964 JAN 28 to 1964 NOV 28 for the National Aeronautics and Space Administration under contract NASw 888. General direction has been provided by Roland Chase of Headquarters, Office of Advanced Research and Technology, Washington, D. C. In October 1964 the contract direction was transferred to Dr. M. H. Nagel of the Electronics Research Center, Cambridge, Mass.

The work at Wheeler Laboratories has been performed by E. Ronald Schineller, Donald W. Wilmot, and Herman M. Heinemann under the direct supervision of Henry W. Redlien. Advice and general direction have been provided by Harold A. Wheeler, Frank H. Williams and Henry L. Bachman.

VIII. References.

The following references are listed in chronological order and numbered consecutively starting at number (1). It is to be noted that an additional list is included in Appendix A also starting with the number (1). The references in the report and appendix each apply to their own reference section, unless otherwise indicated.

(1) A. M. Zarem, F. R. Marshall and F. L. Poole, "An Electro-Optic Shutter for Photographic Purposes", Trans. of AIEE, vol. 68; 1949.

(2) H. G. Booker, V. H. Rumsey, G. A. Deschamps, M. L. Kales, J. I. Bohnert, "Techniques for Handling Elliptically Polarized Waves," Proc. IRE, vol. 39, p. 533; May 1951.

(3) H. M. Barlow and A. L. Cullen, "Surface Waves", Proc. IEE, vol. 100, part III, p. 329; 1953.

(4) R. W. Ditchburn, "Light", Interscience Publishers, New York, p. 528; 1953.

(5) S. E. Miller "Coupled Wave Theory and Waveguide Applications", BSTJ, vol. 33, p. 661; May 1954.

(6) D. D. King, "Properties of Dielectric Image Lines", IRE Trans. on Microwave Theory and Techniques, vol. MTT-3, no. 2, p. 75; March 1955.

(7) J. S. Cook, "Tapered Velocity Couplers", BSTJ, vol. 34, no. 4, p. 807; July 1955.

(8) A. G. Fox, "Wave Coupling by Warped Normal Modes", BSTJ, vol. 34, no. 4, p. 807; July 1955.

(9) W. H. Louisell, "Analysis of the Single Tapered Mode Coupler", BSTJ, vol. 34, no. 4, p. 853; July 1955.

(10) M. Newstein and N. Solimene, "Analysis of Laser Modulation Techniques", Technical Research Group, Report ASD-TDR-62-9; June 1962, ASTIA AD 283 462.

(11) D. W. Wilmot, "Macroscopic Optical Waveguide", Wheeler Labs. Report 1100.2; Oct. 1962.

(12) V. R. Bird, D. R. Carpenter, P. S. McDermott, and R. L. Powell, "Rectangular Optical Dielectric Waveguides as Lasers", paper from "Lasers and Applications", edited by W. S. C. Chang, Eng. Exp. Sta., Ohio State, Columbus, p. 147; Nov. 7-8, 1962.

(13) C. G. Montgomery, R. H. Dicke and E. M. Purcell, "Principles of Microwave Circuits", Boston Tech. Lithographers; 1963. (Rad. Labs. Series, vol. 9, McGraw-Hill; 1948 p. 299).

(14) W. W. Rigrod and I. P. Kominow, "Wideband Microwave Light Modulation", Proc. IEEE, vol. 51, no. 1, p. 137-140; Jan. 1963.

(15) C. J. Peters, "Gigacycle Bandwidth Coherent Light Traveling Wave Phase Modulator", Proc. IEEE, vol. 51, no. 1, p. 147-153; Jan. 1963.

(16) D. W. Wilmot and R. A. Kaplan, "Concepts of Optical Waveguide Components", Wheeler Labs. Report 1112; March 1963.

(17) D. W. Wilmot and R. A. Kaplan, "Development of Macroscopic Waveguide Components for Optical Systems", Wheeler Labs. Report 1139; April 1963.

(18) R. A. Kaplan, "Optical Waveguide of Macroscopic Dimensions in Single-Mode Operation", Proc. IEEE, vol. 51, no. 8; Aug. 1963.

(19) R. W. Hermansen, "Experimental Evaluation of Macroscopic Optical Waveguide", Wheeler Labs. Report 1172; Sept. 1963.

(20) M. J. Beran and G. B. Parrent, "Theory of Partial Coherence", Prentice Hall; 1964.

(21) E. Snitzer, "Neodymium Glass Laser", paper from "Quantum Mechanics", vol. 2, Col. Univ. Press, p. 999; 1964.

(22) R. C. Hansen, "Microwave Scanning Antennas, vol. I, Apertures", Academic Press, New York; 1964, p. 179.

(23) J. Kane and H. Osterburg, "Optical Characteristics of Planar Guided Modes", JOSA, vol. 54, no. 3, p. 347; March 1964.

(24) D. W. Wilmot, "Macroscopic Optical Waveguide for Constructing Optical Components", Paper presented at 1964 International Symposium of the Professional Group on Microwave Theory and Techniques; May 1964.

(25) D. Dutton, M. P. Givens, R. E. Hopkins, "Some Demonstration Experiments in Optics Using a Gas Laser", Am. Jour. of Physics; May 1964.

(26) E. R. Schineller, D. W. Wilmot and H. M. Heinemann, "A Macroscopic Waveguide Medium for Laser System Components", Wheeler Labs. Report 1209 to NASA; June 1964.

(27) H. Osterberg and L. W. Smith, "Transmission of Optical Energy Along Surface: Part I Homogeneous Media", p. 1073; "Part II Inhomogeneous Media", p. 1078, JOSA, vol. 54, no. 9; Sept. 1964.

(28) R. Y. Chiao, E. Garmire, C. H. Townes, "Self-Trapping of Optical Beams", Phy. Rev. Letters, vol. 13, p. 479; Oct. 12, 1964.

(29) H. M. Heinemann and H. W. Redlien, "The Observation of Mode Impurity in Gas Lasers Apparently Resonating in the TEM-00 Mode", Wheeler Labs. Report 1253P; Oct. 1964. (To be published as a correspondence in the Proc. IEEE).

(30) E. R. Schineller and H. W. Redlien, "Development of Macroscopic Optical Waveguide Components - Progress", Tech. Letters from Wheeler Labs. to National Aeronautics and Space Administration, Nos. 1 to 8; prepared to cover each month from Feb. 1964 to Oct. 1964.

(31) L. Holland, "The Properties of Glass Surfaces", John Wiley, 1964.

(32) M. DiDomenico, O. Svelto, "Solid State Photodetection: A Comparison between Photodiodes and Photodetection", Proc. IEEE, vol. 52, no. 2, p. 136; Feb. 1964.

Appendix A of NASA CR-332

A MACROSCOPIC WAVEGUIDE MEDIUM FOR LASER SYSTEM COMPONENTS

By E. R. Schineller, D. W. Wilmot
and H. M. Heinemann

To National Aeronautics and
Space Administration
Contract Number NASw 888

1964 JUN 10 Job 466

This report has been previously submitted to the National Aeronautics and Space Administration as Wheeler Laboratories' Report 1209. Subsequently typographical errors have been corrected and technical changes have been made on pages 7A and 25A; this revised report was designated as Report 1209A, and is included as an appendix of the Final Report, NASA CR-332. The page numbers of the appendix are suffixed with an "A" to differentiate them from the body of the final report.

Summary

Many applications in the fields of radar, communications, measurements, etc. have been proposed for coherent laser radiation. One approach to the design of systems for these applications is the utilization of conventional optical components; an alternative approach, which is being studied at Wheeler Laboratories, is the development of new optical components patterned after microwave devices. The initial step in the design of microwave-analagous components is the development of a single-mode optical waveguide large enough to permit component fabrication. Single-mode operation is required to prevent signal distortion due to modal dispersion.

A dielectric waveguide for this purpose has been studied and its feasibility has been demonstrated at optical frequencies. The waveguide dimensions are macroscopic in the sense that they are visible to the naked eye. It has been shown that a single-mode waveguide may be as large as 100 wavelengths with stringent but feasible tolerances on dielectric constant and surface quality. Single-mode and controlled multimode operation have been correlated with theory. In addition, a survey of materials and fabrication techniques has been made. One possible approach utilizes chemical diffusion techniques to obtain the needed control of dielectric constant.

Contents

List of Figures

Contents (continued)

List of Figures — Page

Contents (continued)

List of Figures — Page

I. Introduction.

A laser system is generally composed of a laser oscillator and a collection of conventional optical components, such as lenses, prisms, beam splitters, etc. It has been recognized at Wheeler Laboratories that there is an alternate approach to the design of such systems. This approach is based on the realization that many of the proposed laser applications, particularly in the fields of communication and tracking, are analagous to currently existing microwave systems. This realization suggests the possibility of utilizing microwave-type components in the optical frequency range. Under the sponsorship of the National Aeronautics and Space Administration, Wheeler Laboratories is currently studying the feasibility of such an approach. This study involves (1) the development of a waveguide medium in which microwave-type components may be fabricated, (2) an evaluation of various component configurations, and (3) the fabrication of one or more microwave-type components to demonstrate the feasibility of this approach. This report covers the first phase of the study concerned with the development of the waveguide medium; a final report covering the development of components will be prepared upon completion of this study.

Microwave components are generally designed within a single-mode or controlled multimode medium. This approach has definite advantages over the unbounded character of conventional optical components. For instance, the power within a single-mode medium is constrained to propagate at only one set of angles determined by the waveguide dimensions and the frequency of the signal. Therefore, variations in the angle of incidence of the radiation at the input to the system affect only the excitation efficiency and not the character of the propagating mode. In an unbounded medium there is no such angular restriction and a variation in the angle of incidence at the system input many result in a variation of the properties of each individual component. An additional advantage of single-mode operation is that signal distortion caused by modal dispersion is prevented. In general, microwave components have well-defined phase characteristics. They are also angle insensitive and inherently more compact and stable than conventional optical components.

In order to duplicate the properties of microwave components the optical waveguide medium should operate in a single-mode or controlled multimode condition. It should also be macroscopic in size for ease of handling, feasibility of component fabrication and high-power capability. Waveguide operation at optical frequencies has been demonstrated in dielectric fibers (Refs. 13 and 16). However, conventional dielectric fibers with diameters of the order of 100 wavelengths are known to support many propagating modes. In cases where single mode operation was observed, it was necessary to reduce fiber diameters to the order of one wavelength.

Dielectric waveguide consists of a core material of high dielectric constant embedded in a cladding material with a lower dielectric constant. It may be shown that the maximum cross-sectional dimension for single-mode operation is inversely proportional to the square root of the difference between the dielectric constants of the core and cladding. This principle has been employed to obtain single-mode operation with cross-sectional dimensions exceeding 100 wavelengths. This waveguide exhibits an attenuation of several db/meter which makes it suitable for lengths of a few centimeters containing several components. The design and fabrication of such a waveguide is the topic of this Report.

The theoretical and experimental steps involved in the waveguide development are outlined herein. Section III presents the theory of optical dielectric waveguide and pertinent design data. Material considerations and fabrication techniques are summarized in Section IV. The experimental evaluation of the waveguide is outlined in Section V and results are reviewed in Section VI. The appendix contains an illustration of the theory of transverse resonance — a commonly used microwave technique which has proved invaluable in this study.

II. Symbols and Definitions.

x, y, z = rectangular coordinates. z is direction of propagation; x, y are transverse dimensions.

r = radial dimension of circular waveguide.

d = total width of core of slab waveguide.

D = diameter of core of circular waveguide.

Da = diameter of waveguide field.

W = total width of waveguide field.

W_i = width of focused incident field at half-amplitude points.

W_r = width of waveguide field at half-amplitude points.

A = area of waveguide field.

h = height of waveguide in y direction.

R = region of integration at waveguide aperture.

a = parameter indicative of width of gaussian curve.

P_r = total power received in waveguide.

P_i = total power incident on waveguide.

f_i = amplitude function of field incident on waveguide.

f_r = amplitude function of waveguide field.

ρ = power density of wave incident on waveguide.

η_a = aperture efficiency = ratio of power incident on aperture to that received.

θ = angle of plane wave in waveguide.

θ_c = critical angle for total internal reflection.

φ_o = angle of incident radiation in air.

φ = angle of incident radiation in waveguide medium.

k = dielectric constant.

k_1 = dielectric constant in core.

k_2 = dielectric constant in cladding.

Δk = $k_1 - k_2$.

ϵ_o = permittivity of free space.

λ = wavelength in free space.

λ_g = wavelength in waveguide.

K_o = free space propagation constant $(2\pi/\lambda)$.

K_z = longitudinal propagation constant $(2\pi/\lambda_g)$.

K_1 = transverse propagation constant in core.

K_2 = transverse propagation constant in cladding.

p = propagation parameter in core $(K_1 d/2)$.

q = propagation parameter in cladding ($|K_2|d/2$).
Z = impedance.
Z_1 = transverse wave impedance in core.
Z_2 = transverse wave impedance in cladding.
Z_z = longitudinal wave impedance.
A_m = amplitude factor which determines absolute field strength.
n = integer.
m = mode number.
μ_{mn} = solutions of $J_n(\mu_{mn}) = 0$.
N = density of molecules.
α = polarizability.
e = charge on electron.
M = mass of electron.
f_s = oscillator strength.
ω_s = resonant frequency.
γ_s = damping term of quantum transition.

III. Optical Dielectric Waveguide Theory.

The theory of operation of dielectric waveguides is well-established and has received considerable treatment in the literature. Such waveguides have been treated for the microwave region in Refs. 11, 14, where the waveguide dimensions are generally of the order of a wavelength and the ratio of dielectric constants of the inner and outer regions is two or three to one. These microwave guides are usually constrained to a single mode of propagation.

Dielectric waveguides suitable for operation at optical frequencies have been treated in Refs. 5, 13, 16, 17. In some of these cases the difference in relative dielectric constants (Δk) between the inner (core) and outer (cladding) regions is large, and the waveguide size is many wavelengths, as is the case for many dielectric fibers employed in fiber optics applications. Therefore, these guides are highly multimode and the characteristics can generally be determined by a geometric optics analysis (Ref. 13). In other cases, the Δk has been reduced to about 0.01 by using a glass cladding with dielectric constant close to that of the glass core. However, even though the Δk is small, these waveguides still operate multimode unless the guide size is reduced to about one wavelength (Ref. 16).

The optical waveguide discussed in this report has dimensions large with respect to the wavelength, but operates with a very small Δk (0.0001). Under these conditions the guide can be constrained to operate in only a single mode or a few controlled low order modes, thus combining the advantages of large size with single mode propagation.

In the first part of this Section the properties of dielectric waveguide modes are discussed and a few of the structures capable of propagating such modes at optical frequencies are indicated. Then the conditions for obtaining single mode propagation with structures having large (macroscopic) dimensions are indicated. Various propagation characteristics of this "macroscopic" single mode guide are presented and finally the excitation and radiation properties of the guide are discussed.

In the more familiar case of metal waveguides, such as those used at microwave frequencies, the wave is guided along the structure by multiple reflections at the metal boundaries. For dielectric guides, the wave may also be guided by multiple reflections from the dielectric interfaces by the process of total internal reflection. The particular configuration of the guide may take on many forms; the primary requirement is that the dielectric constant of the inner medium (core) be greater than the outer medium (cladding), so that total internal reflection may occur. Two common configurations of dielectric waveguides are shown in Fig. 1. The slab configuration (Fig. 1(a)) is an unbounded structure on two sides and hence is limited to controlled-mode propagation in only one transverse direction. However it is very useful experimentally because of its simplicity, both of analysis and of construction. The dielectric rod waveguide shown in Fig. 1(b) is limited to controlled mode propagation in both transverse planes and hence can be true single mode.

A simple concept of propagation along these structures can be obtained by considering rays reflecting back and forth along the guide, as illustrated in Fig. 2, for the slab configuration. The propagating modes correspond to rays which are totally reflected at the dielectric interfaces and therefore travel down the guide without loss, as in Fig. 2(a). Only certain discrete angles of propagation are permitted, corresponding to angles which satisfy all the field conditions at the boundaries of the structure. The waveguide parameters can be chosen so that only one such angle will propagate; this is a single (fundamental) mode guide. In a single mode transmission medium, energy may propagate with only one stable field configuration. This means the field patterns in any cross-sectional plane of the transmission line are identical in shape. In guides capable of supporting a few modes, there are a few different field configurations which also may satisfy the conditions for propagation.

There is another class of modes called "leaky" modes which correspond to rays which are incident on the dielectric interfaces at an angle of incidence less than the critical angle and hence are not totally reflected. In this case, illustrated in Fig. 2(b), the energy traveling down the guide is strongly attenuated because power is lost at each reflection. The angles of propagation permitted in

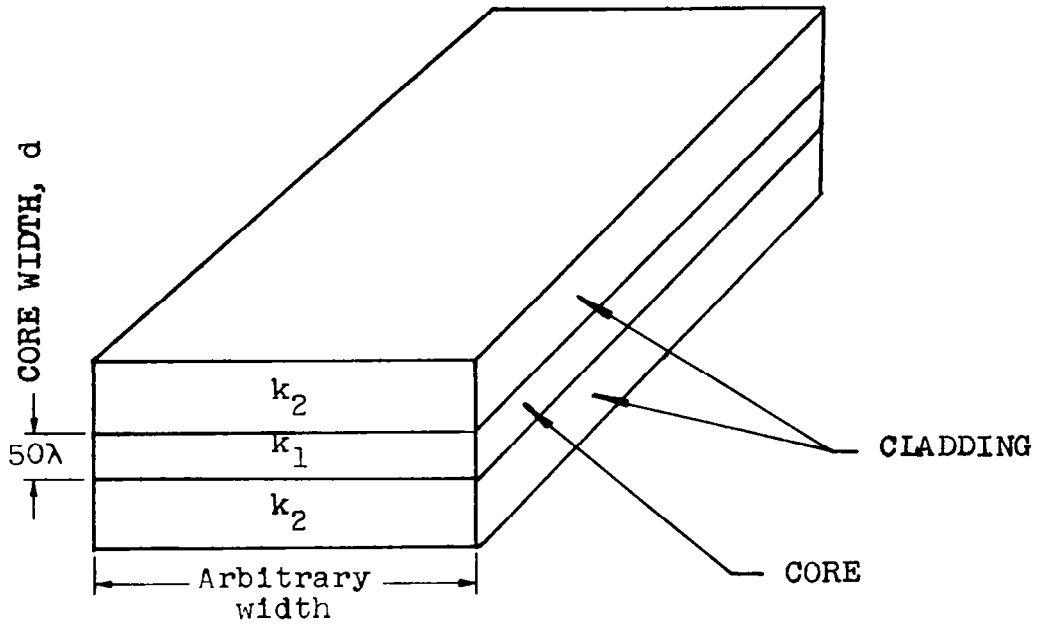

(a) Dielectric slab waveguide.

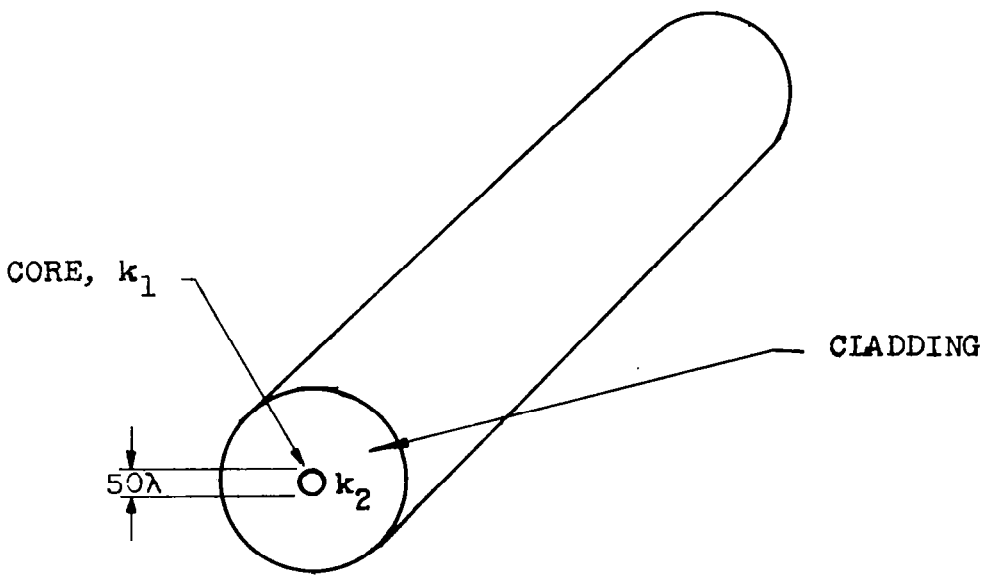

(b) Dielectric rod waveguide.

Fig. 1 - Macroscopic dielectric waveguide.

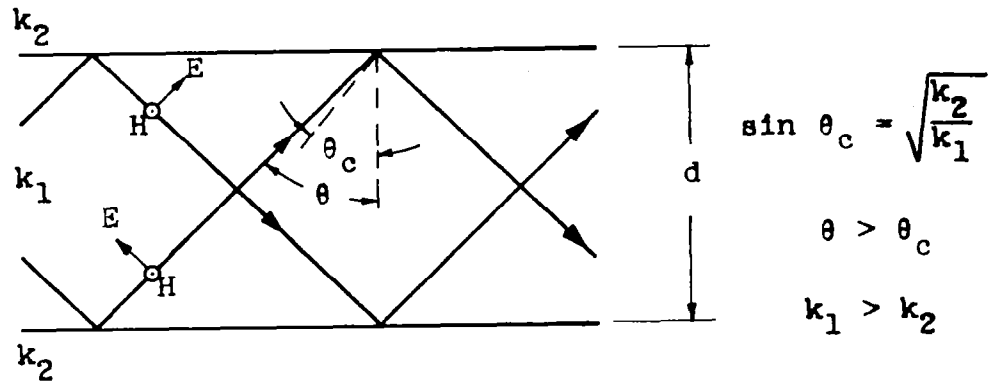

(a) Propagating TM mode.

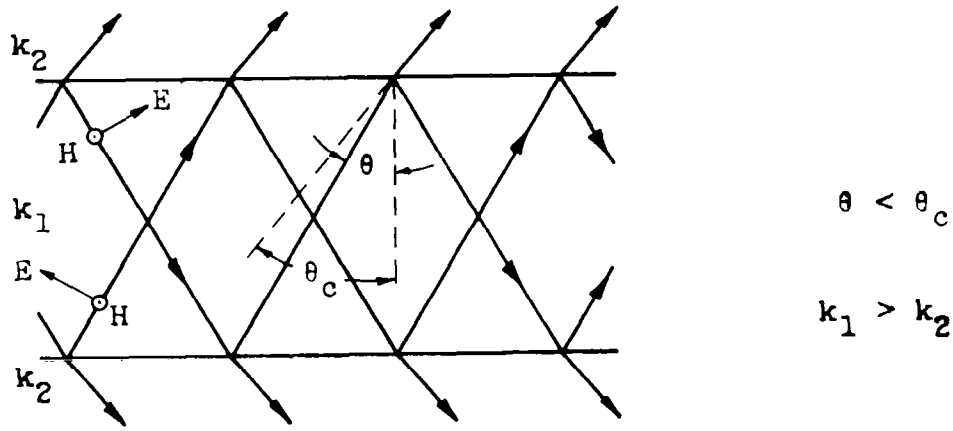

(b) "Leaky" TM mode (not propagating).

Fig. 2 - Propagation in a dielectric slab waveguide.

the waveguide are discrete for the leaky waves also; however, it is not possible to limit the number of leaky modes for a given size structure.

A more rigorous and complete analysis of propagation in dielectric waveguides is required to obtain the detailed propagation characteristics. These analyses have been presented in the literature in general terms using both field matching techniques (Ref. 5) and waveguide techniques (Ref. 14). In order to gain further insight into the characteristics of these waveguides, a complete analysis has been performed in the present study, using the transmission line approach known as "transverse resonance". The transverse resonance analysis (Ref. 6) seeks resonant conditions in the transverse plane as a criterion for propagation in the longitudinal direction. From this analysis, the propagation constants, field distributions, etc., can be determined. The basic details of the analysis are given in Appendix I, which presents a complete analysis for the slab configuration; the significant results are given in the remaining parts of this Section.

As shown in the Appendix, the properties of any dielectric waveguide can be determined from two pairs of characteristic equations. Each pair of equations corresponds to the transverse electric (TE) and transverse magnetic (TM) modes. The TM and TE modes are orthogonal, since they are linearly polarized in mutually perpendicular directions. In the special case of waveguides with very small differences in dielectric constants between the core and cladding, the propagation characteristics are degenerate and apply equally well to TE and TM modes, so that only one pair of equations need be specified. The two characteristic equations for the slab waveguide with small Δk are:

$$p \tan\left(p - \frac{m\pi}{2}\right) = q \qquad (1)$$

and

$$p^2 + q^2 = K_o^2 \frac{d^2}{4} (k_1 - k_2) \qquad (2)$$

where p and q are parameters related to the transverse propagation constants in the core and cladding regions respectively, K_o is the free space propagation constant $(2\pi/\lambda)$, d is the core width and k_1 and k_2 are the dielectric constants of the core and cladding respectively. These symbols are also defined in Section II. The conditions for waveguide propagation correspond to values of p and q which simultaneously satisfy the above equations. Since equation (1) is transcendental, the solutions are obtained by graphical techniques. The two equations are plotted on p vs. q coordinates in Appendix I; solutions of the two equations occur where the two curves intersect.

The condition for the waveguide to support propagation in a particular mode can therefore be readily determined from these characteristic curves. In order for a TM-m or TE-m mode to propagate, the following condition must be satisfied:

$$\frac{d}{\lambda}\sqrt{\Delta k} \geq \frac{m}{2}, \qquad (3)$$

where $m = 0, 1, 2, \ldots$ and $\Delta k = k_1 - k_2$. For the above condition, all modes of order m or lower will propagate. If $(d/\lambda)\sqrt{\Delta k}$ is less than $m/2$ the modes of order m and higher are leaky. This equation therefore defines a waveguide cutoff condition, where cutoff is defined as the transition point between propagating and leaky (or cutoff) modes. A convenient method of representing these relationships is by means of a mode chart (Ref. 19). This chart, shown in Fig. 3 has Δk plotted vs. d/λ. On these coordinates are drawn constant-m contours which graphically represent equation (3). These contours form the cutoff lines of the individual modes. A particular set of waveguide parameters (Δk and d/λ) define an operating point on the chart. For an operating point to the right of a given mode line m, all of the TM and TE modes of order m and lower will propagate. If the operating point is to the left of a given mode line m, the modes of order m or greater are leaky.

The number of propagating TM or TE modes in a given guide is one more than the mode number of the highest propagating mode, since $m = 0$ is the first mode. For the above condition there are actually $2(m + 1)$ propagating modes, since there are both TM and TE modes for each m. However, since these have identical propagation

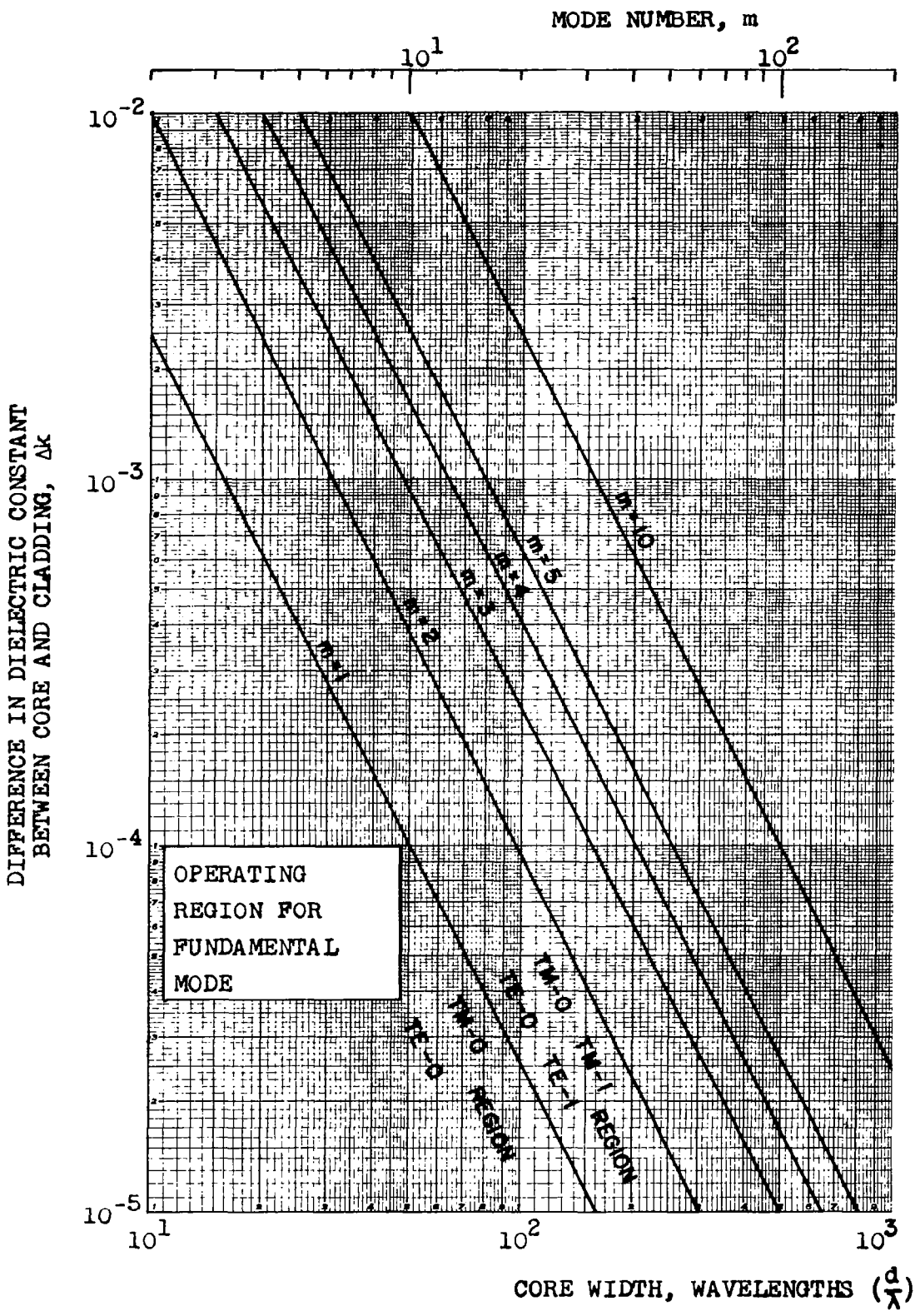

Fig. 3 - Mode chart for dielectric slab waveguide.

characteristics and since one or the other can be selected by choosing the appropriate polarization, the number of modes will be considered as m + 1 rather than 2(m +1). If the aperture field pattern in the waveguide were observed, the maximum number of lines (corresponding to peaks of the field pattern) which would be seen is also equal to m + 1. This fact is discussed further in connection with the experimental work presented in Section V.

In order to construct a single mode guide, the parameters must be chosen so that operation is restricted to the region to the left of the m = 1 line; this is the region marked TM-0, TE-0 on the chart. Such a guide is called single mode because although it supports both the TM-0 and TE-0 modes, these modes are degenerate for small Δk as mentioned previously. Also, since the modes are orthogonally polarized, one or the other can be selectively excited by choosing the appropriate polarization.

The characteristic equations and mode chart presented above have been derived for dielectric waveguide of the slab configuration. A similar set of equations can be derived for the case of a circular geometry. Although the details of the analysis differ, the general approach is identical to the slab configuration and so is not presented in this Report. The characteristics of circular waveguides have been treated in Refs. 5, 15, 17, and only the results are presented here.

A set of characteristic equations similar to equations (1) and (2) can be obtained for the circular guide and plotted on p vs. q coordinates as before. The corresponding mode cutoff relation for the special case of small Δk is

$$\frac{D}{\lambda}\sqrt{\Delta k} > \frac{\mu_{nm}}{\pi} \qquad (4)$$

The parameter, μ_{nm}, is a number obtained from the roots of the Bessel function (Ref. 17) whose value depends on the particular mode. (The mode notation follows that in this Reference.) A listing of the values of μ_{nm} for several low order modes is given on the mode chart for the circular dielectric waveguides shown in Fig. 4. This chart is analogous to the mode chart for slab waveguide (Fig. 3); as in the case of the slab configuration, the lowest order mode (HE-11) has no low frequency cutoff.

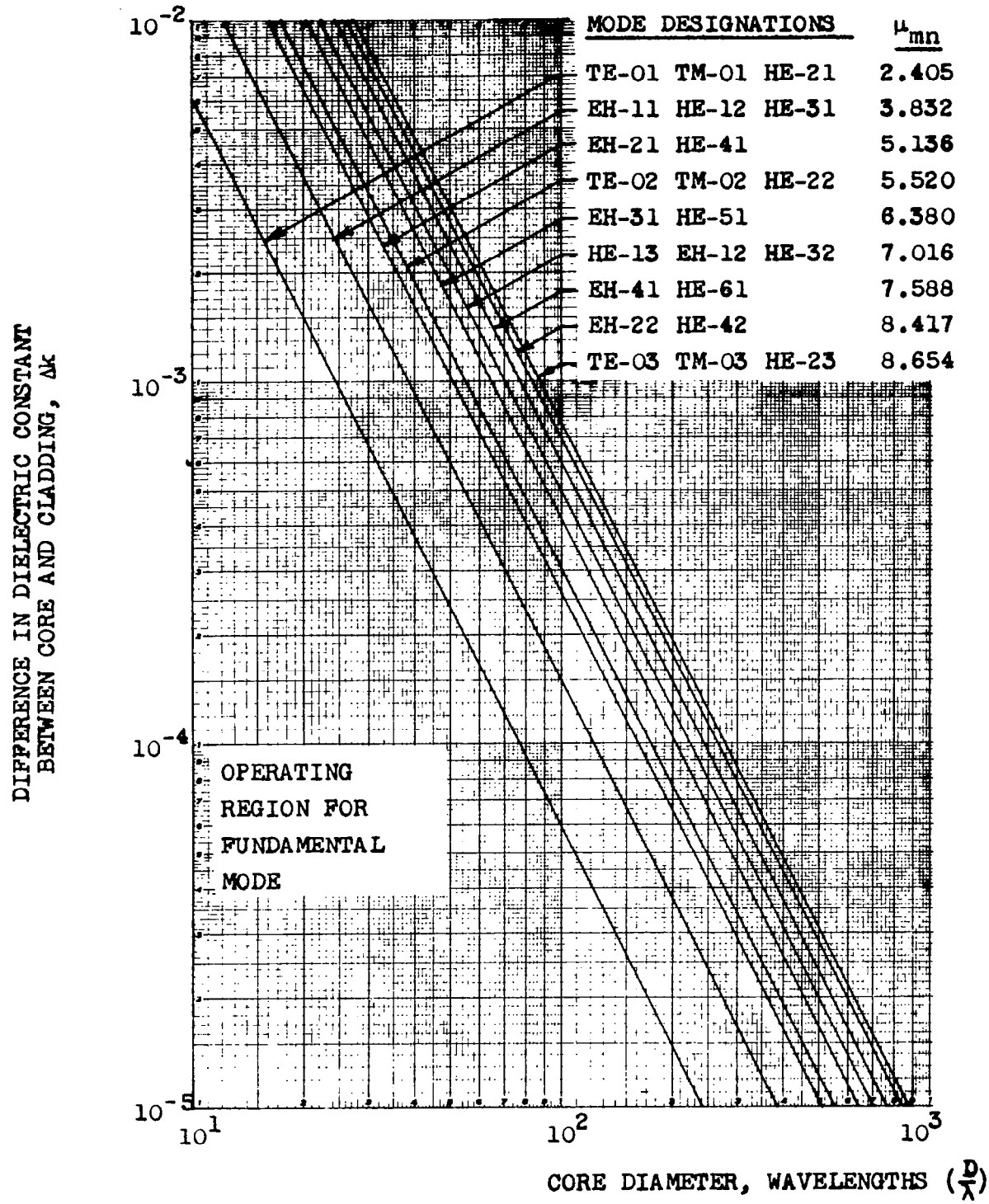

NOTE: Mode notation as in Ref. 17.

Fig. 4 - Mode chart for circular dielectric waveguide.

The distribution of the electric and magnetic fields within the waveguide, and the directions of the field lines has been determined for the slab guide, from the analysis in Appendix I.

The directions of the field lines of the TM-0 mode in slab waveguide are shown in Fig. 5(a); a sketch of the amplitude distribution of the transverse fields is shown in Fig. 5(b). Field patterns of the TM-1 mode are shown in Fig. 6. The patterns of the corresponding transverse electric (TE) modes may be obtained by interchanging the electric and magnetic field lines in these figures. It can be seen that the fields extend across the dielectric interface into the cladding region so that energy propagates in both the core and cladding regions. This result is not apparent from the simple analysis with reflecting rays mentioned earlier. Figs. 5 and 6 are intended to give a qualitative description of the fields, applicable to most operating conditions, rather than an accurate quantitative picture for a particular operating point.

A more accurate quantitative plot of the distribution of the transverse fields of the two lowest order modes of propagation is shown in Fig. 7, for a few different operating conditions. In all cases, the field distributions vary sinusoidally in the core region and exponentially in the cladding. The amplitude of the fields at the edge of the core depends on the operating conditions; the field strength at the edge increases as the mode becomes closer to cutoff. At the cutoff condition, the fields extend indefinitely into the cladding; consequently such a mode would require infinite energy to excite and is not useful. A typical operating point has been chosen as a condition where only the desired number of modes may propagate, and the highest mode is about 10 percent away from cutoff of the next higher mode on the p vs. q curves. The graphical determination of the operating points are shown in Appendix I and indicated on the plots in Fig. 7.

It can be seen from the field patterns of Fig. 5 for the TM-0 mode, that the electric field direction is normal to the waveguide surfaces at a plane through the center of the guide. Consequently a metal bisecting wall could be placed at this plane without affecting propagation. Similarly, for the TE-0 mode, a magnetic bisecting wall (open circuit) could be placed in the

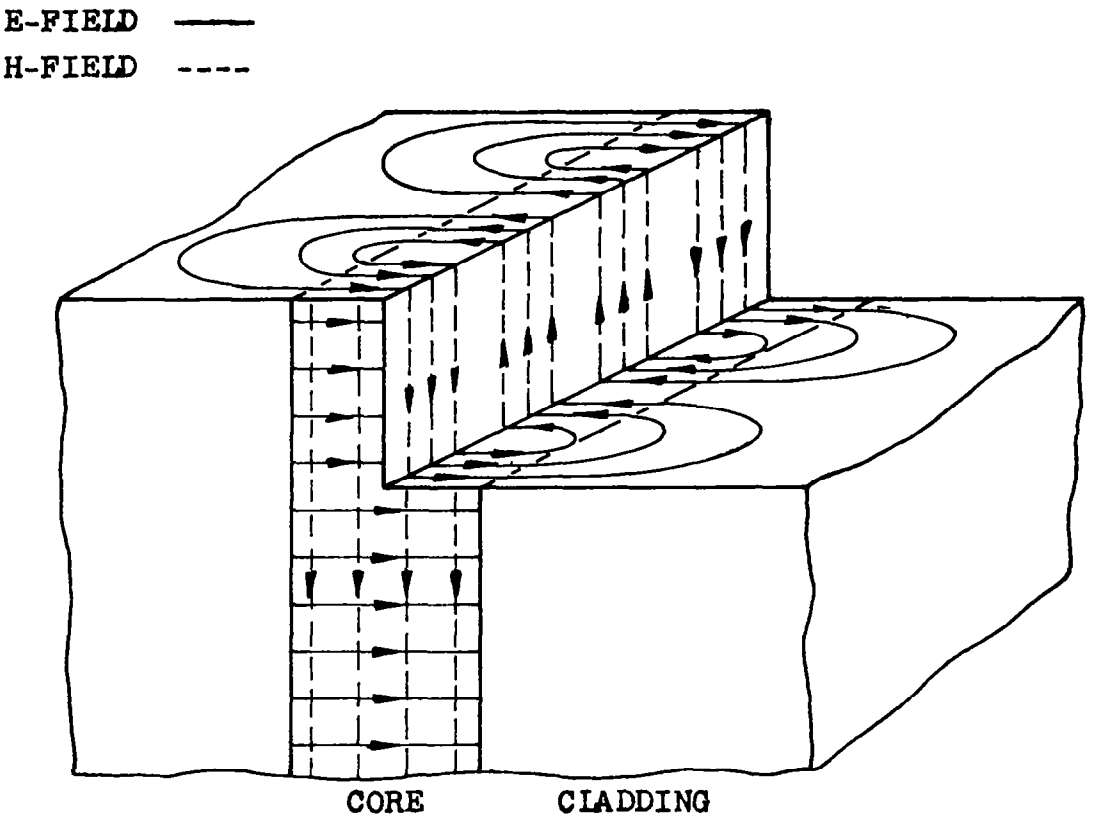

(a) Directions of field lines.

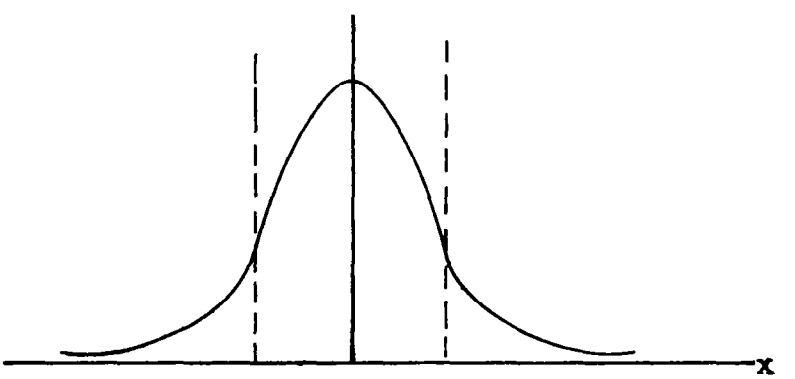

(b) Amplitude distribution of transverse field.

Fig. 5 - Field patterns of TM-0 mode in dielectric slab waveguide.

E-FIELD ——

H-FIELD ----

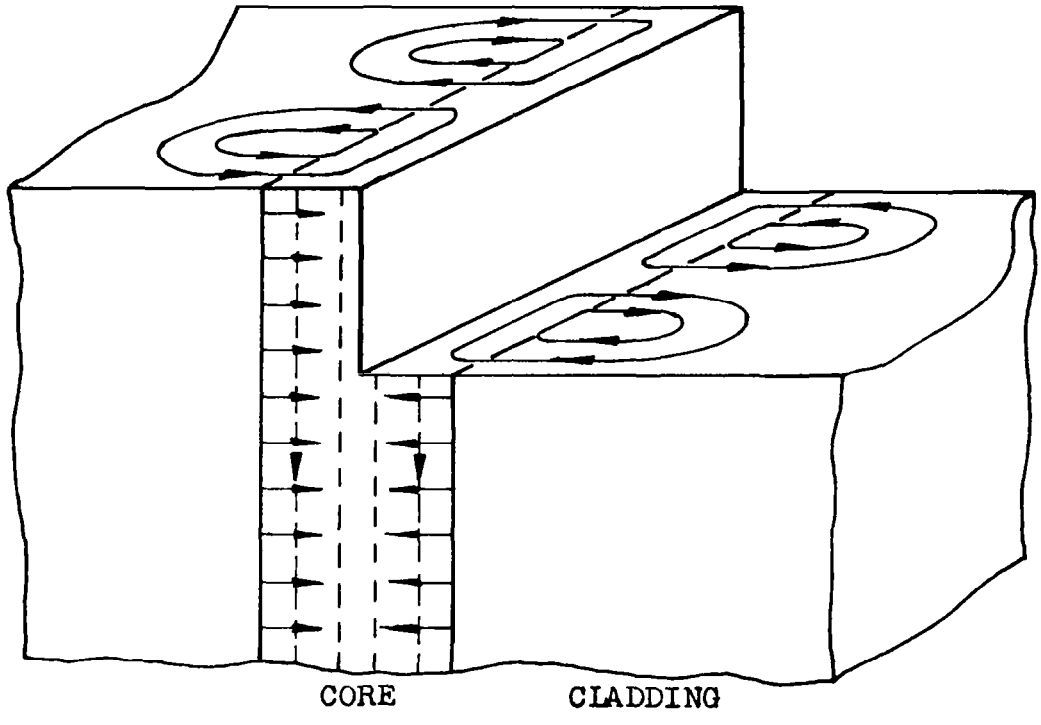

(a) Directions of field lines.

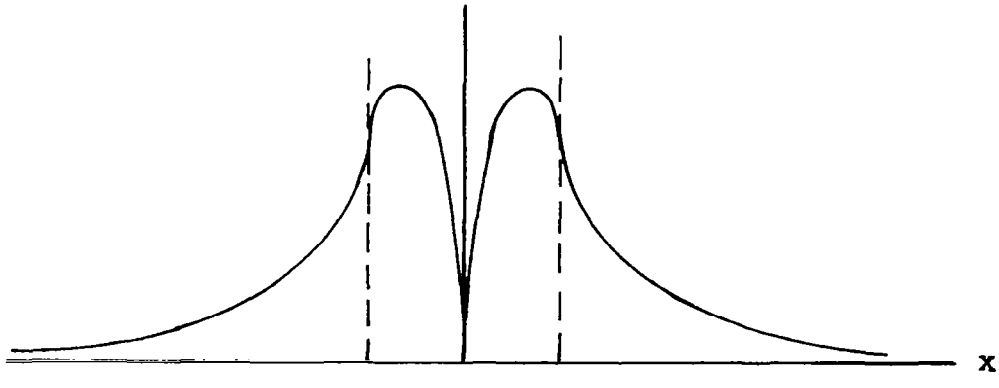

(b) Amplitude distribution of transverse fields.

Fig. 6 - Field patterns of TM-1 mode in dielectric slab waveguide.

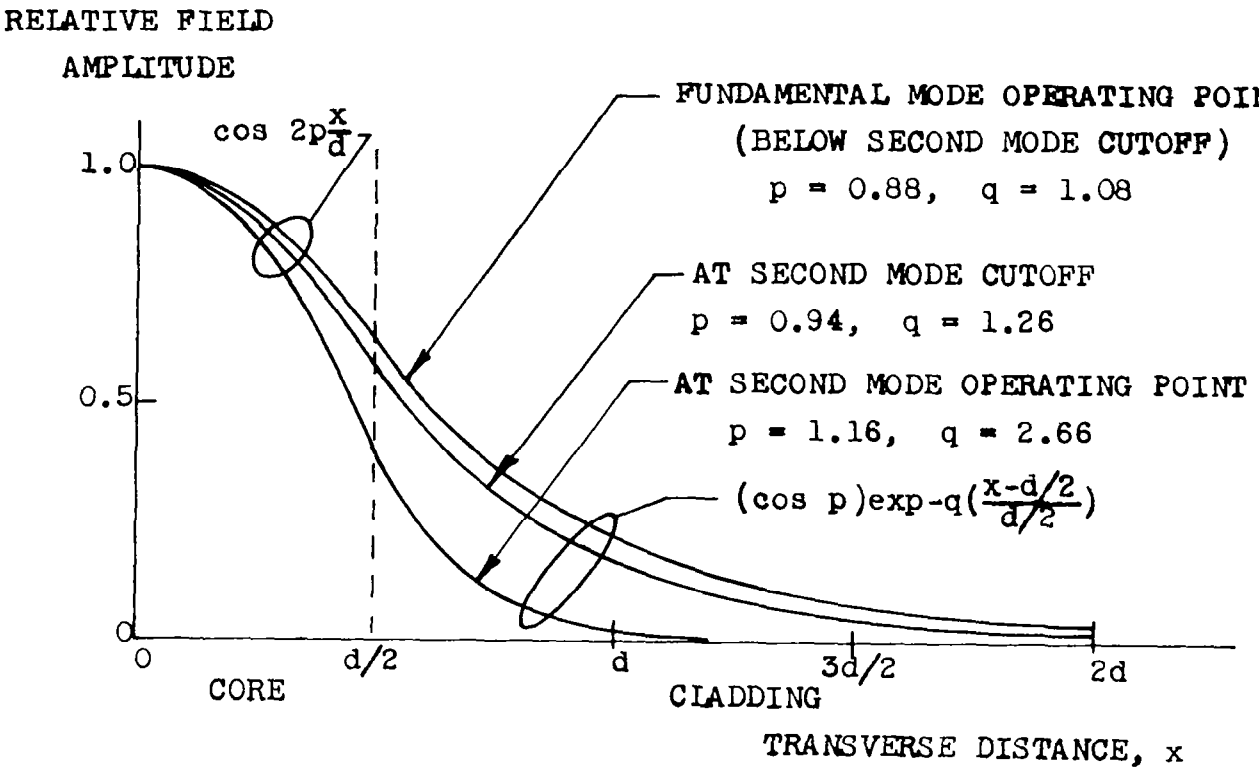

(a) Fundamental mode (TM-0 or TE-0).

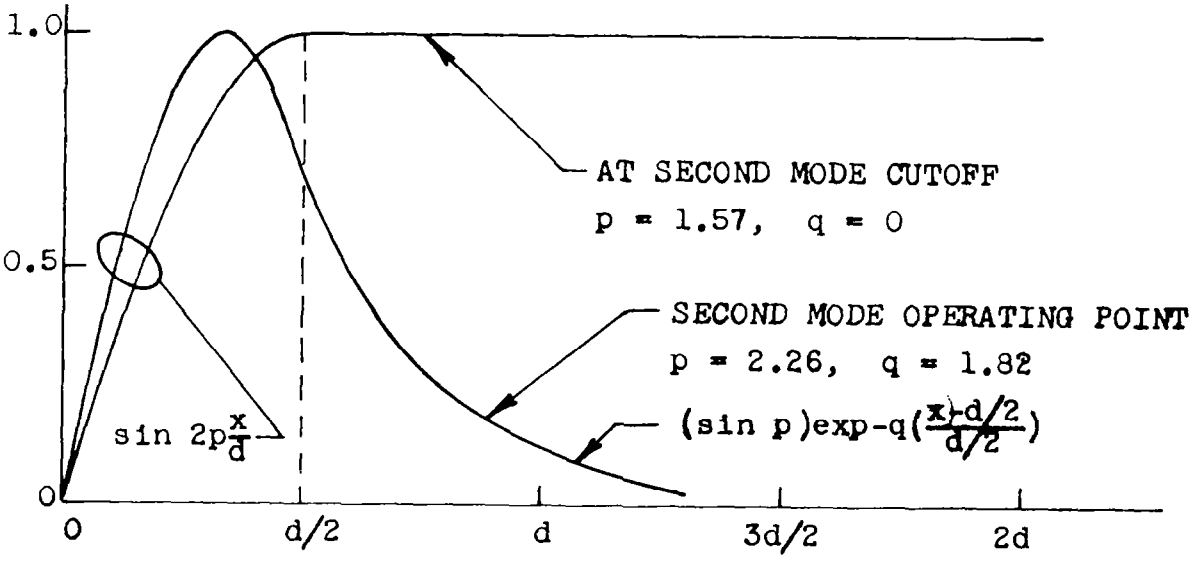

(b) Second mode (TM-1 or TE-1).

Fig. 7 - Transverse field distribution in dielectric slab.

center of the guide without affecting propagation. It is shown in the Appendix that a metal bisected waveguide propagates half of all the possible modes of a full width guide, and a magnetic bisected waveguide propagates the other half.

The field distribution in cylindrical dielectric waveguide can be calculated in a similar manner as for the slab (Ref. 5, 15). In this case, the fields in the core region are given by Bessel functions and in the cladding by Hankel functions. A sketch of the field lines of the fundamental (HE-11) mode in cylindrical guide is shown in Fig. 8(a). The field lines in the cladding have not been shown since this simplifies the picture, and as a practical matter, the field intensity is very low in the cladding for most operating conditions. It can be seen that the field lines in the core are parallel, and hence this mode is linearly polarized. Most of the higher order modes are not so simply polarized and hence not as adaptable to simple excitation techniques.

The distribution of the transverse fields in the cylindrical guide is shown in Fig. 8(b). This pattern is for the HE-11 mode, operating about 10% below the cutoff of the second mode.

Another important property of any waveguide is the variation of the propagation constant with frequency. This property, commonly called dispersion is calculated for the slab waveguide in Appendix I. A convenient method for presenting the dispersion properties of this type of waveguide is to plot normalized guide wavelength (λ/λ_g) vs. waveguide size normalized to free space wavelength (d/λ). A plot of the dispersion properties of the first and second modes is given in Fig. 9, for three different operating conditions. From these curves, the difference in guide wavelength between modes can be determined for any waveguide operating with a given Δk, guide size and frequency. It is interesting to note the limits of the guide wavelength for this type of waveguide. When operating far from cutoff, the guide wavelength approaches the wavelength of an unguided plane wave in the core region ($\lambda/\sqrt{k_1}$); when operating near cutoff, the guide wavelength approaches that of a plane wave in the cladding ($\lambda/\sqrt{k_2}$). Therefore for the waveguide under consideration, where the difference in dielectric constants between core and cladding is very small, the maximum dispersion between modes is also very small. The dispersion is

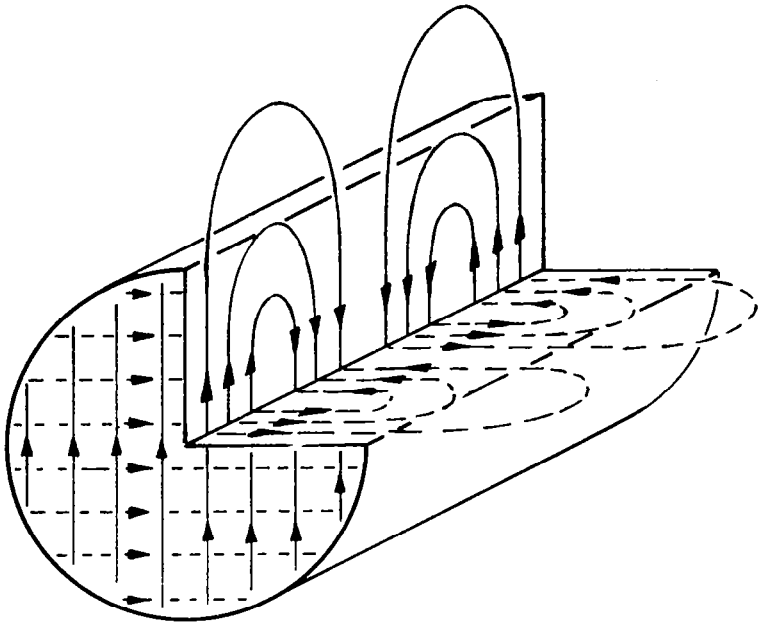

(a) Directions of field lines.

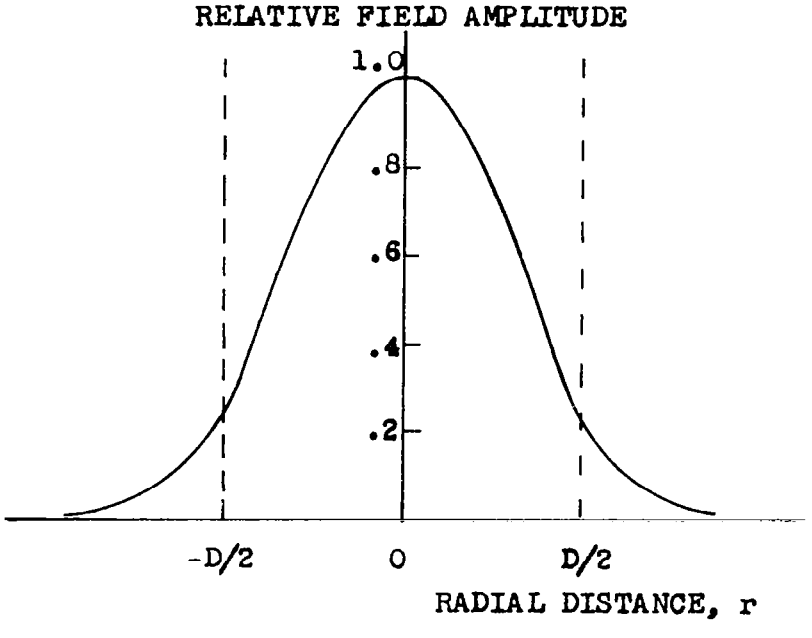

(b) Field amplitude (at fundamental mode operating point).

Fig. 8 - Field pattern of fundamental (HE-11) mode in cylindrical dielectric waveguide.

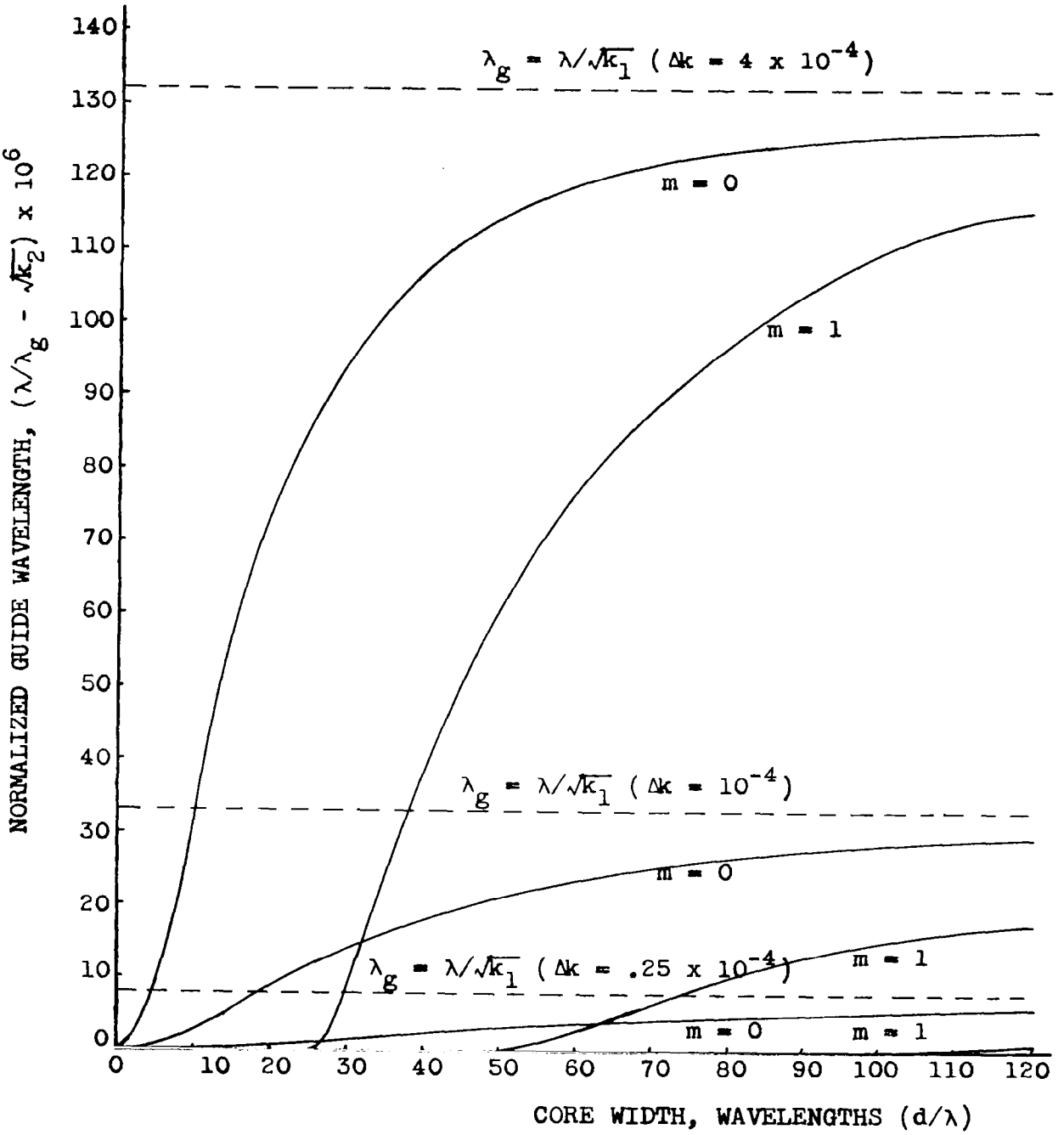

Fig. 9 - Dispersion properties of dielectric slab waveguide.

sufficiently large to permit construction of directional couplers which rely on dispersion between modes however, and in fact corresponds to coupling regions which are of convenient (macroscopic) size (about 1/2 inch).

All the previous calculations of propagation characteristics have assumed lossless media for both the dielectric materials and the metal bisecting walls (in the case of bisected waveguide). Under these conditions, there is zero attenuation for the propagating modes; the leaky modes are of course highly attenuated in the direction of propagation.

The effects of lossy propagation media on propagation have been investigated briefly. For a waveguide composed of dielectric materials only (core and cladding) the waveguide attenuation is very nearly equal to the attenuation of an unguided plane wave through the same medium. If the losses of the core and cladding regions differ, the resultant attenuation of the waveguide is equal to the sum of the unguided attenuation in each medium multiplied by the percentage of the total power in the respective region (Ref. 8). For normal operation, most of the power is concentrated in the core region and so if the losses of the two regions are of the same magnitude, the attenuation is determined almost entirely by the loss of the core medium. Data on typical values of loss for some of the materials being considered for waveguide construction are given in the next Section on materials and fabrication. The attenuation of the experimental waveguide presently being tested is about 3 db per meter.

The attenuation of a bisected waveguide configuration is caused by the loss of the dielectric medium and the bisecting wall. The loss caused by the dielectric medium is the same as for the ordinary waveguide discussed above. The loss caused by the bisecting wall is more complex because it may not only introduce attenuation, but can also affect the phase of the propagation constant.

A simple analysis of the affect of the lossy wall can be performed if it is assumed that the loss contributes only a small perturbation on the real propagation constant. The distribution of the fields in the bisected waveguide is then identical to the distribution in one half of a normal guide operating in the same mode. A simple method of calculating the loss then, is to consider the wave-

guide propagation as comprising two plane waves reflecting back and forth down the guide. The reflectance of the metal wall is less than 100% however, and so some power is absorbed at each reflection. The attenuation is therefore equal to the number of reflections per unit length multiplied by the power lost at each reflection. The reflectance, and hence the attenuation, is different for the two polarizations, and varies as a function of the angle of incidence. Therefore, the attenuation of the TM and TE sets of modes should be different. This simplified approach to the attenuation of the bisected guide predicts small attenuation for the TE modes and very large attenuation for the TM modes, at normal operating conditions.

However, a more detailed analysis of the propagation characteristics of a waveguide with a lossy-metal bisecting wall indicates that the propagation constant is affected strongly by the wall and so the simple analysis presented above is not adequate. The essential difference between the behavior of a perfectly conducting metal and a finite conducting metal occurs at angles of incidence near grazing (as is the case for the waveguide being considered). Here the lossy metal acts as a lossy dielectric, and consequently exhibits a Brewster angle effect, which changes the phase of the reflected wave, relative to that obtained with a perfect metal. The phase of the reflected wave is therefore the same for both polarizations, and as a result both TM and TE modes propagate in an almost identical manner. This phenomenon will be investigated further in this job; however, preliminary experimental results, presented in Section V, indicate that the propagation characteristics of both TM and TE modes are identical, as this theory predicts.

The problem of exciting the waveguide, treated here, concerns the coupling of optical power from some external source to the operating mode of the waveguide. The excitation characteristics of interest are the efficiency of excitation, the relative coupling for each mode of operation, and the dependence of coupling on angle of incidence. Usually, the external source is either far removed so that there is a uniform plane wave incident on the aperture, or the source is nearby so that there may be a sharply focused field on the aperture. The definition of efficiency depends on which case is being considered.

For the case of plane waves incident on a waveguide aperture, it is convenient to first select an aperture area and then consider the amount of power incident on that area. This power is equal to the power density, in watts per unit area, multiplied by the area. To determine the coupling of the incident power to the aperture, an efficiency factor is defined, which is the ratio of the power coupled (or received) to the power incident within the aperture area. Therefore, the power received is (assuming impedance matching):

$$P_r = \rho A \eta_a$$

where ρ = incident power density (watts/unit area), A = aperture area and η_a = aperture efficiency. The aperture area is defined so as to include the fields developed by the mode under consideration as shown in Fig. 10. The aperture efficiency herein defined is called the "gain factor" in microwave antenna theory (Refs. 3, 18). The aperture efficiency shown in Fig. 10 for the slab waveguide is for a unit height, so the area of the aperture must be multiplied by the height of the guide under consideration.

The effect of angle of incidence on the coupling may also be computed from antenna pattern theory. In Fig. 11 are shown the normalized aperture distributions (waveguide field distribution) and the corresponding radiation patterns for several low order modes, which could be developed in rectangular metal waveguide (Refs. 3, 7). It should be noted that the particular distributions also apply to the dielectric slab waveguides when all the modes are "far from cutoff". This means that the guide will support additional higher modes besides those shown. It is observed that the higher modes have peak responses at angles far from the waveguide axis, and that these modes are therefore excited strongest by incident fields from off-axis directions. The relative excitation of each of these modes is illustrated in Fig. 12. In this case the aperture width is the core width (field amplitudes are very small in the cladding). The peak amplitudes shown are the aperture efficiencies, expressed as a voltage ratio ($\sqrt{\eta_a}$). A plane wave incident at the angle φ, as shown will excite the first, second and third modes in the voltage ratio 0.24, 0.74, 0.51 respectively.

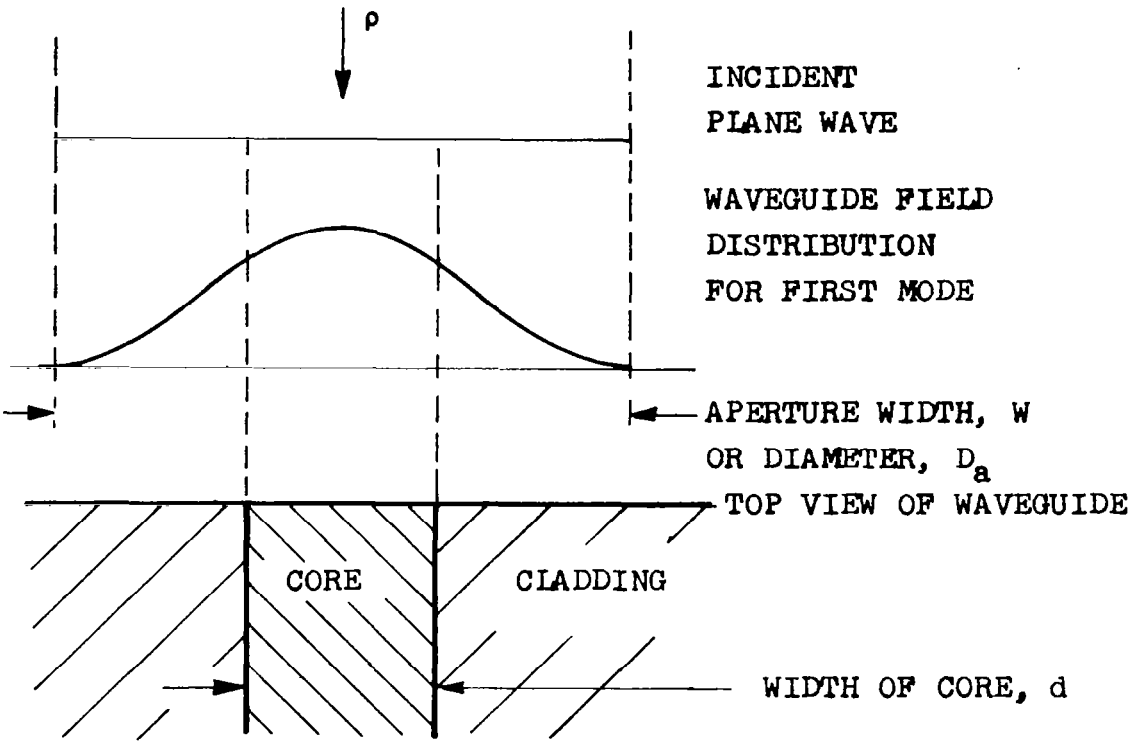

P_r = power coupled to waveguide mode

= $\rho A \eta_a$

where ρ = incident power density, watts/unit area

SLAB CONFIGURATION

A = W x h

η_a = 0.67 (for cosine-squared field distribution)

h = height of waveguide under consideration

CIRCULAR CONFIGURATION

$A = \pi D_a^2/4$

η_a = 0.56 (cosine-squared)

Fig. 10 - Coupling to waveguide with plane wave.

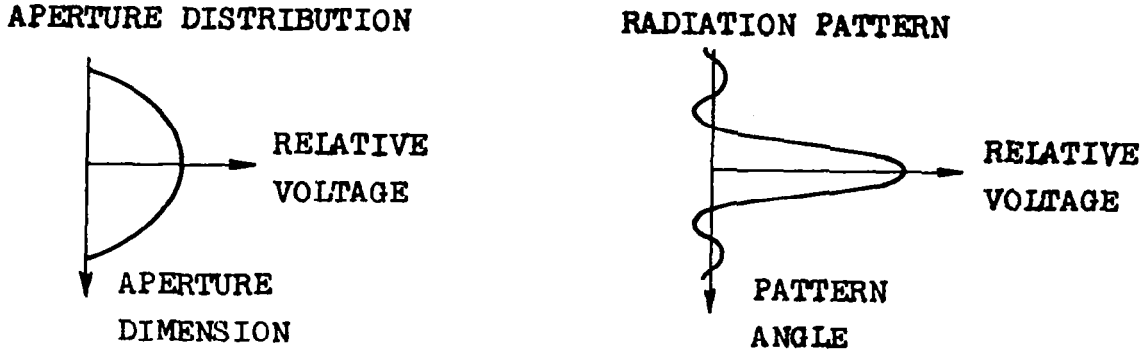

(a) TE-0, TM-0 modes.

(b) TE-1, TM-1 modes.

(c) TE-2, TM-2 modes.

(d) TE-3, TM-3 modes.

(Note: all modes far from cutoff).

Fig. 11 - Waveguide field distribution with far-field radiation patterns.

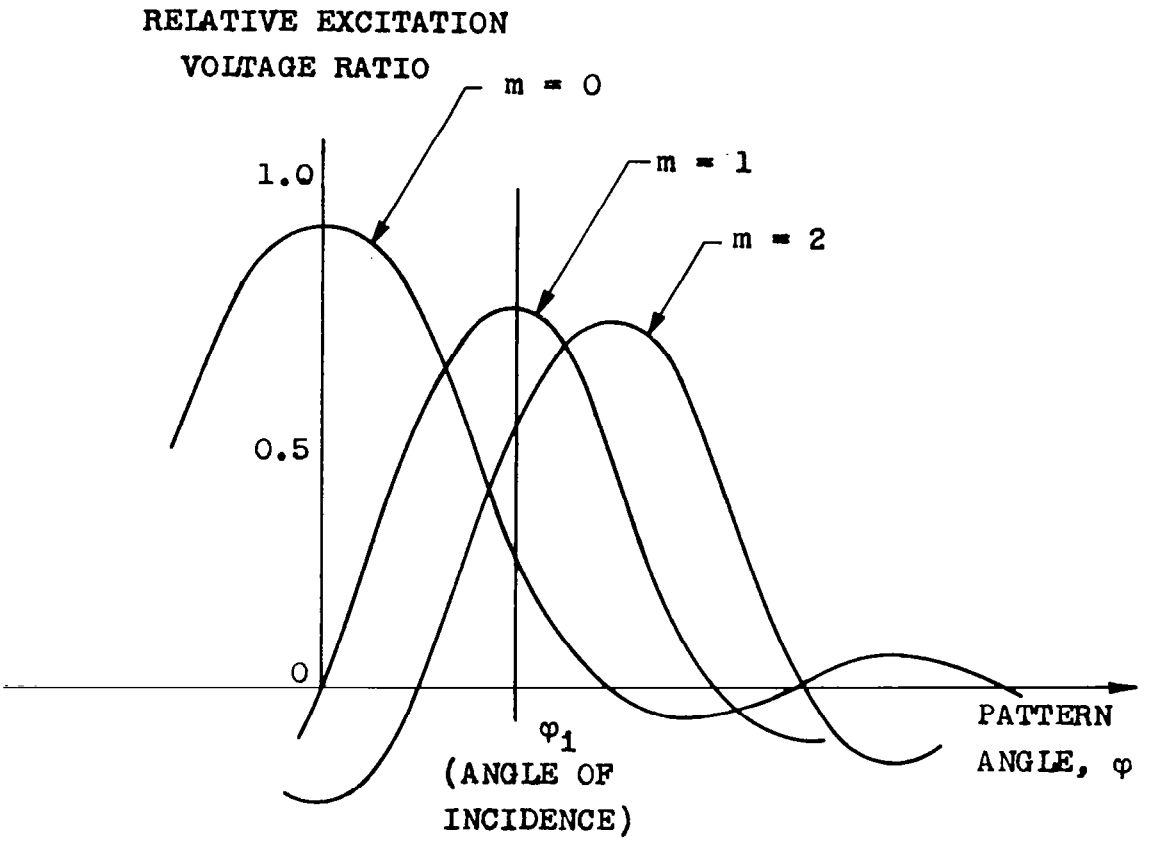

(a) radiation patterns.

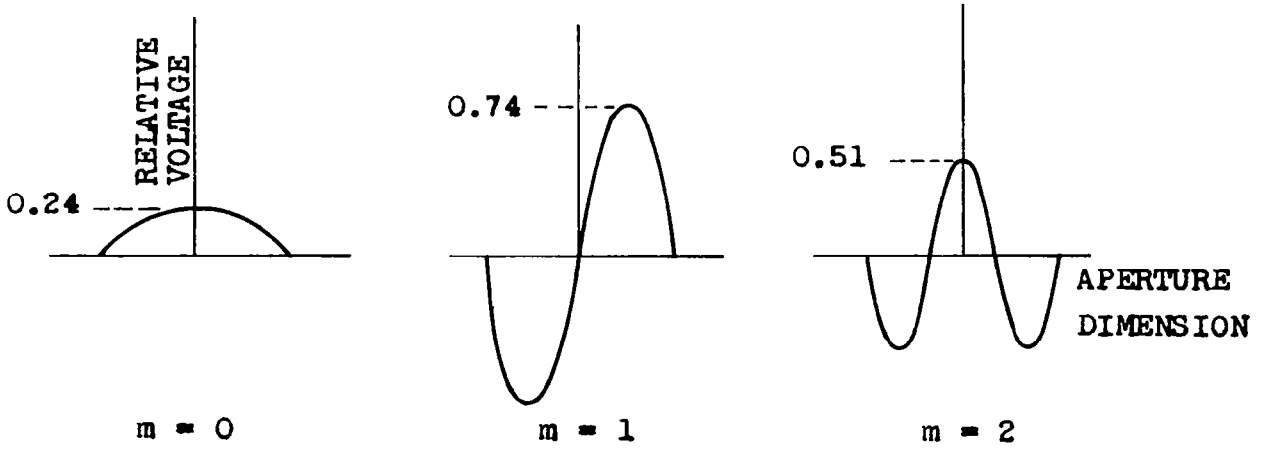

(b) aperture fields.

Fig. 12 - Relative mode excitation for a given angle of incidence.

For the case of external fields focused on the waveguide, not only is the width of the aperture significant, but also the width of the incident excitation. The coupling of power into the waveguide mode from the incident field depends on the similarity of the shapes of the incident and waveguide fields (Refs. 12, 20). When the fields have the same shapes, all the power of the incident field is coupled (assuming impedance matching). When the fields have different shapes, not all the power is coupled. The ratio of the power received to that incident is,

$$\frac{P_r}{P_i} = \frac{\left| \int_R f_i \, f_r \, dR \right|^2}{\int_R f_i^2 dR \int_R f_r^2 dR} \tag{5}$$

where f_i and f_r are the distribution functions of the incident and waveguide fields and R is the aperture region. This formula may be evaluated in simple terms if the incident and waveguide fields are approximated by Gaussian shapes ($\exp - ax^2$); the results are summarized in Fig. 13. For the case of the slab waveguide, the coupled power applies to the coupling per unit height. If the incident field varies along the height dimension, each section along the height may be considered separately. For example, if the incident field is a circularly symmetric Gaussian and the widths of the incident and waveguide fields are the same, all the power may be coupled. However, the field in the waveguide in the height dimensions will then have the Gaussian shape. For circular fields and circular guides, the coupling applies to the total power.

For other angles of incidence and displacements of the fields, equation (5) may be applied, but evaluation is complex and is not carried out here. Qualitative considerations indicate that lateral displacement of the incident field will primarily affect the amplitude of the coupled signal, while changes of the angle will excite different higher modes, as in the case of plane waves incident.

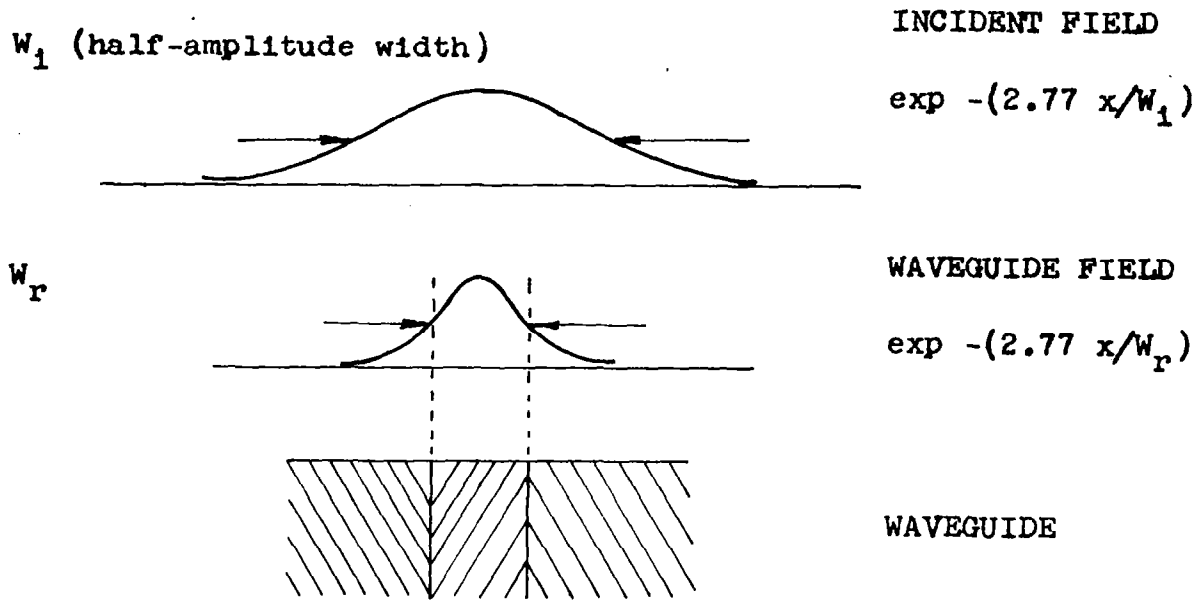

SLAB WAVEGUIDE

$$\frac{P_r}{P_i} = \text{ratio of power coupled per unit height}$$

$$= \frac{2}{\frac{W_i}{W_r} + \frac{W_r}{W_i}}$$

CIRCULAR WAVEGUIDE

$$\frac{P_r}{P_i} = \text{total power coupled}$$

$$= \left[\frac{2}{\frac{W_i}{W_r} + \frac{W_r}{W_i}}\right]^2$$

Fig. 13 - Coupling to waveguide with focused field.

IV. Waveguide Fabrication.

The ultimate objective of this optical waveguide study is the development of a medium in which practical optical components may be fabricated. In order to achieve this goal it is necessary to evaluate waveguide configurations and materials with respect to fabrication feasibility and practicality as well as propagation characteristics.

A. Configurations and Techniques.

Fabrication feasibility has been considered for two classes of waveguide models -- (1) experimental models intended primarily for laboratory analysis of waveguide characteristics and (2) prototype models, with performance stable over a wide environmental range, to demonstrate practicality. The desired characteristics for these two classes are indicated in Table I.

Several experimental waveguide configurations are shown in Fig. 14 and their general characteristics are outlined in Table II. In all of these configurations either the waveguide core or cladding is a liquid. Such an arrangement eliminates the necessity for mating glass surfaces, reducing fabrication time and cost. Also, the temperature dependence of the dielectric constant of the liquid provides a convenient control of the difference in dielectric constant (Δk). However, this same temperature sensitivity will probably preclude its use as a prototype waveguide.

The box assembly shown in Fig. 15 has been used for most of the initial testing. The waveguide structure consists of two optically flat plates, 77 mm long, of Schlieren quality, borosilicate crown glass ($k = 2.2952$), suspended in chlorobenzene. The chlorobenzene in the gap between the plates serves as the waveguide core with the glass plates as the cladding. This construction permits easy adjustment of core size. The temperature of the waveguide is controlled to $.03^{\circ}C$ by a temperature-regulated, water-circulation system connected to the bottom of the box. Experimental data taken with this configuration is reported in Section V.

EXPERIMENTAL WAVEGUIDE MODELS	PROTOTYPE WAVEGUIDE MODELS
INTENDED USE: (1) Experimental verification of propagation constants and field configurations. (2) Medium for initial testing of component configurations. (3) Laboratory operation only.	INTENDED USE: (1) Demonstrate practicality of component construction. (2) Design stage preceding operational models. (3) Demonstrations external to the laboratory.
DESIRED CHARACTERISTICS: (1) Ease of parameter adjustment. (2) Tight control of all parameters to avoid ambiguity. (3) Adaptable to component feasibility studies.	DESIRED CHARACTERISTICS: (1) Fixed, stable parameters. (2) Loose tolerances to reduce fabrication costs. (3) Insensitivity to position. (4) Capability of operation over a reasonable temperature range. (5) Power capacity sufficient to handle conventional cw and pulsed lasers.

Table I. Desired characteristics of experimental and prototype waveguide models.

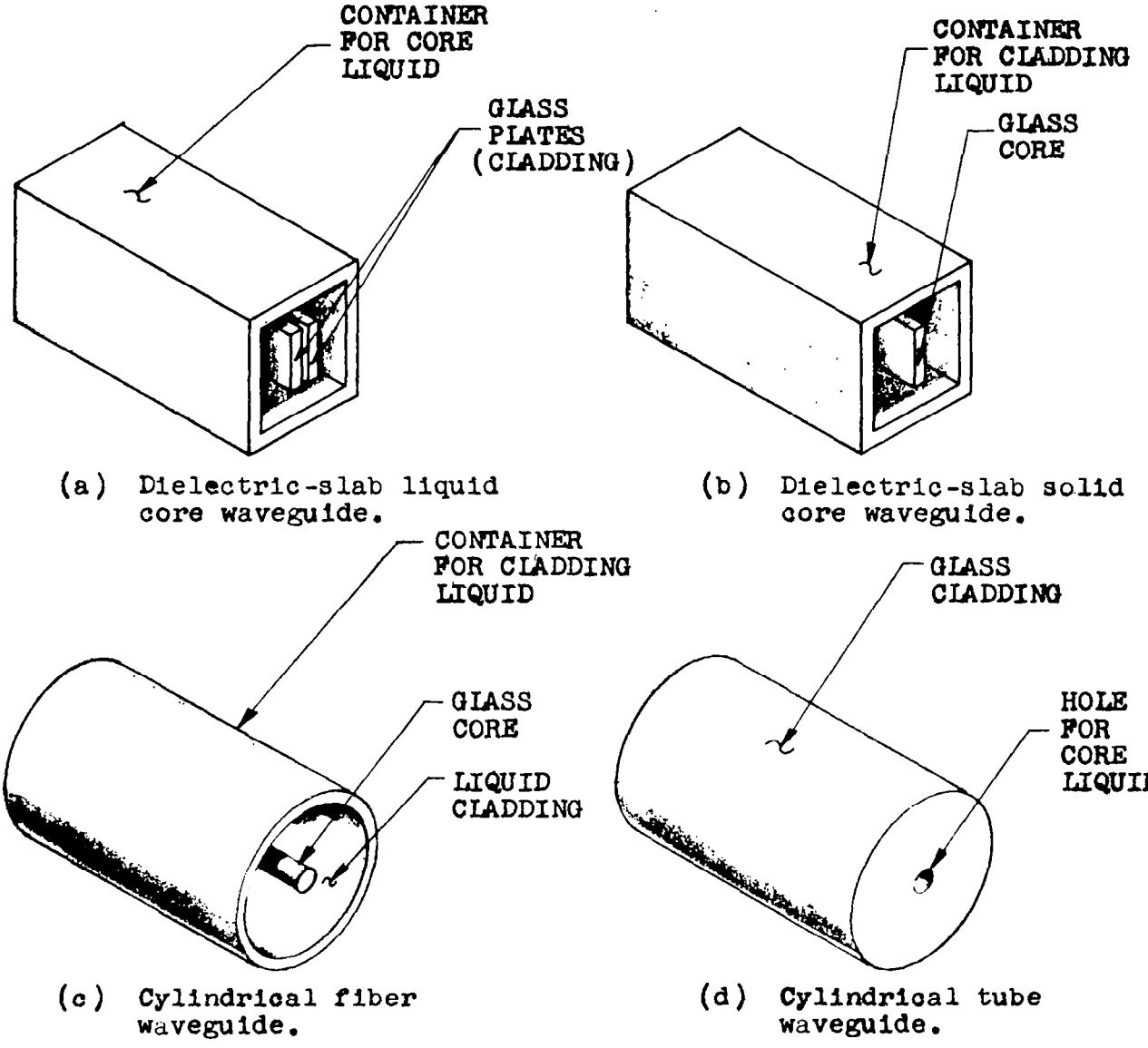

(a) Dielectric-slab liquid core waveguide.

(b) Dielectric-slab solid core waveguide.

(c) Cylindrical fiber waveguide.

(d) Cylindrical tube waveguide.

Fig. 14 - Sketches of experimental waveguide models.

WAVEGUIDE TYPE	CHARACTERISTICS
Dielectric-slab liquid core [Fig. 14(a)]	(1) Adjustable thickness. (2) Δk can be adjusted by temperature control. (3) Adaptable to component studies. (4) Easily modified to short circuit bisected configuration. (5) Inherently homogeneous liquid core. (6) Simple fabrication.
Dielectric-slab glass core [Fig. 14(b)]	(1) Δk can be adjusted by temperature control. (2) Adaptable to component studies. (3) Easily modified to short circuit bisected configuration. (4) Permits evaluation of effect of inhomogeneities in typical glass core. (5) Fabrication from available drawn sheets.
Cylindrical fiber [Fig. 14(c)]	(1) Δk can be adjusted by temperature control. (2) Single-mode in both cross-sectional dimensions. (3) Fabrication from available drawn glass or quartz fibers.
Cylindrical tube [Fig. 14(d)]	(1) Δk can be adjusted by temperature control. (2) Single-mode in both cross-sectional dimensions. (3) Fabrication from available glass capillary tubes or drawn quartz tubes. (4) Liquid may be sealed in tube, removing necessity for external container.

Table II. General characteristics of various experimental waveguide models.

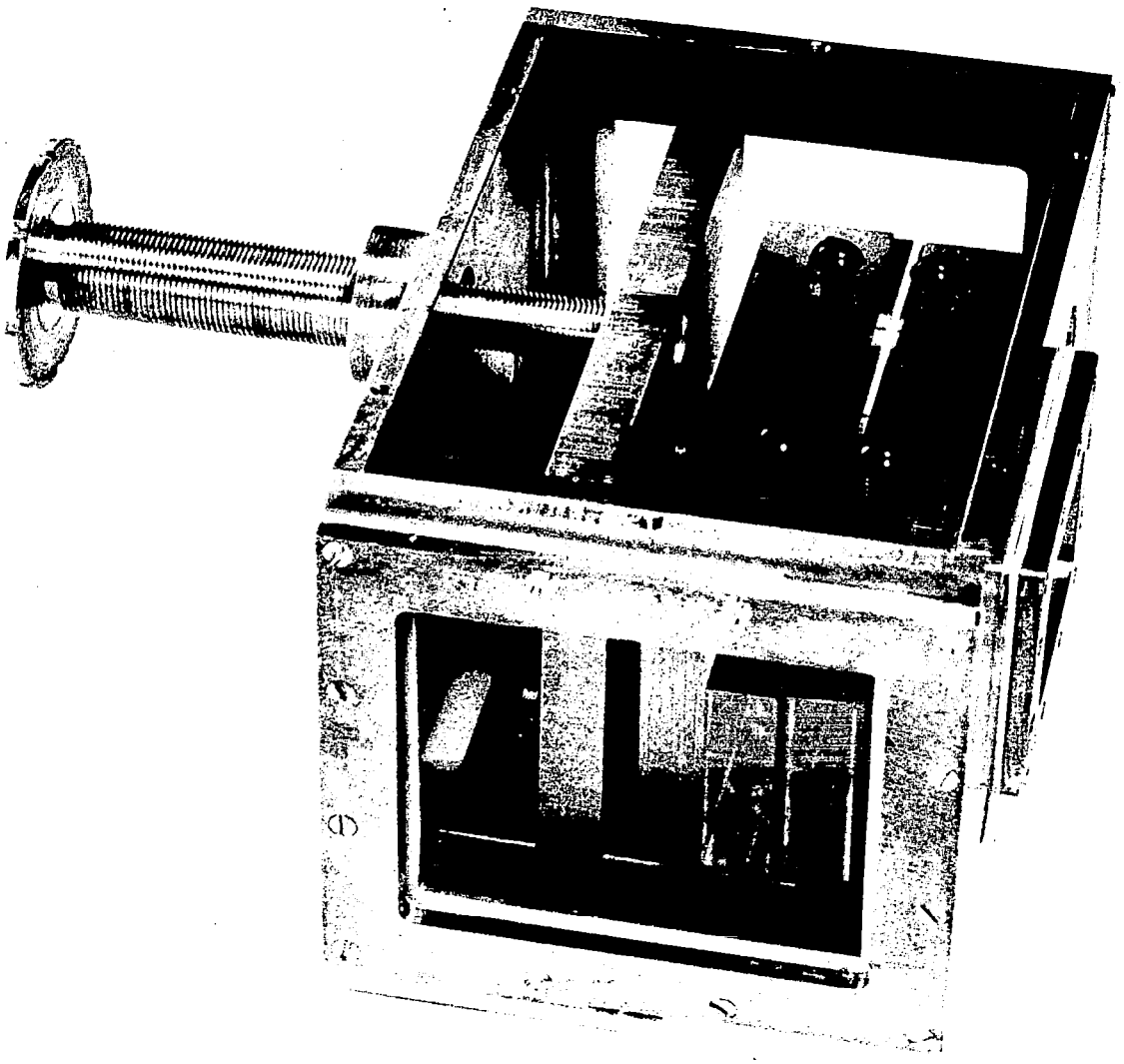

Fig. 15 - First experimental model of macroscopic optical waveguide.

For prototype waveguides several fabrication techniques have been considered. The general objective has been to obtain a waveguide fabricated entirely from solid materials. This objective is complicated by the small difference (10^{-4}) required between the dielectric constants of the core and cladding materials. Among the possible techniques are:

(1) Vacuum depositing of a dielectric cladding on a thin glass core. The dielectric constant of the cladding may be accurately controlled relative to the core by depositing a precise mixture of several dielectrics simultaneously.

(2) Diffusion of an impurity into the core material. The core and cladding would be fabricated from the same material and the diffused impurity would raise the dielectric constant of the core to the required value.

(3) Heavy doping of the cladding and controlled removal of the dopant to obtain the required dielectric constant for the cladding. In this case the core would be a pure material and the cladding material would be chosen so that its dielectric constant before doping was below that of the core. The adjustment of the dielectric constant could be made after the waveguide was assembled by immersing it in a chemical which removes the dopant in the cladding. Waveguide characteristics could be monitored during this process and the waveguide removed from the chemical when the desired Δk is obtained.

(4) Modification of the physical properties of a single glass slab to establish a k-gradient across it. The modal characteristics of this waveguide will differ somewhat from those discussed in Section III, but the important properties will be similar. Among the possible techniques for obtaining a k-gradient are: heat treating to change structure, diffusion of impurities into the slab, chemical reactions, nuclear processing, etc.

While the present experimental, partially liquid, models are suitable for waveguide studies and the evaluation of component

designs, the ultimate usefulness of macroscopic waveguide is its application to operational systems. Therefore, the fabrication of a prototype waveguide, consisting entirely of solid materials is of paramount importance.

B. Materials.

The fabrication of any optical waveguide involves a choice of materials which must be based on the effect of the material properties on waveguide propagation. A brief summary of pertinent material properties is presented in this subsection.

The properties of most interest are dielectric constant and dielectric loss. In addition, since metals may be used for waveguide bisections, metallic loss is also of interest. However, relatively high losses may be tolerated because the waveguide is to be used primarily for component fabrication, as opposed to long-run power-transfer applications. For instance an attenuation of 10 db/meter results in a loss of only 0.1 db for a one centimeter long component. On the other hand the tolerance on the homogeneity of the dielectric constant is quite critical. The required difference in dielectric constant between the core and cladding materials is of the order of .0001 for single-mode dimensions of a hundred wavelengths. Therefore, it is estimated that the dielectric constant throughout the core should not deviate by more than .00001 from its design value. The dielectric constant of the cladding must meet similar specifications in the region of the interface. However, this tolerance on the cladding becomes less critical at distances of one or two core thicknesses from the interface.

Dielectric losses arise from both absorption and scattering phenomena. In solid dielectrics scattering may be caused by large discontinuities such as air bubbles or scratches. These losses may be reduced to a negligible value by specifying optical quality, precision-annealed glass with a high quality surface finish.

Molecular scattering, which occurs in both liquids and solids, also contributes to dielectric loss (Ref. 10). This effect is directly proportional to the fourth power of frequency. Therefore,

this type of scattering, which is commonly neglected at microwave frequencies, must be evaluated at optical frequencies. For typical solid materials molecular scattering contributes about 1 db/meter to the attenuation at 1 micron.

Absorption is another important loss factor at optical frequencies. From an engineering point of view optical absorption need only be considered as a mechanism which reduces the intensity of the radiation in an exponential manner. The mechanism of absorption is related to the atomic structure of the material and is discussed in standard optical textbooks (Ref. 9).

Total loss is the important parameter for dielectric waveguide materials and this quantity may be easily measured. Therefore, detailed computations of dielectric absorption and scattering are not necessarily needed for the evaluation of dielectric materials. Empirical values for the total attenuation of glass and various liquids appear in the literature (Ref. 1). The total attenuation of transparent glass is generally given as less than 10 db/meter in the visible region. The attenuation of benzene and carbon disulfide have both been measured at WL to be about 3 db/meter at 0.6328 microns. As indicated previously, this magnitude of attenuation is considered acceptable for waveguide applications.

Metallic losses are significant because of their effect on reflection. In the short-circuit bisected waveguides a reflectance of 100% is desired. The degradation of waveguide performance with decreasing reflectance is indicated in Section III. The approximate reflectance of silver and aluminum are plotted in Fig. 16 as a function of frequency. This property is also a function of the angle of incidence. Fig. 16 is plotted for normal incidence; whereas, the reflectance at grazing incidence approaches 100% for both metals. In general, reflectance improves at the lower frequencies. Although silver has a higher reflectance, aluminum is usually preferred for its corrosion resistance.

Since the precise control of the dielectric constant of the waveguide materials has a critical effect on waveguide characteristics, it is necessary to understand the functional variation of this parameter. The dielectric constant of a pure material is related to molecular density and molecular polarizability by the formula;

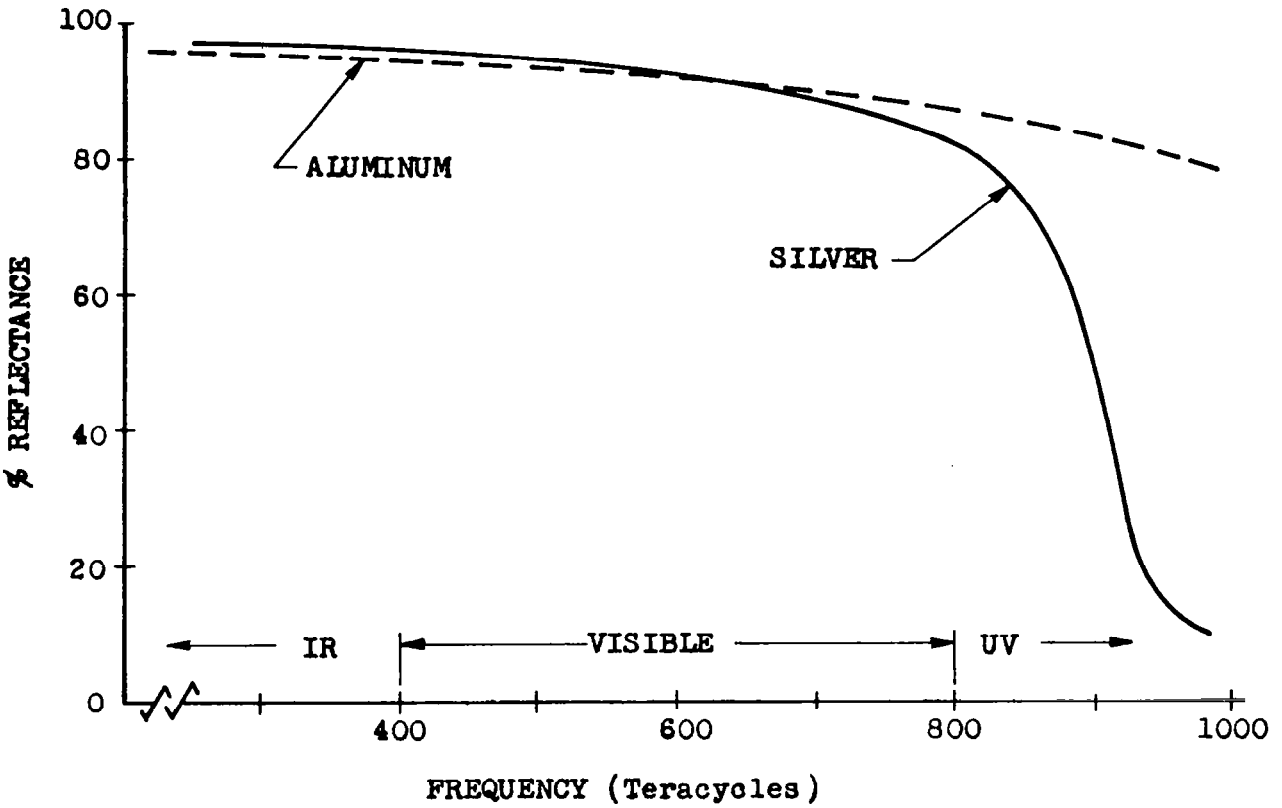

Fig. 16 - Reflectance of metals as a function of frequency.

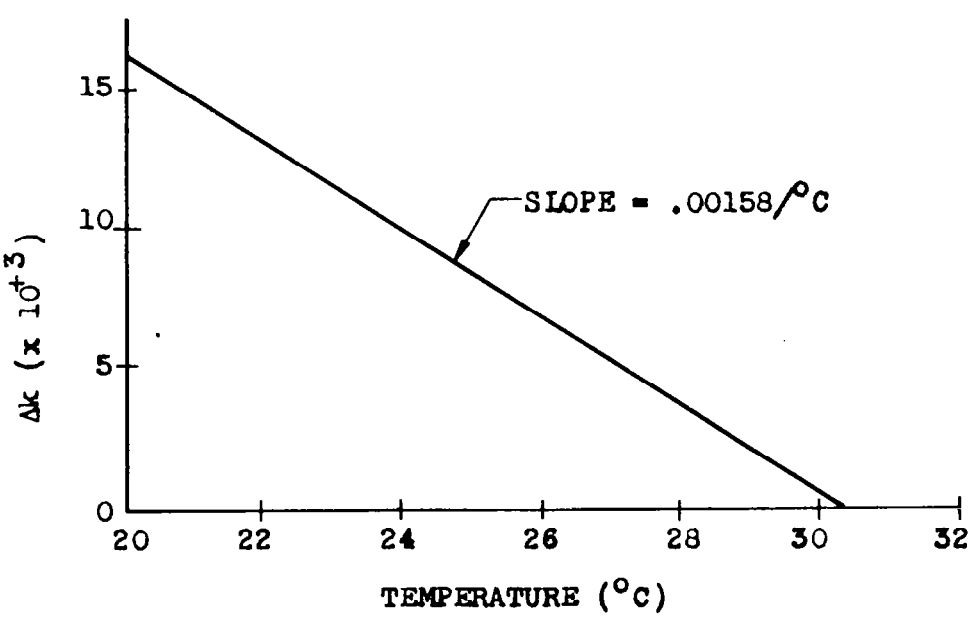

Fig. 17 - Temperature dependence of Δk for a chlorobenzene and glass waveguide.

$$\frac{k - 1}{k + 2} = \frac{4\pi}{3} N\alpha \, , \qquad (6)$$

where N is the density of molecules and α is the polarizability. For materials consisting of a variety of different molecules the $N\alpha$ product may be replaced by the summation of $N\alpha$ products over the different molecules. The polarizability, α, is a function of the quantum-mechanical state of the molecules (Ref. 10) and, is known to exhibit both a temperature and a frequency dependence.

The temperature variation of the dielectric constant arises from two separate effects. The predominant one for liquid dielectrics is the variation of density, N, with temperature and normally results in a decrease of dielectric constant with rising temperatures. The other factor is the temperature dependence of the polarizability. This is caused by thermal pumping of molecules into higher vibrational levels. The effect of the thermal pumping may be either to raise or lower the dielectric constant depending on the atomic structure of the material.

The dielectric constant of a solid is generally less temperature sensitive than that of a liquid. For typical glasses the dielectric constant changes by $0.00001/^{\circ}C$ while for typical liquids, it varies by $.001/^{\circ}C$. Therefore, in a completely solid waveguide the core and cladding have a similar temperature dependence so that Δk, the important parameter for waveguide propagation, will tend to remain constant even though the absolute value of the dielectric constant changes. The liquid-solid experimental waveguides, however, are very temperature sensitive because the dielectric constant of the liquid varies relative to that of the solid. The temperature dependence of Δk for a typical experimental waveguide is plotted in Fig. 17.

The frequency dependence of the dielectric constant is related to the molecular polarizability of the material. The polarizability exhibits various singularities as a result of molecular and atomic resonances. The frequency variation may be obtained from Eq. (6) by taking into account the frequency dependence of the polarizability which is given by;

$$\alpha = \frac{e^2}{M} \sum \frac{f_s}{(\omega_s^2 - \omega^2) + j\gamma_s\omega} \quad , \tag{7}$$

where f_s is the "oscillator strength" associated with each resonant frequency, ω_s, and γ_s is a damping term associated with each quantum transition. The summation is over all the resonant frequencies of the molecule. This theory has been developed from both classical and quantum mechanical viewpoints in Ref. 2 and will not be presented here. The dielectric constant as a function of frequency for a transparent dielectric is plotted over a large frequency band in Fig. 18, and the dielectric constant of borosilicate crown glass is shown in Fig. 19 for the visible portion of the spectrum. This material is typical of transparent optical materials in that dielectric constant increases with frequency.

The fabrication of a macroscopic optical waveguide is considered feasible for both experimental and prototype models. Experimental waveguides have already been demonstrated and the choice of waveguide materials may be based on published data and on simple laboratory measurements. Techniques for fabrication of more practical, prototype waveguides have been indicated. However, this application of these techniques is sufficiently different from conventional applications so that careful design and experimentation will be required for their development.

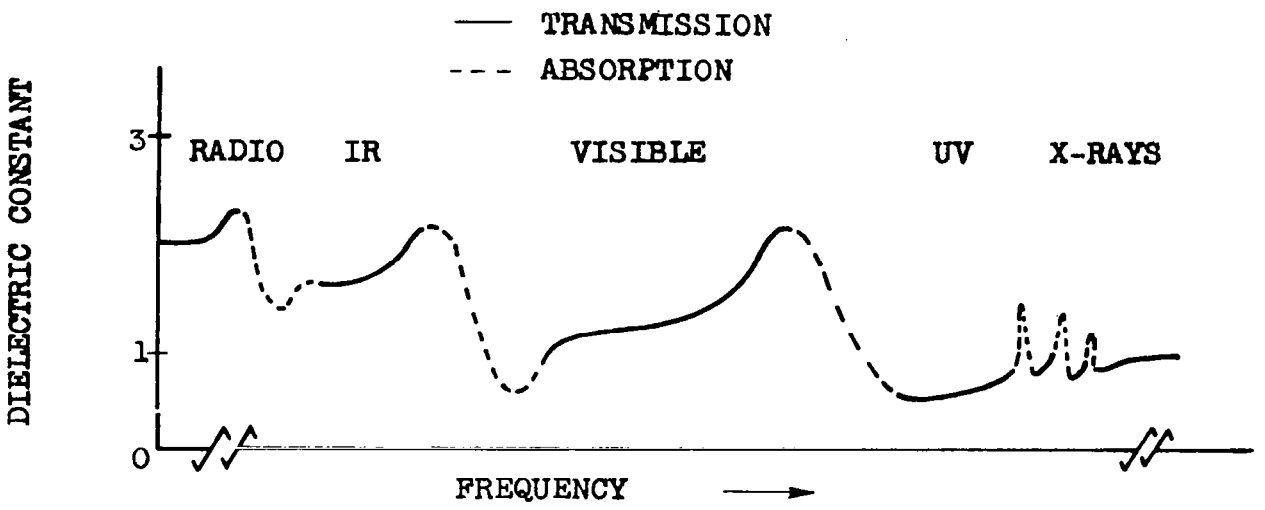

Fig. 18 - Typical variation of dielectric constant with frequency.

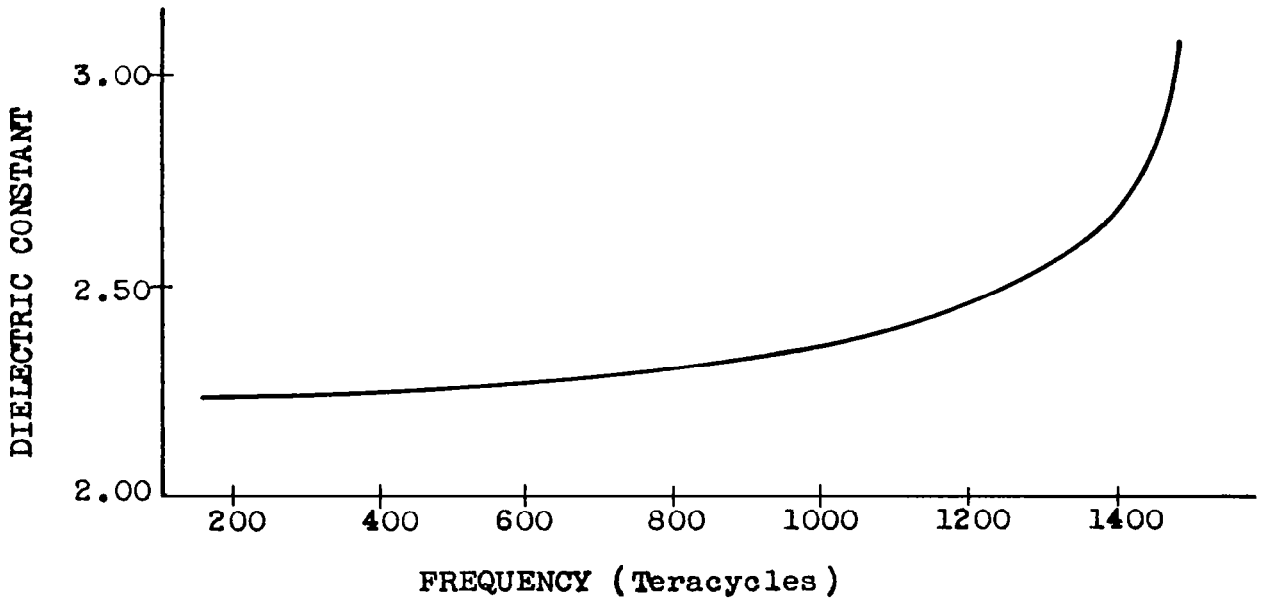

Fig. 19 - Dielectric constant versus frequency for borosilicate crown glass in the visible band.

V. Experimental Evaluation.

The objective of the experimental study is the verification of waveguide performance as predicted by the theoretical analysis. Positive verification will indicate that there is sufficient understanding of the waveguide propagation, and that adequate tolerances have been held on materials and configurations to justify the various assumptions of the analysis. The experimental program has included the observation of waveguide modes, the measurement of field patterns, and comparison of these characteristics with theoretical calculations, for several experimental waveguide configurations.

Three waveguide configurations have been investigated: (1) a liquid-core, solid-cladding dielectric-slab waveguide, (2) a solid-core, liquid-cladding dielectric-slab waveguide, and (3) a short-circuit-bisected dielectric-slab waveguide. These configurations are described below.

The experimental model of the first configuration, a liquid-core, solid-cladding dielectric-slab waveguide, was designed with the features shown in Fig. 20; a photograph of this waveguide is given in Fig. 15. The waveguide structure consists of two 77 mm plates of Schlieren quality borosilicate crown glass ($k = 2.2952$), suspended in chlorobenzene; the inside surfaces of the plates are optically flat. The glass plates serve as the waveguide cladding, and the chlorobenzene in the gap between the plates serves as the core.

The spacing between the plates is adjusted by means of a differential screw, shown in Fig. 20. One turn of the screw changes the spacing by ten microns. The spacing is observed through a 100X microscope, and measured with a calibrated reticle in the microscope eyepiece; the measurement accuracy is approximately $\pm$ 3 microns.

To provide a uniform waveguide, the plates have to be parallel. This is accomplished by directing a collimated laser beam through a side window on the waveguide tank, and observing the beams reflected from the surfaces of the glass plates with a telescope, as illustrated in Fig. 21. Each reflection appears as a point in the field of view of the telescope. When the points corresponding to reflections from the inner surfaces of the plates are superimposed, the plates are parallel. The adjustment is made with three differ-

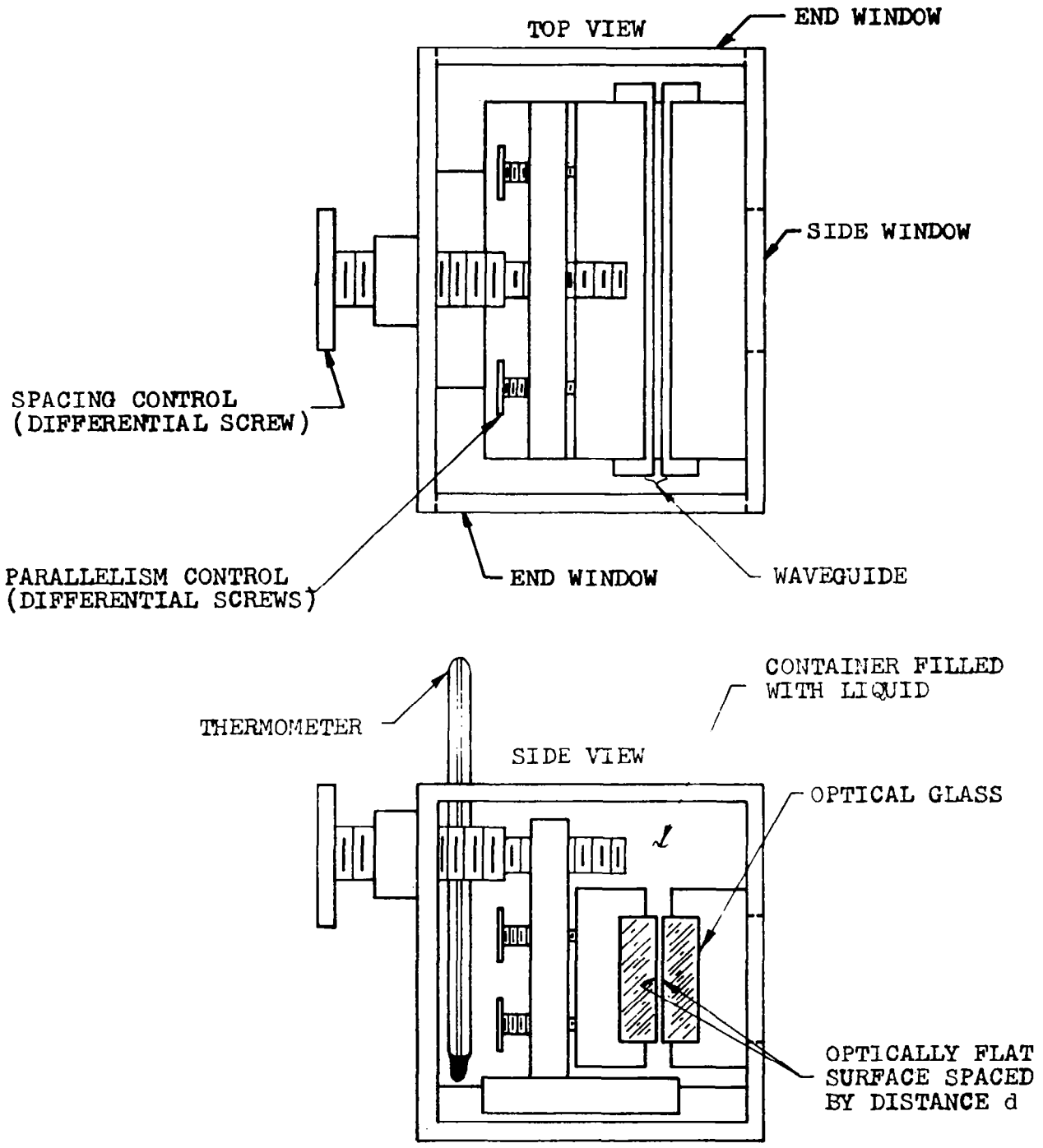

Fig. 20 - Experimental model of dielectric-slab waveguide.

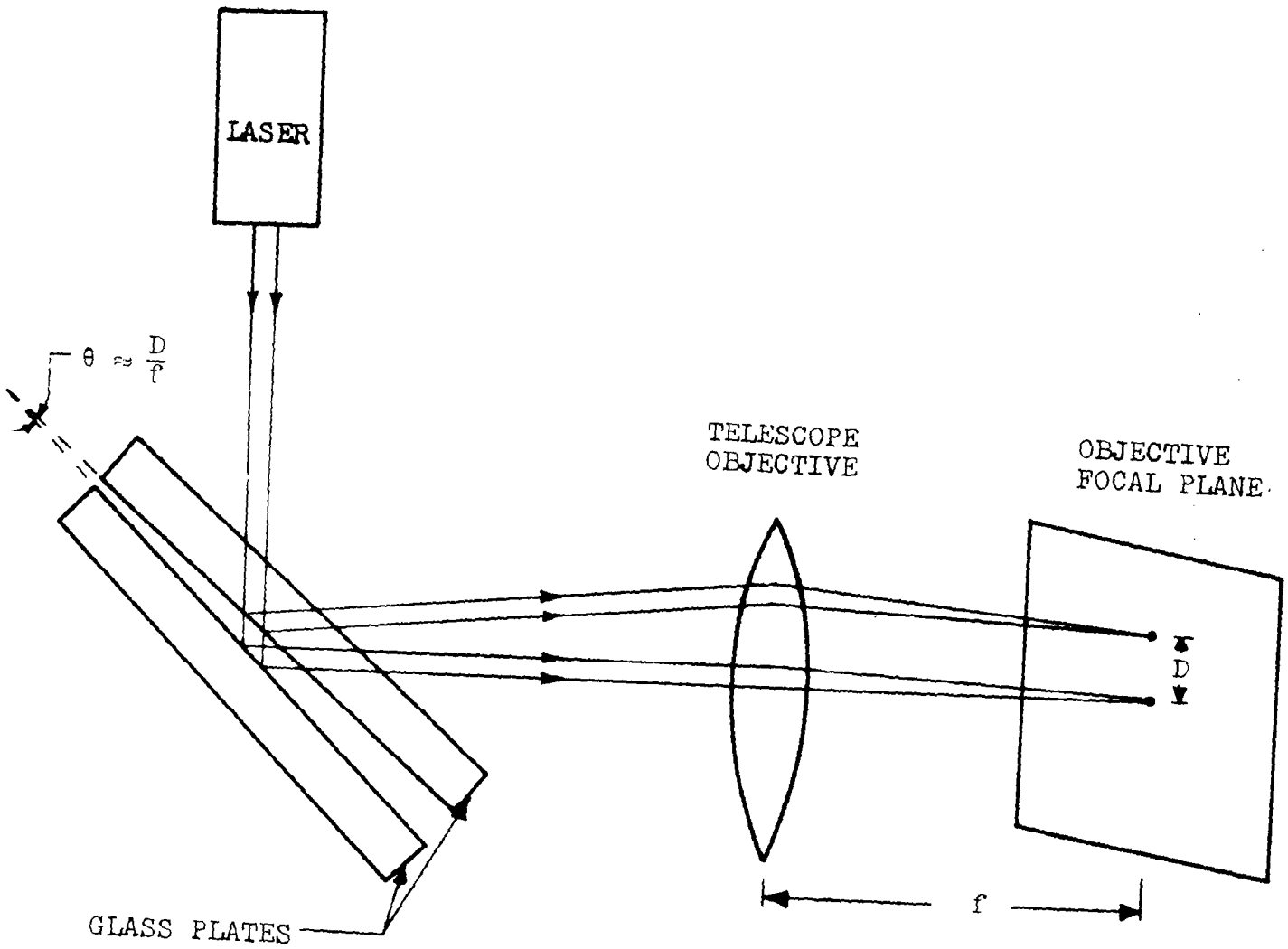

Fig. 21 - Technique for aligning glass plates.

ential screws, shown in Fig. 20. After adjustment, the plates are parallel to within 0.01 milliradian.

The experimental model of the second configuration, a short-circuit-bisected dielectric-slab waveguide, is similar in construction to the dielectric-slab waveguide described above; the only difference is that one of the glass plates has been replaced by an identical plate having a thin layer of aluminum deposited on the optically flat surface. The glass plate again serves as the cladding, and the chlorobenzene in the gap between the glass plate and the aluminized surface serves as the core. The adjustment of spacing and parallelism with this waveguide configuration are identical to those described above for the dielectric-slab waveguide.

The experimental model of the third configuration, a solid-core, liquid-cladding dielectric-slab waveguide, employs the same supporting structure as the waveguides described above. For the solid core guide, the two glass plates are removed and replaced by a thin (89 ± 3 microns) sheet of optical quality glass, 76 mm long, which serves as the waveguide core; the chlorobenzene in which it is suspended serves as the cladding.

In order to measure the number of modes and the field patterns, a test range has been implemented. This range comprises three basic systems: the source system, the waveguide system, and the detection system. A block diagram of the test range is given in Fig. 22; a photograph is shown in Fig. 23.

The source system, illustrated in Fig. 24, comprises a CW He-Ne gas laser having a collimated output at 0.6328 microns, provision for introducing a calibrated value of attenuation into the laser beam, and a lens for focusing the beam on the input aperture of the waveguide. The laser output is linearly polarized in the vertical plane; a half-wave plate may be placed in the beam to rotate the polarization to the horizontal plane when desired. A 1000 cps square-wave generator provides amplitude modulation of the laser.

The waveguide system, illustrated in Fig. 25, comprises the waveguide test fixture described previously, a thermostatically-controlled water-circulation system connected to the bottom of the waveguide tank, and provisions for adjusting the orientation of the

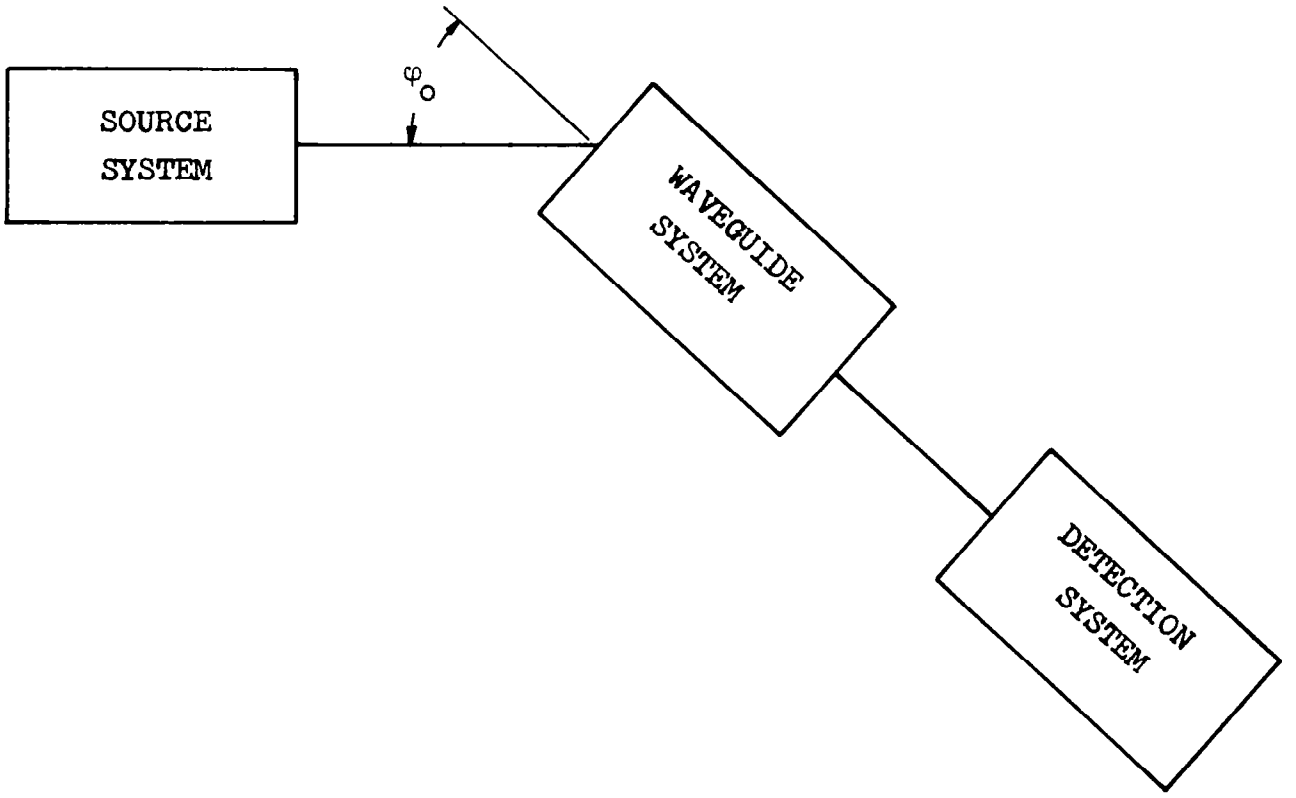

Fig. 22 - Block diagram of test range.

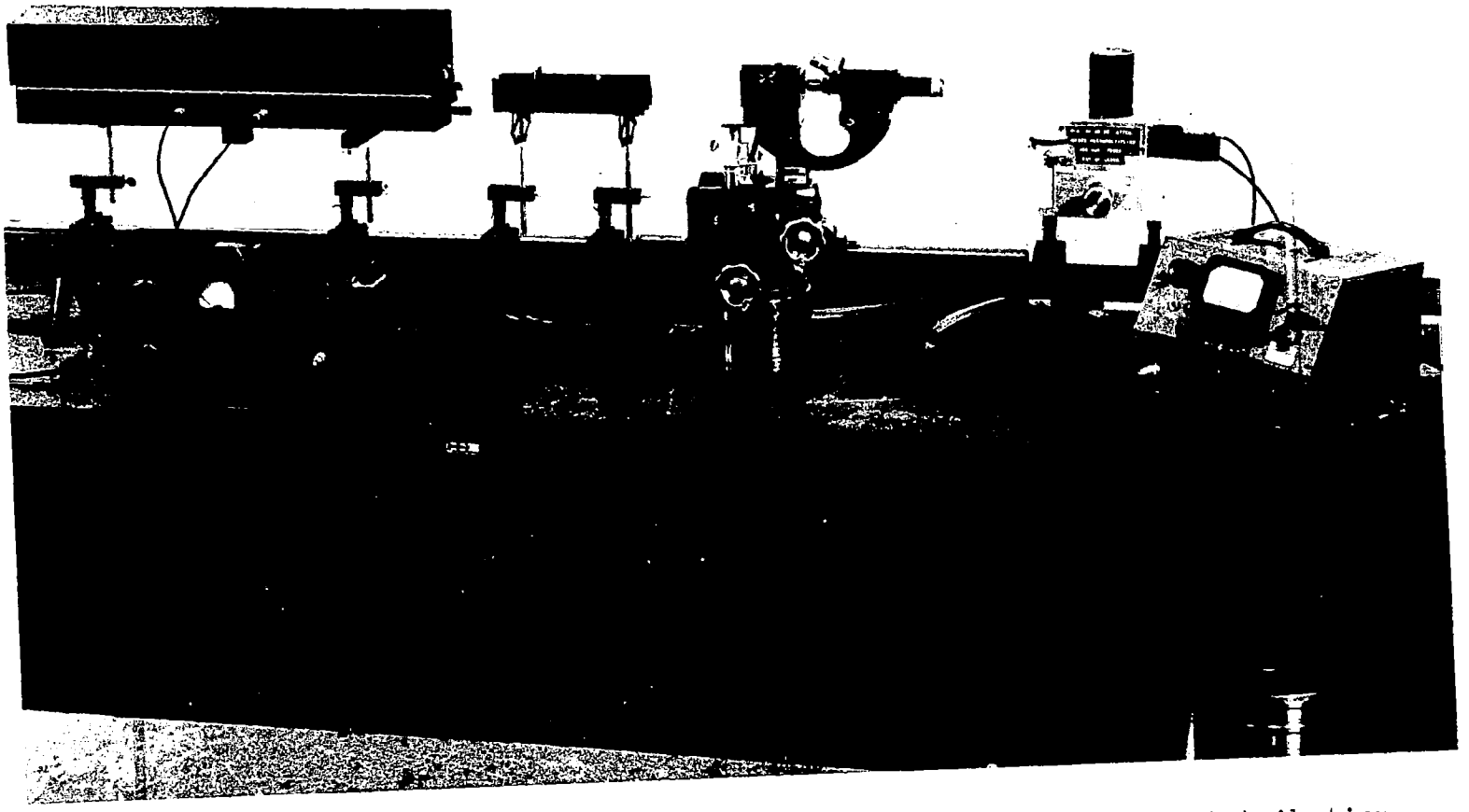

Fig. 23 - Photograph of test range for measurement of aperture distribution.

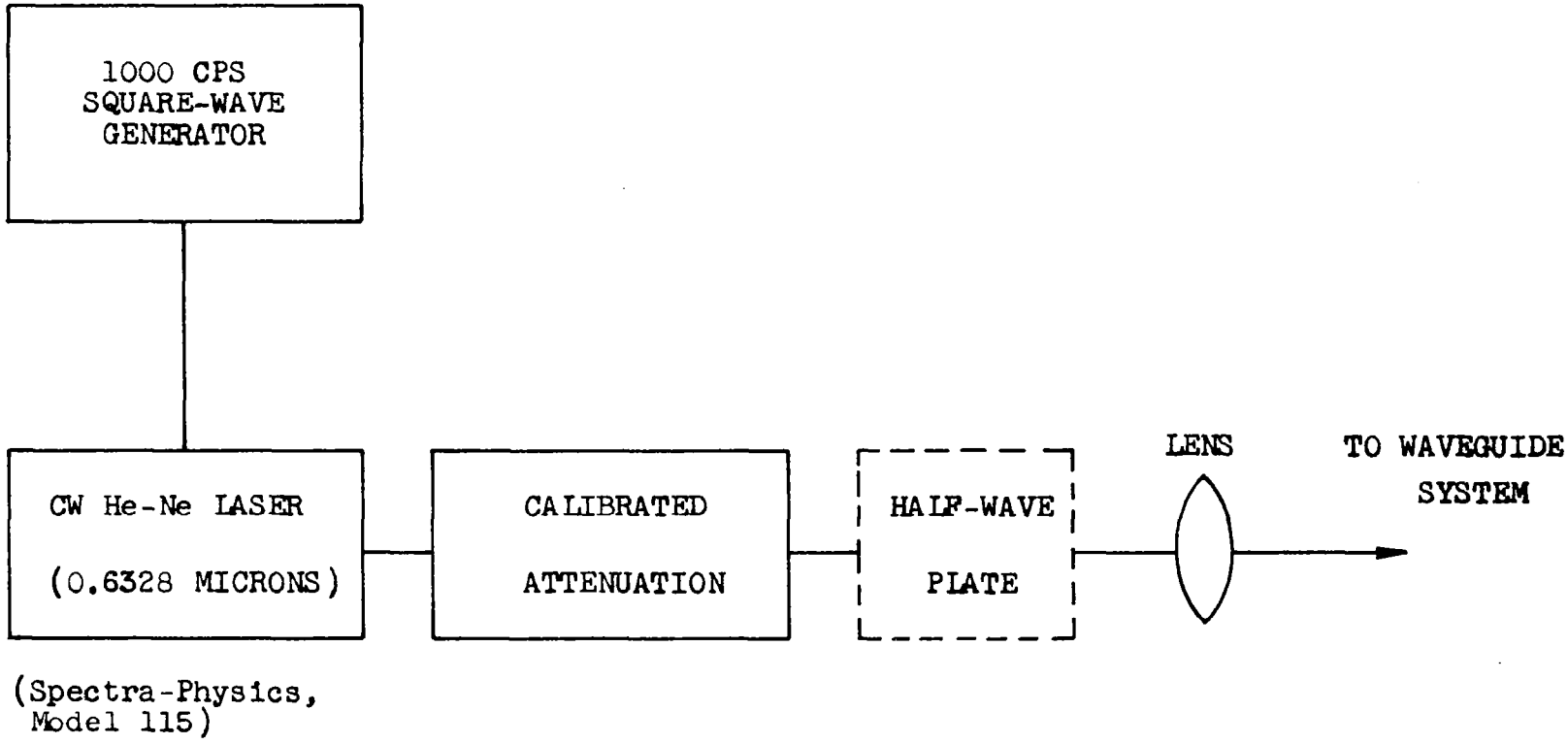

Fig. 24 - Block diagram of source system.

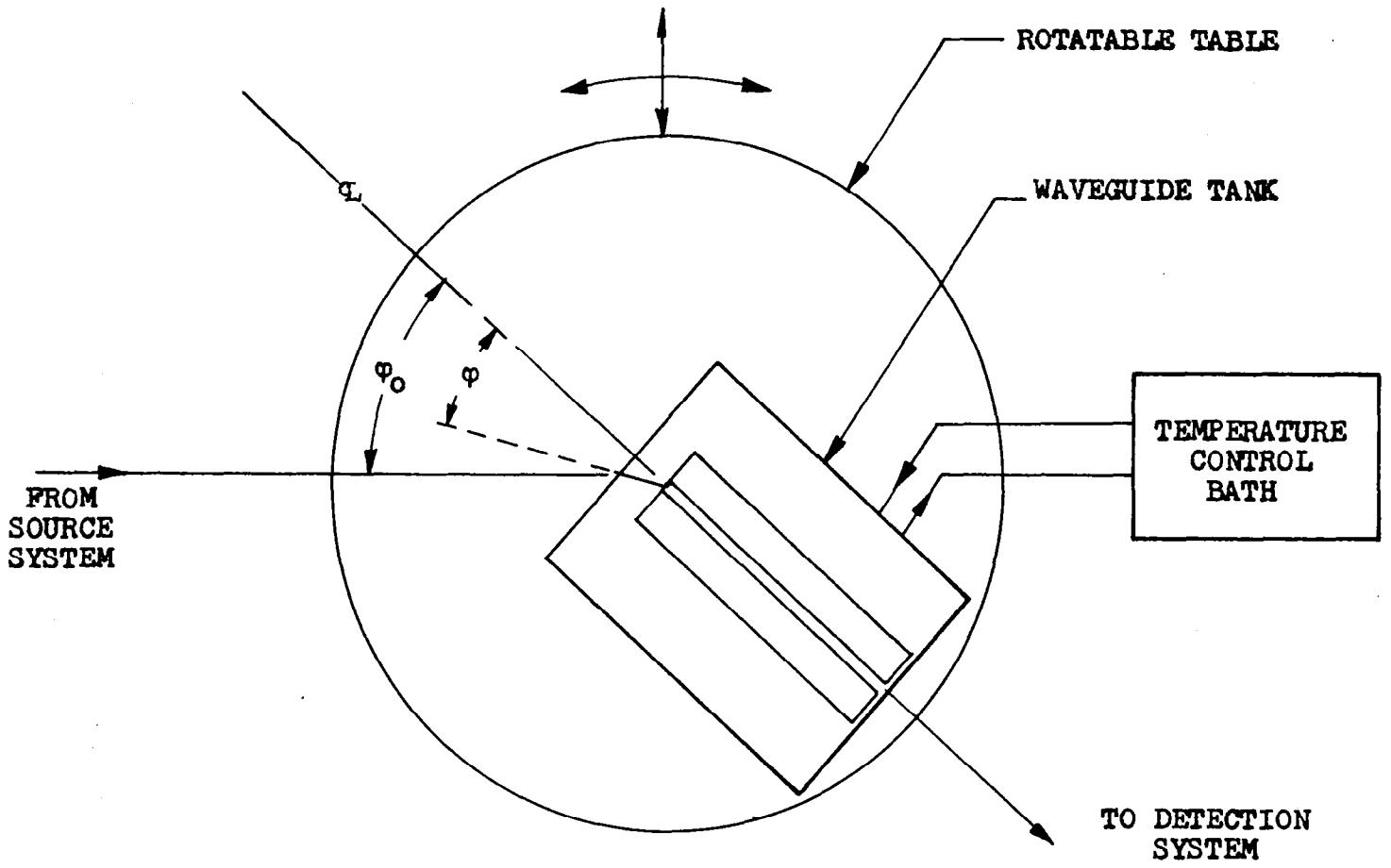

Fig. 25 - Block diagram of waveguide system.

waveguide relative to the incident laser beam. The temperature-regulation system is necessary to control the dielectric constant of the liquid in the waveguide, and therefore the difference in dielectric constant between the core and the cladding, as discussed in Section IV, Part B. The temperature of the waveguide may be controlled to $\pm 0.03^{\circ}$ C, and, therefore, the difference in dielectric constant is controlled to ± 0.00005. The waveguide tank is mounted on a table and may be rotated in the horizontal plane, in order to vary the angle of incidence of the laser beam (excitation angle). The table may also be moved transverse to the incident laser beam, in order to sample different portions of the beam.

The detection system, illustrated in Fig. 26, comprises a 1P22 photomultiplier tube and power supply, and either a tuned amplifier or a chart recorder, both of which respond to the 1000 cps modulation frequency of the laser. Both the recorder and amplifier are calibrated in decibels. A small rectangular aperture is placed in front of the photomultiplier to provide the requisite spatial resolution. In order to measure the aperture distribution of the waveguide, a 100X microscope is focused on the output aperture, and the pattern observed with the microscope is measured. The microscope is not employed when measuring the far-field (radiation) pattern of the waveguide. In addition to the above apparatus for pattern measurements, provision has been made for photographically recording the waveguide output.

The tests of the three waveguide configurations are described separately below.

1. Liquid-Core, Solid-Cladding Dielectric-Slab Waveguide.

For this waveguide configuration tests were made both of mode excitation and of aperture field distribution. The three parameters which could be adjusted are the difference in dielectric constant between the core and the cladding, the waveguide width, and the excitation angle of the waveguide. The width was adjusted to 35.7 microns (57λ) and then held constant throughout the test for the mode excitation study. The first step in the measurement was to increase the temperature until the waveguide became dark; at this

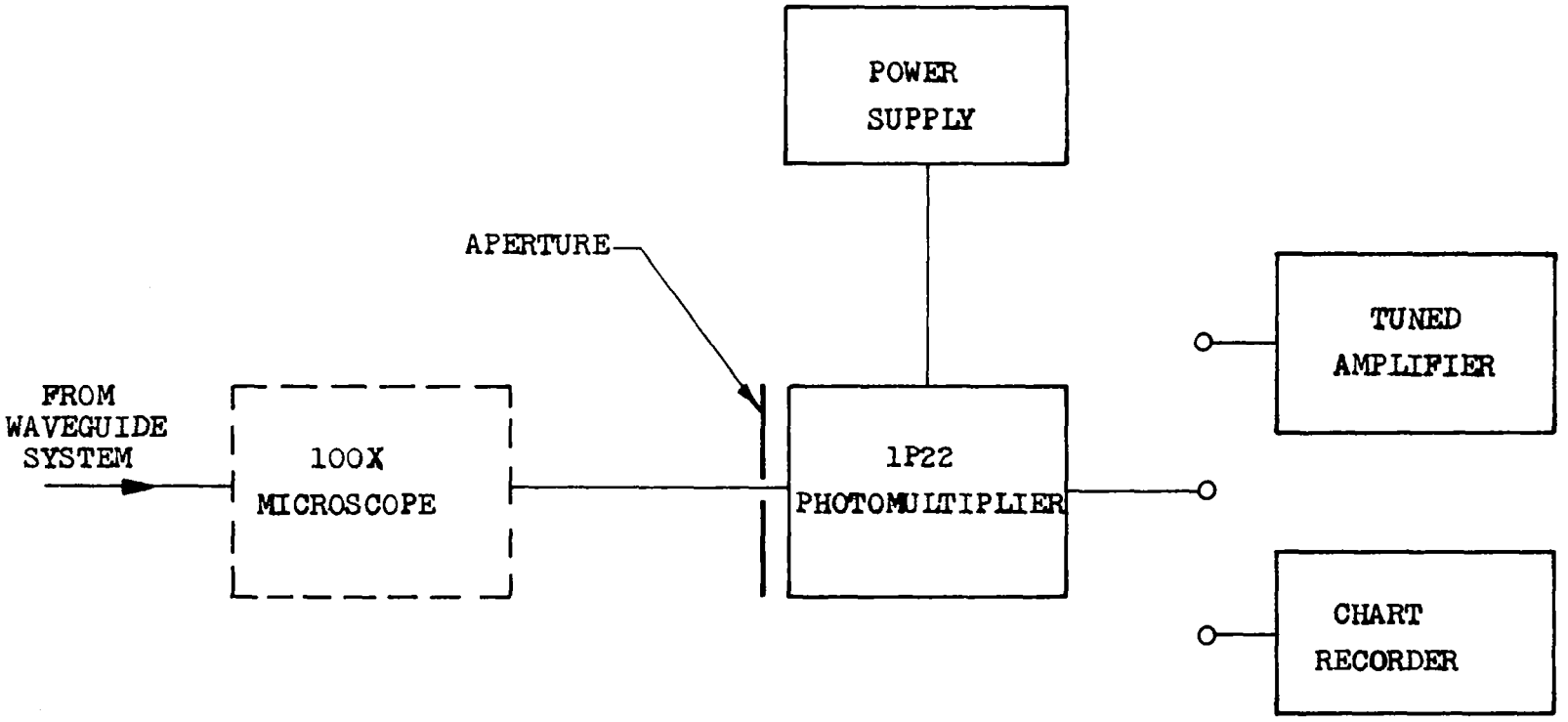

Fig. 26 - Block diagram of detection system.

temperature, the difference in dielectric constant between the core and cladding is zero. The temperature was then decreased in discrete steps to increase the difference in dielectric constant. At each temperature level, the temperature was allowed to stabilize, and the excitation angle was varied. The highest propagating mode was noted, by counting the maximum number of lines observed in the core, and the corresponding mode number was indicated at a point on the mode chart (Fig. 27) corresponding to the measured values of waveguide spacing and difference in dielectric constant. It should be noted that the number of lines observed in the aperture for a given mode is one greater than the mode designation "m". For agreement between measurements and theory to be indicated, a highest mode number "m" would be observed for a point on the chart between the lines labeled "m" and "m+1". For small differences in dielectric constant, the data agrees with theory; as the difference increases, fewer modes were observed than predicted. However, within the precision and tolerances of the measurements and waveguide construction, it is considered that the waveguide modes observed are consistent with the theoretical analysis.

For the measurements of aperture field distributions, the waveguide width was first adjusted to be 75λ, the temperature of the waveguide was adjusted so that only the fundamental mode (TM-0, TE-0) was supported, and the excitation angle was adjusted for maximum output. A measured and theoretical pattern are shown in Fig. 28. The theoretical curve was obtained by noting the measured field amplitude at the edge of the core. This amplitude determines the values of the waveguide parameters "p" and "q", which in turn determine the theoretical field pattern (Appendix I). Good agreement between measurements and theory is obtained, indicating that waveguide performance is correctly explained by the analysis. A "noise" level at about -22 db is observed, and is caused by scattered light in the waveguide region. An additional aperture field pattern is presented in Fig. 29 for 50λ guide spacing. Although some asymmetry is present in this pattern, indicating that more than one mode is present, the general shape of the field is the same as that predicted by the analysis.

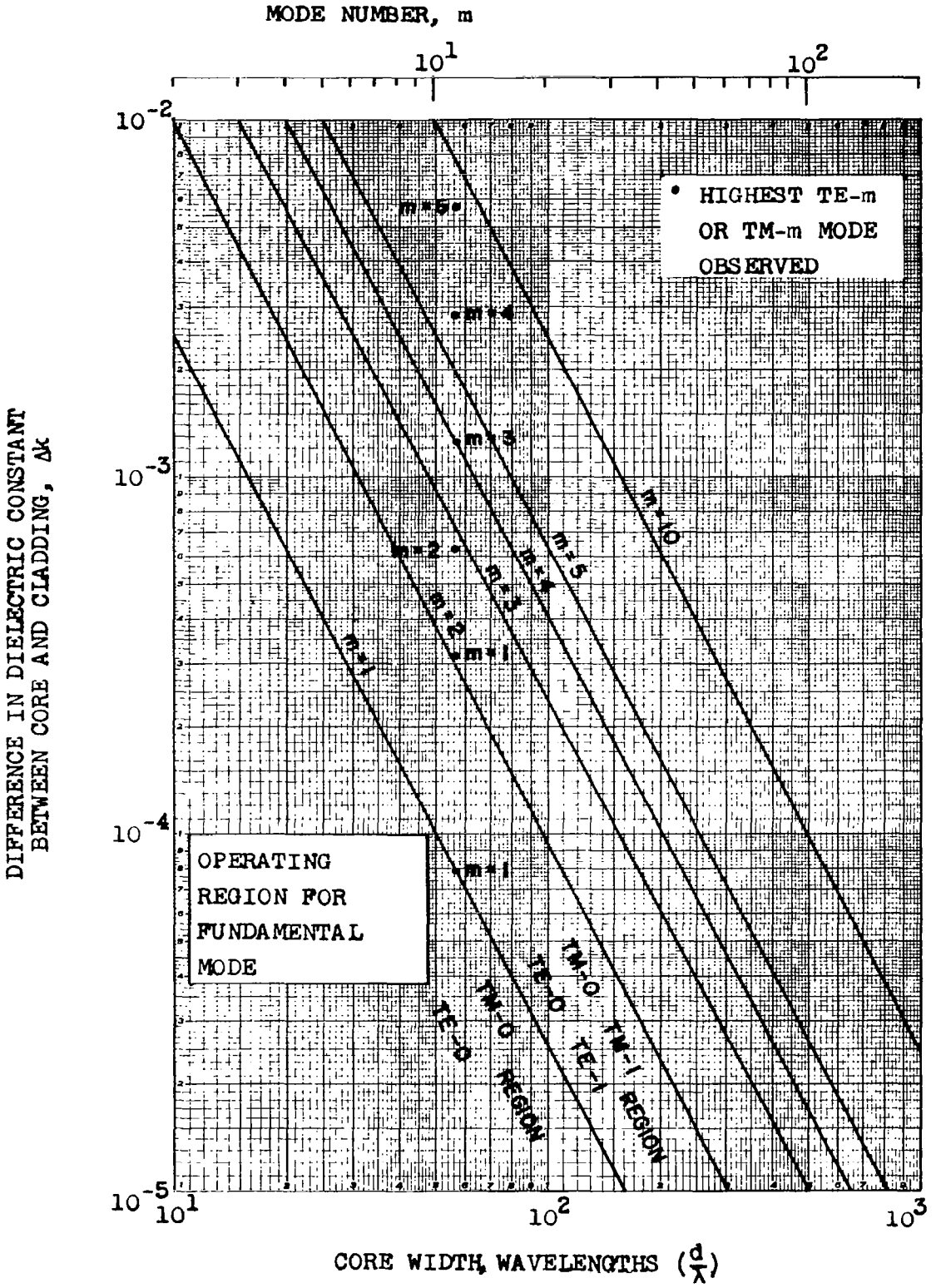

Fig. 27 - Mode chart, showing data for liquid-core, solid-cladding dielectric-slab waveguide.

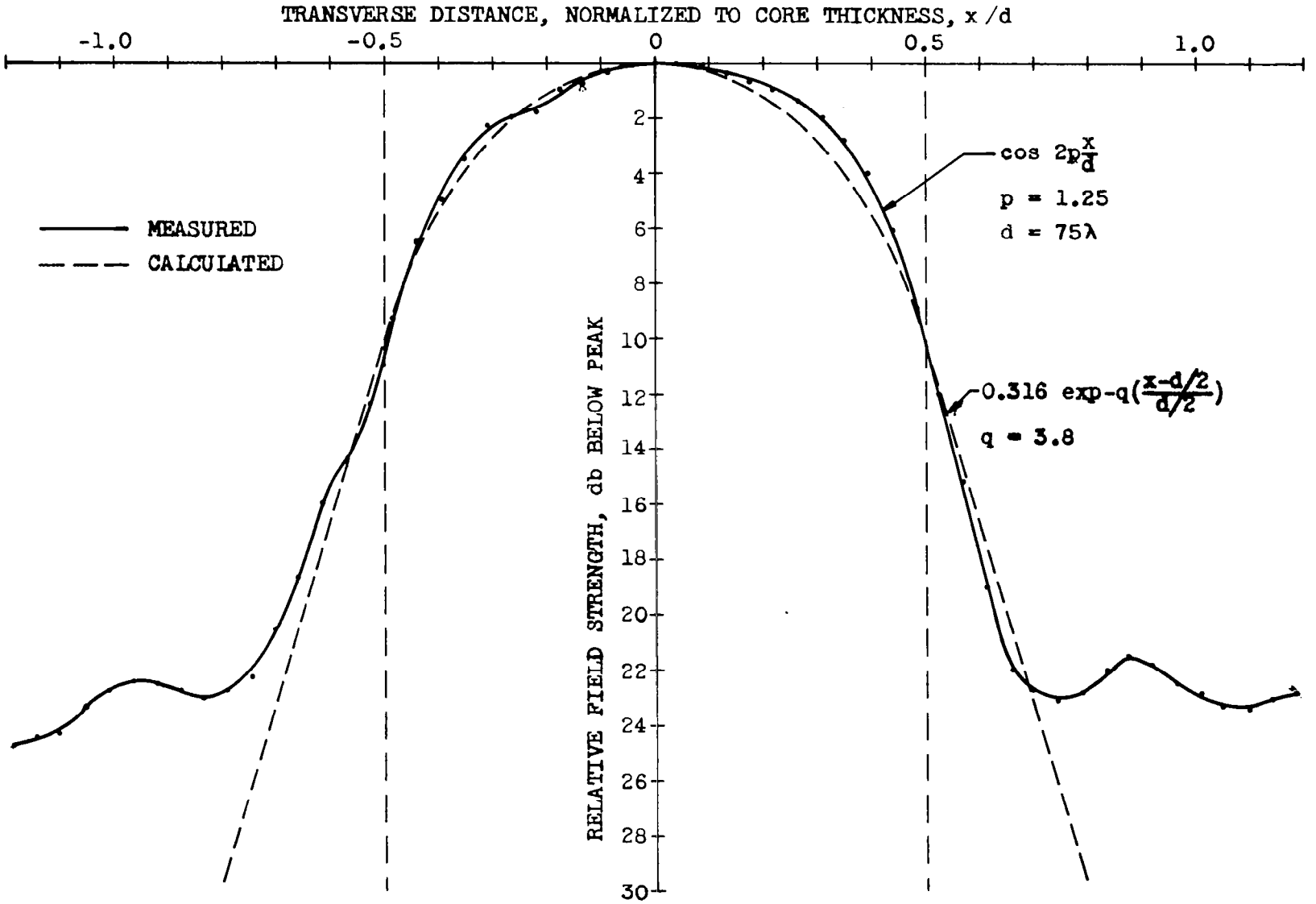

Fig. 28 - Aperture distribution, fundamental mode (TE-0) in liquid-core, solid-cladding dielectric-slab waveguide; 75λ spacing.

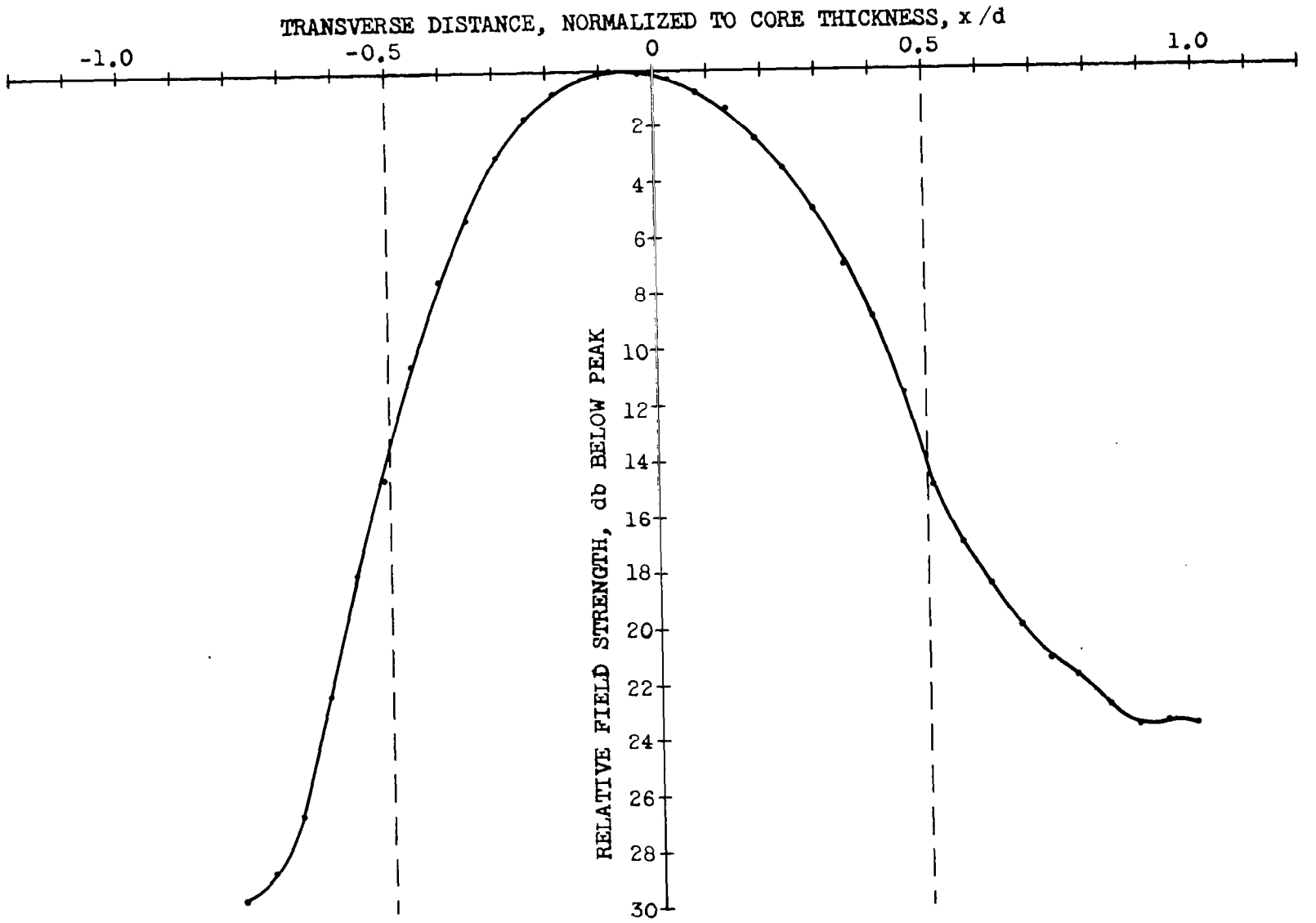

Fig. 29 - Aperture distribution, fundamental mode (TE-0) in liquid-core, solid-cladding dielectric-slab waveguide; 50λ spacing.

The temperature and excitation angle of the waveguide were subsequently adjusted to provide pure second-mode operation with a guide spacing of 31.6 microns (50λ). The measured pattern is plotted in Fig. 30. As in the fundamental-mode case, the pattern has the general characteristics predicted by the theory. However, the value at the center should be a null, but only a minimum was measured. This effect is caused by the photomultiplier, which has an aperture of some extert, and is an intensity-responding device. Therefore the depth of the minimum could not be measured accurately. The noise level was again approximately -22 db. The waveguide was then adjusted so that both the first and second modes propagated, in a guide of 83.0 micron (131λ) spacing, and the pattern was measured (Fig. 31). The general characteristics of the pattern again agree with the theory. The asymmetry in the pattern is a result of the vector addition of the fields of the two modes.

An attempt was made to observe and measure the radiation pattern for each of the three aperture distributions above. Because of spurious light transmission in the waveguide region, these observations were not possible at that time. However, observations were made for two cases of individual higher modes in a waveguide with 65.5 micron (103λ) spacing. When only the third mode was being propagated, the measured pattern angle was 0.03 radians, the same as the theoretical value. When the eighth mode was propagated, the measured pattern angle was 0.08 radians, also the theoretical value. These results further verify that the guide is operating according to the theoretical model assumed in the analysis.

2. Short-Circuit-Bisected Dielectric-Slab Waveguide.

This waveguide configuration was tested both for mode excitation and for field patterns as described above for the all-dielectric guide. The theoretical performance of this bisected waveguide, based on the assumption of a perfectly conducting metal wall, is similar in some respects to the dielectric guide, but differs in certain significant details. A metal wall forms a mirror and images some of the allowed modes, but does not permit others. To summarize briefly, every alternate TM mode is permitted starting

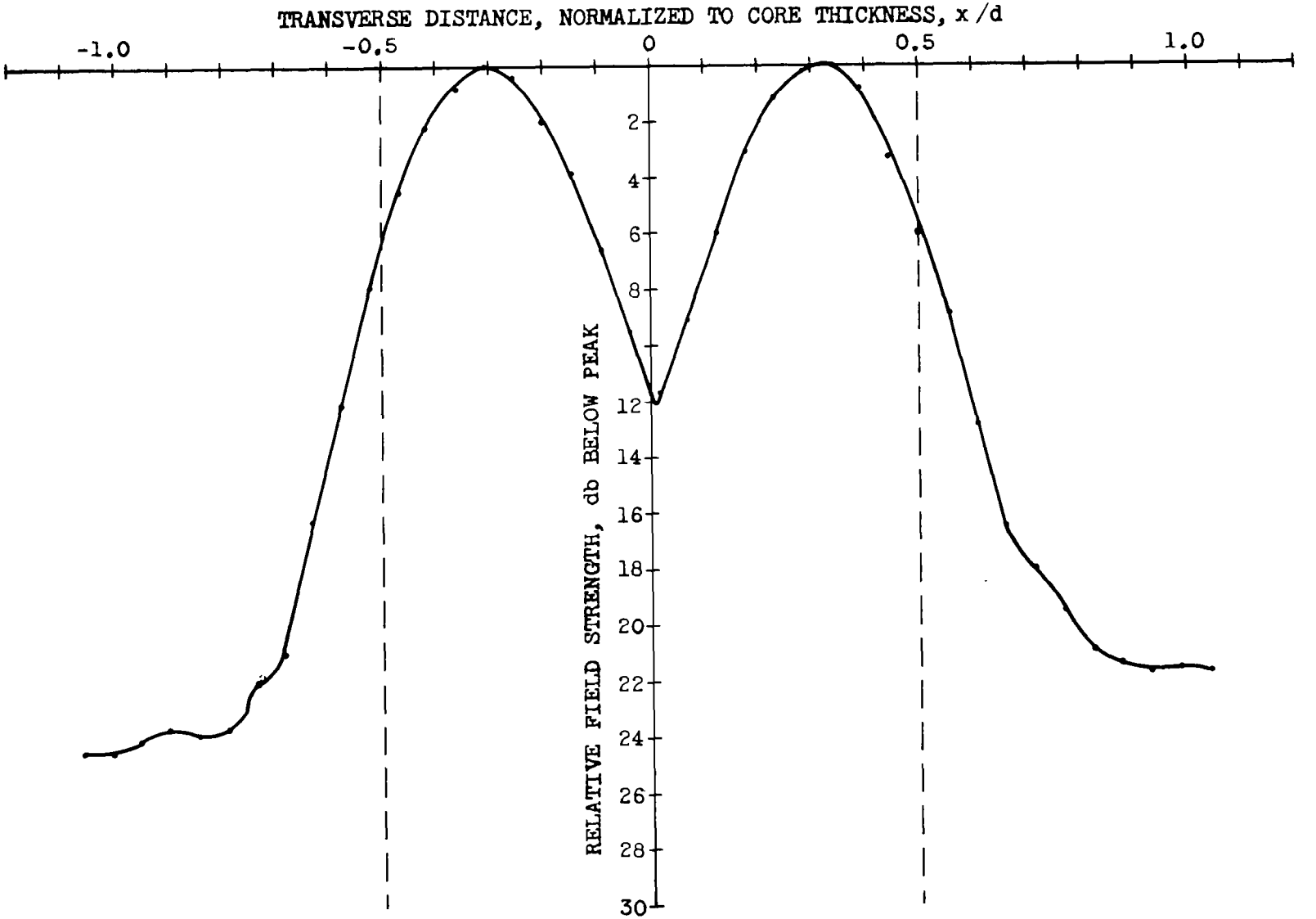

Fig. 30 - Aperture distribution, second mode (TE-1) in liquid-core, solid-cladding dielectric-slab waveguide; 50λ spacing.

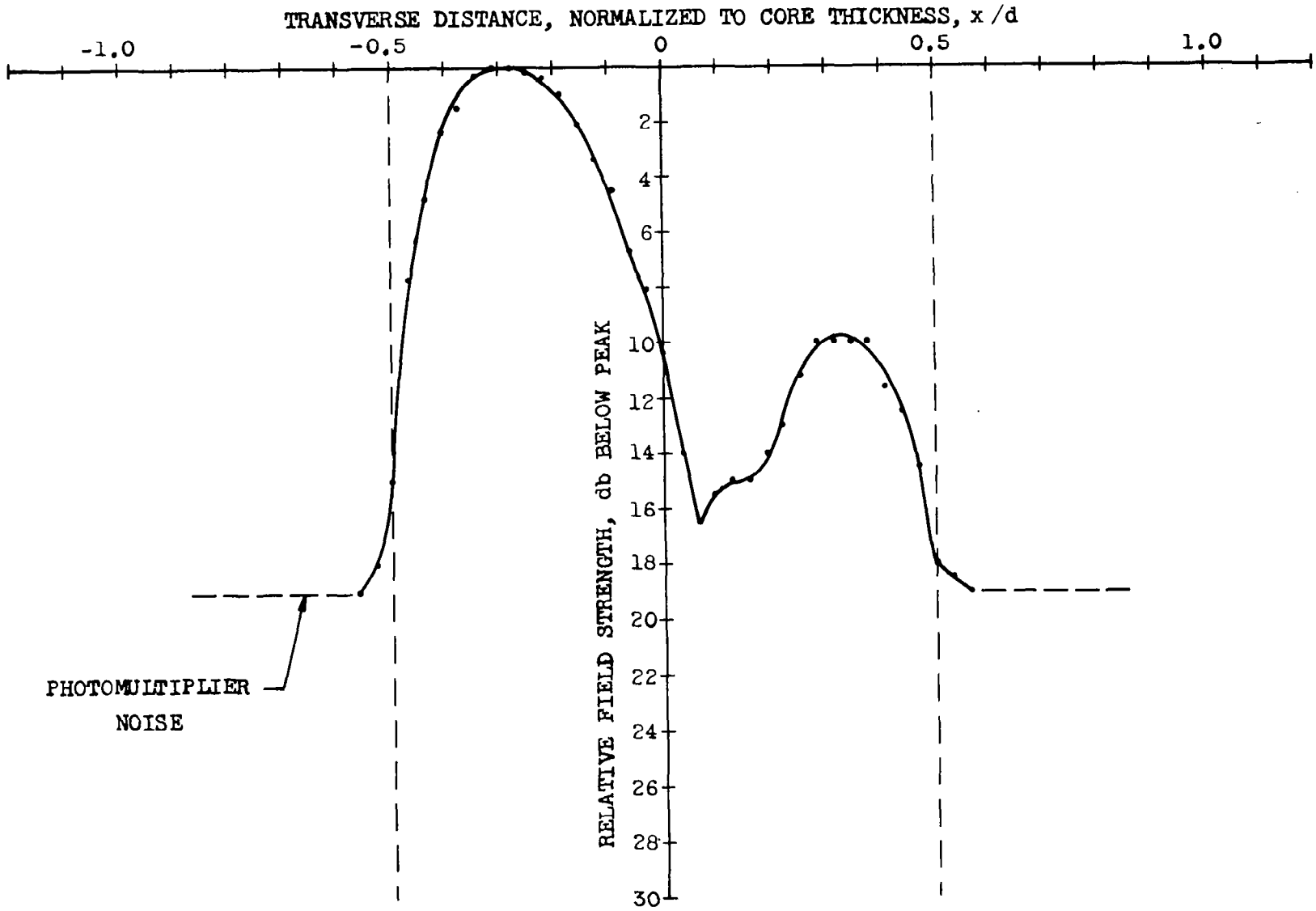

Fig. 31 - Aperture distribution, combination of first and second modes in liquid-core, solid-cladding dielectric-slab waveguide; 1.31λ spacing.

with the TM-0 mode (all modes with even mode number "m"). The lowest order TE mode is not allowed, but all modes with odd mode number "m" are permitted. The mode chart has the same cutoff lines as that for the dielectric guide, but represents only half of the modes. Each line represents the introduction of either a TE or TM mode, but not both simultaneously as for the unbisected guide. The width of the waveguide on the chart is equal to twice the actual separation between the metal surface and the boundary. The TM modes are characterized by maximum electric field amplitude on the metal wall and the TE modes by minimum electric field amplitude.

The first tests had as an objective the identification of the different shapes for the TM and TE modes, and the verification of the different cutoff conditions for the two types of modes. For these tests the waveguide temperature was adjusted so that only the fundamental mode was supported, and the excitation angle was adjusted for maximum output. The aperture distribution was then measured for both the TE and the TM modes by changing the incident polarization — Figs. 32 and 33 respectively. Both patterns are identical within experimental accuracy, indicating that contrary to theory the propagation characteristics are identical for the two modes.

The waveguide was then adjusted to provide second-mode operation, and the aperture distribution was measured for both the TE and the TM modes — Figs. 34 and 35 respectively. Both patterns are again, contrary to theory, identical within experimental accuracy. The fact that both peaks are not of equal amplitude indicates the presence of some fundamental mode, in addition to the desired second mode.

Additional tests were performed with greater difference in dielectric constant and additional TE and TM modes were observed. The main characteristic that became evident in all the above tests is that the TE and TM modes were identical in shape and cutoff characteristics, and therefore indicate a departure of measured performance from the theoretical model. A preliminary analysis suggests that this departure is caused by ohmic losses in the metal surface. These losses are great enough to change the phase of the reflection coefficient for parallel polarization (TM waves) from 0^{o} to 180^{o}, thus giving the TM waves the same propagation character-

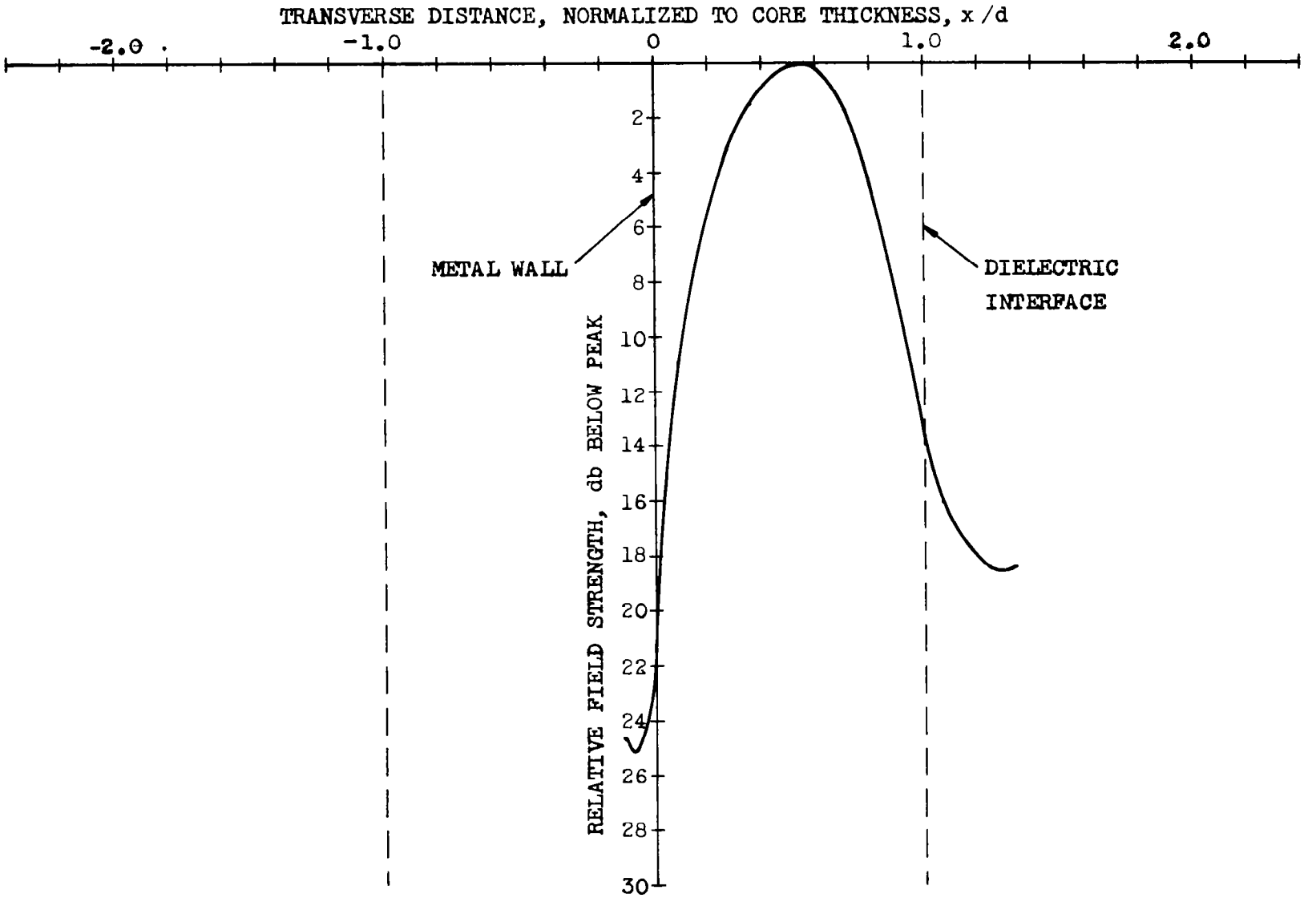

Fig. 32 - Aperture distribution, fundamental TE mode in bisected dielectric-slab waveguide; 50λ spacing.

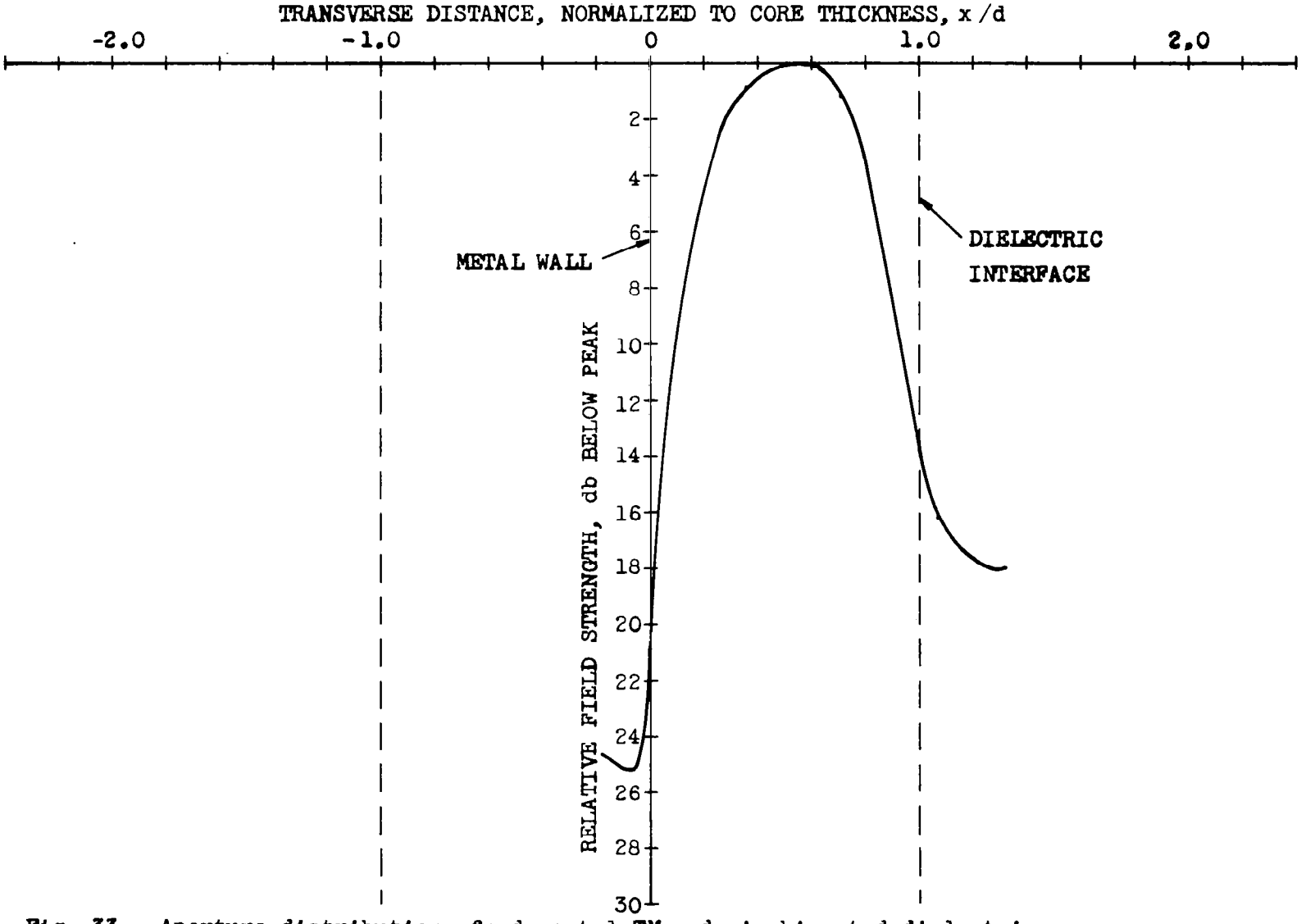

Fig. 33 - Aperture distribution, fundamental TM mode in bisected dielectric-slab waveguide; 50λ spacing.

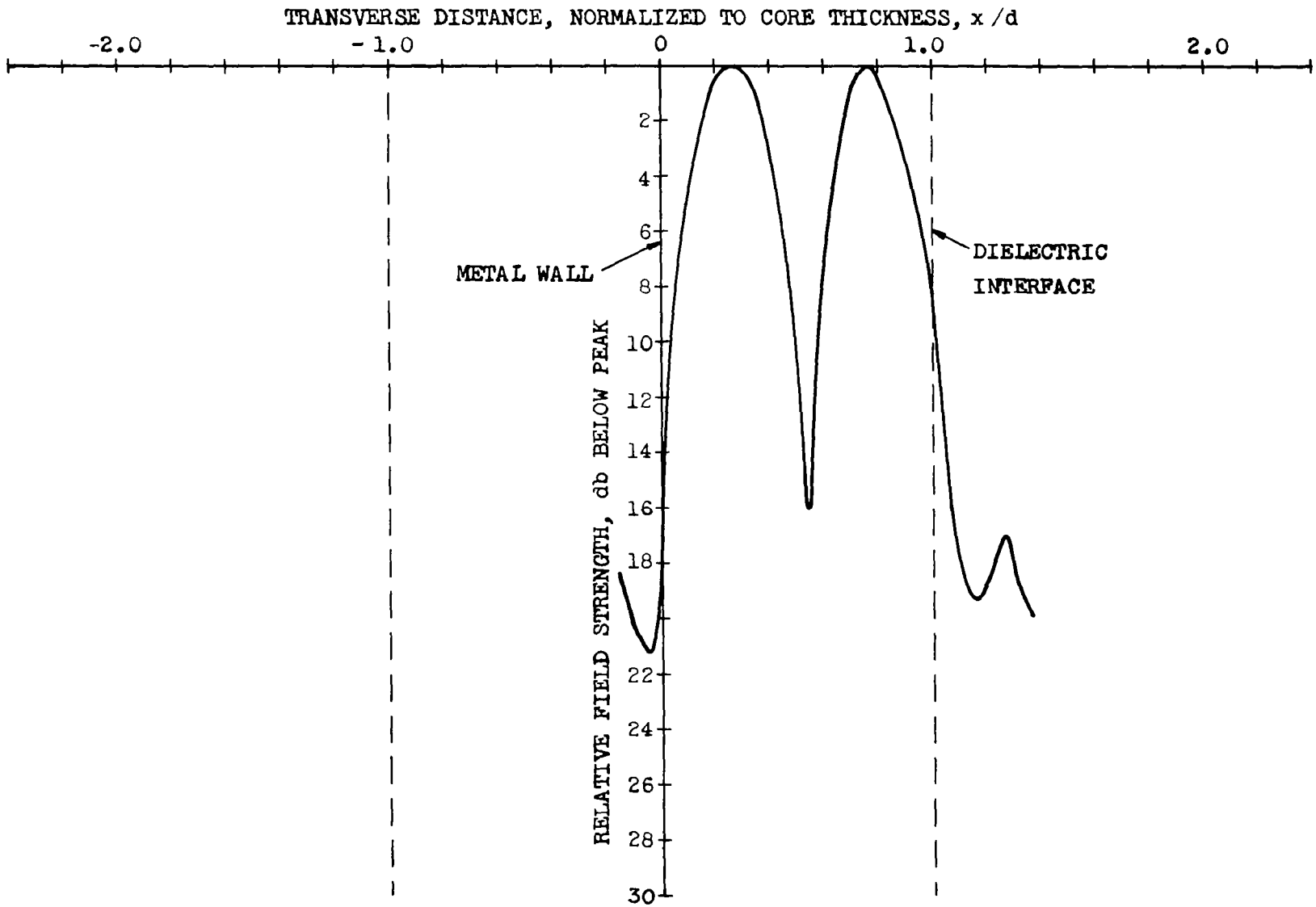

Fig. 34 - Aperture distribution, second TE mode in bisected dielectric-slab waveguide; 50λ spacing.

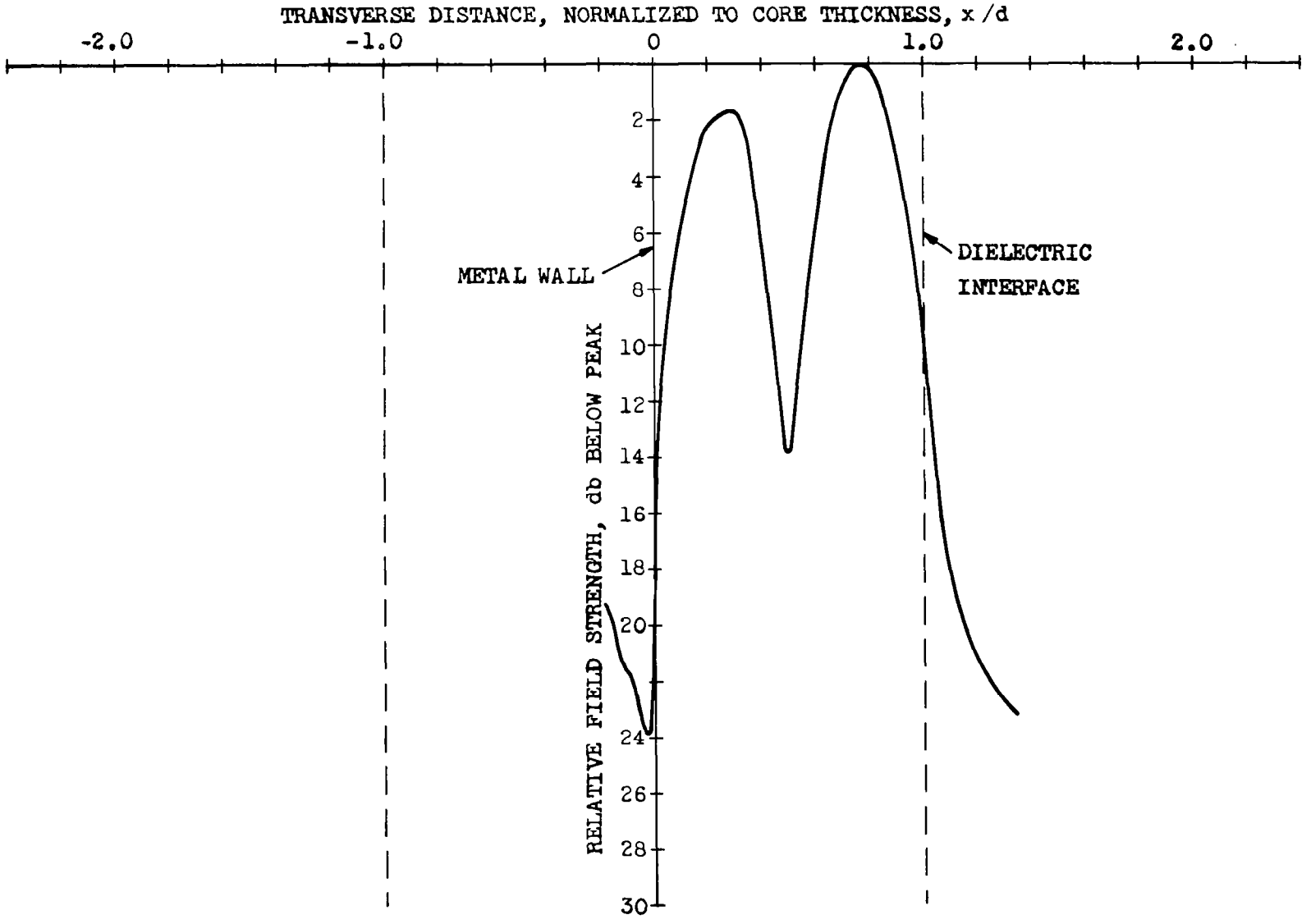

Fig. 35 - Aperture distribution, second TM mode in bisected dielectric-slab waveguide; 50λ spacing.

istics as TE waves. This type of behavior is often exhibited at microwaves and lower frequencies; one example is propagation of a ground wave over the earth, which has a finite conductivity. Since this behavior departs from the simple theoretical model assumed, further study is planned to understand the propagation characteristics for application to component design.

3. Solid-Core, Liquid-Cladding Dielectric-Slab Waveguide.

Preliminary observations were made with this configuration using a glass core of good, but not controlled, quality: no specifications were available on the dielectric constant, the homogeneity, or the flatness of the surfaces defining the core-cladding interfaces. The initial investigation revealed that individual higher modes could be propagated in this guide; they appeared to have the expected general characteristics.

An attempt to adjust this configuration for fundamental-mode operation, and measurement of the aperture distribution of the first several modes, is being deferred until thin glass sheets with controlled properties are received.

VI. Conclusions.

The properties of optical dielectric waveguide have been investigated for the case where the difference in the dielectric constants of the core and cladding materials is extremely small. In this waveguide, single-mode operation may be obtained with core dimensions of many wavelengths; thereby facilitating the fabrication of proposed microwave-type components.

The propagation characteristics of the waveguide have been analyzed using the conventional microwave technique of transverse resonance. From these computations the variations of the field intensities for the core and cladding regions have been obtained. This approach also yields the cut-off conditions which have been presented graphically in the form of mode charts. While the attenuation of this guide has been found to be high enough to preclude its use as a long distance transmission line, it is low enough so that lengths of a few centimeters, containing several microwave-type components, are considered feasible.

The problem of efficient waveguide excitation has also been studied theoretically; both for single-mode and multi-mode waveguides. It has been found that nearly all the power in an incident beam may be coupled into the lower waveguide modes by simple focusing techniques.

A number of techniques for waveguide fabrication have been considered. Throughout this work a distinction has been made between experimental waveguides, containing a liquid dielectric, and more practical, prototype waveguides which must be constructed entirely of solid dielectrics. Fabrication feasibility has been demonstrated by the operation of a laboratory model and sufficient design data has been obtained to permit the "electrical" design of a solid waveguide. However, the fabrication of an all solid waveguide is complicated by the tight tolerances required on the dielectric constants of the waveguide materials. Fabrication techniques are being studied and it is believed that the fabrication of a solid waveguide is feasible. Among the more promising techniques are (1) vacuum depositing of the cladding and (2) adjustment of the dielectric constant of a glass slab by physical or chemical changes.

The experimental program to date has consisted of a study of field distributions and cut-off conditions for several configurations. The cut-off conditions were determined by observing the highest order mode which could propagate for a given core thickness and difference in dielectric constant. The field plots were obtained in a manner similar to the measurement of microwave antenna patterns. The waveguide aperture distribution was transferred to a more accessible location by the focusing action of a microscope. Then this field distribution was scanned by a photomultiplier with a small sampling aperture. A servo system linked the scanning photomultiplier to a recorder which plotted the field distribution. The results of these measurements are in agreement with dielectric waveguide theory. An interesting result of these experiments was the realization that a short-circuit-bisected waveguide at optical frequencies does not exhibit the mode structure predicted by assuming a perfect conductor at the bisecting plane. It was found necessary to include the effect of the metallic losses to explain the observed modes.

In general, this study has demonstrated that single-mode waveguide with macroscopic dimensions at optical frequencies may be constructed and that the performance of this waveguide follows theoretical predictions.

VII. Acknowledgements.

The work described in this report has been performed during the period of 1964 JAN 28 to 1964 MAY 28 for the National Aeronautics and Space Administration under contract NASw 888. General direction has been provided by Roland Chase of NASA.

The work at Wheeler Laboratories has been performed by E. Ronald Schineller, Donald W. Wilmot, and Herman M. Heinemann under the direct supervision of Henry W. Redlien. Advice and general direction have been provided by Harold A. Wheeler and Frank H. Williams.

VIII. References.

(1) F. W. Fowle, "Smithsonian Physical Tables", 8 ed., Smithsonian Inst.; 1934.

(2) F. Seitz, "Modern Theory of Solids", 1 ed., McGraw-Hill; 1940.

(3) J. A. Ramsay, "Fourier Transforms in Aerial Theory", Marconi Review, no. 83, vol. 9 to no. 89, vol. 11; 1946-48.

(4) S. Silver, "Microwave Antenna Theory and Design", Rad. Lab. Series, vol. 12, McGraw-Hill; 1949.

(5) R. E. Beam et al, "Investigations of Multi-Mode Propagation in Waveguides and Microwave Optics", ASTIA No. ATI 94 929; Nov. 1950.

(6) A. A. Oliner, N. Marcuvitz, "Microwave Network Theory and Applications", MRI Report R-262-51, PIB-202, Polytechnic Inst. of Brooklyn; Sept. 1951.

(7) R. Meridith, "Radiation Patterns of Some Fourier Series Aperture Distributions", RRE Tech. Note 562, AD No. 90 782, Radar Research Est.; July 1955.

(8) D. D. King, S. P. Schlesinger, "Losses in Dielectric Image Lines", Trans. IRE, vol. MTT-5, p. 31; Jan. 1957.

(9) F. A. Jenkins, N. E. White, "Fundamentals of Optics", 3 ed. McGraw-Hill; 1957.

(10) E. Condon, H. Odishaw, "Handbook of Physics", 1 ed., McGraw-Hill; 1958.

(11) A. F. Harvey, "Periodic and Guiding Structures at Microwave Frequencies", Trans. IRE, vol. MTT-8, p. 30; Jan. 1960.

(12) A. F. Kay, "Near-Field Gain of Aperture Antennas", Trans. IRE, vol. AP-8, p. 586-593.

(13) N. S. Kapany, "Fiber Optics", Scientific Am., vol. 203, no. 5, p. 2-11; Nov. 1960.

(14) R. E. Collin, "Field Theory of Guided Waves", McGraw-Hill; 1960.

(15) E. Snitzer, "Cylindrical Dielectric Waveguide Modes", Jour. Opt. Soc. Am., vol. 51; May 1961.

(16) E. Snitzer, H. Osterberg, "Observed Dielectric Waveguide Modes in the Visible Spectrum", Jour. Opt. Soc. Am., vol. 51, p. 499; May 1961.

(17) E. Snitzer, "Optical Dielectric Waveguides", Advances in Quantum Electronics (J.R.Singer Ed.) Columbia Univ. Press, p. 348; 1961.

(18) H. Jasik, "Antenna Engineering Handbook", McGraw-Hill; 1961.

(19) R. W. Hermansen, "Mode Charts for Macroscopic Dielectric Waveguide at Optical Frequencies", WL Report 1137; July 1963.

(20) J. A. Ramsay, "Free Space Power Transmission", notes of talk presented to L.I. Chap. of PTGAP; Dec. 3, 1963.

(21) D. W. Wilmot, "Macroscopic Single-Mode Waveguide for the Construction of Optical Components", talk presented at 1964 PGMTT International Symposium, Long Island, N. Y.; May 20, 1964.

Appendix I. Analysis of Propagation in Dielectric Slab Waveguide by Transverse Resonance.

The propagation characteristics of dielectric slab waveguide can be determined either by a solution of the field equations in this structure with application of the appropriate boundary conditions, or by a transmission line type of analysis. This appendix indicates an analysis based on the transmission line technique of transverse resonance (Ref. 6). The basic approach is to consider the structure as a transmission line in the transverse direction and set up the conditions for resonance on this line. Certain resonant conditions in the transverse direction correspond to real propagating modes in the longitudinal direction of the guide.

The configuration of the dielectric slab waveguide is shown in Fig. 36(a). It consists of a dielectric slab of relative dielectric constant, k_1, and width, d, (waveguide core) bounded on both sides by a dielectric of relative dielectric constant, k_2 (cladding). The transverse waveguide equivalent circuit is shown in Fig. 36(b). It comprises a transmission line of length d, impedance Z_1, and propagation constant K_1 with semi-infinite lines of impedance Z_2 and propagation constant K_2 connected to each end as shown. A resonant condition in this waveguide exists if the impedance at some reference plane looking in one direction is equal to the negative of the impedance at this same plane looking in the other direction, that is,

$$\overleftarrow{Z}(x_1) + \overrightarrow{Z}(x_1) = 0 . \qquad (8)$$

This equation can be solved directly for the equivalent circuit indicated; however, because of the symmetry, the circuit can be bisected with an electric wall (short circuit) or a magnetic wall (open circuit) in order to simplify the analysis. The resulting equivalent circuits for these two cases are shown in Fig. 36(c) and (d). In order to find all the possible modes of propagation, both the short circuit and open circuit cases must be solved, and the analysis must be done for both transverse magnetic (TM) and transverse electric (TE) modes.

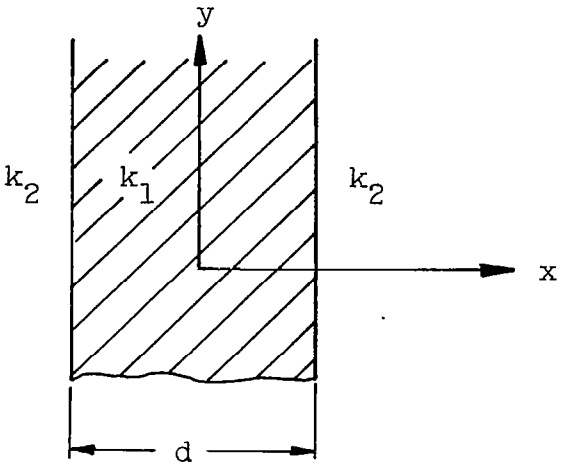

(a) Cross-section of dielectric slab waveguide.

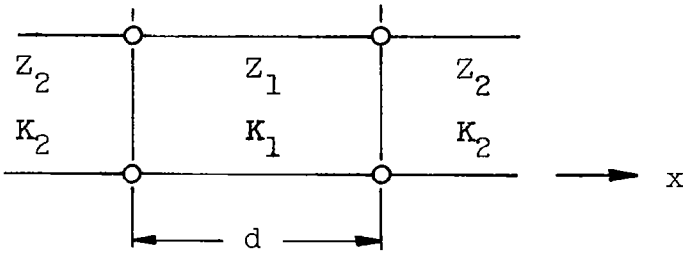

(b) Transverse equivalent circuit.

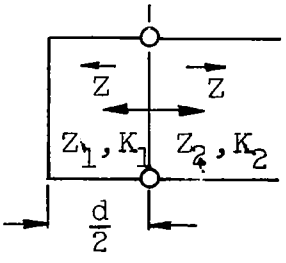

(c) Short circuit bisection.

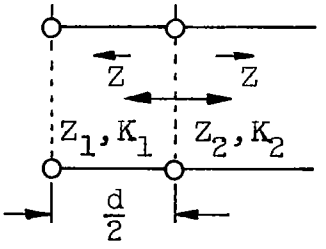

(d) Open circuit bisection.

Fig. 36 - Dielectric slab waveguide and equivalent circuits.

The wave impedances in the core and cladding regions of the transverse equivalent waveguide are as follows. For the TM modes,

$$Z_1 = \frac{K_1}{\omega\epsilon_o k_1} ; \qquad Z_2 = \frac{K_2}{\omega\epsilon_o k_2} . \tag{9}$$

For the TE modes,

$$Z_1 = \frac{\omega\mu_o}{K_1} ; \qquad Z_2 = \frac{\omega\mu_o}{K_2} . \tag{10}$$

The method of analysis will be indicated for the TM modes with short circuit bisection. The other cases can be analyzed in an identical manner, and so only the results will be presented. The impedances looking to the right and left at the plane $x = d/2$ in Fig. 36(c) are substituted into equation (8):

$$jZ_1 \tan K_1 \frac{d}{2} + Z_2 = 0. \tag{11}$$

After substitution for Z_1 and Z_2, this equation can be written as,

$$K_1 \tan K_1 \frac{d}{2} = \frac{k_1}{k_2} |K_2| , \tag{12}$$

where K_2 has been replaced by $-j|K_2|$, since this propagation constant must be imaginary to obtain a solution.

For simplicity, the following parameters are defined, which include the propagation constants in the core and cladding, and the waveguide size:

$$K_1 \frac{d}{2} = p ; \tag{13}$$

$$|K_2| \frac{d}{2} = q . \tag{14}$$

Equation (12) above can now be rewritten in terms of the new parameters p and q as follows:

$$p \tan p = \frac{k_1}{k_2} q . \tag{15}$$

This is one of the basic characteristic equations for the dielectric slab waveguide. As derived above, it applies only to TM modes with a short circuit bisection. However, for the case of small Δk, the factor k_1/k_2 is very nearly equal to unity and can be neglected without appreciable error. This equation is then identical to the equation which would be obtained for TE modes with open circuit bisection. The corresponding equations for the TM open circuit and TE short circuit bisections are identical to equation (15) if the tangent function is replaced by the negative cotangent. Since the tangent and cotangent are related through a constant angle displacement in the argument, a single equation can be written to cover all cases:

$$p \tan \left(p - \frac{m\pi}{2}\right) = q \, . \tag{16}$$

The value of m in this equation designates the particular mode number, i.e., TM-m or TE-m mode. A value of m = 0 corresponds to the fundamental mode (TM-0 or TE-0).

The second characteristic equation is obtained from the following relationships between propagation constants:

$$K_1^2 = K_o^2 k_1 - K_z^2 \tag{17}$$

$$K_2^2 = K_o^2 k_2 - K_z^2 \, . \tag{18}$$

These equations can be combined and written in terms of the p and q parameters defined above to give the second characteristic equation:

$$p^2 + q^2 = K_o^2 \frac{d^2}{4} (k_1 - k_2). \tag{19}$$

Equations (16) and (19) are plotted on p vs. q coordinates in Fig. 37. These curves contain sufficient information to completely specify the propagation characteristics of a slab waveguide. The intersections of the curves given by equations (16) and (19) determine the values of p and q which simultaneously satisfy both equations, and hence satisfy the conditions for propagation. The conditions for mode cutoff can be readily obtained from these curves. For a guide to support

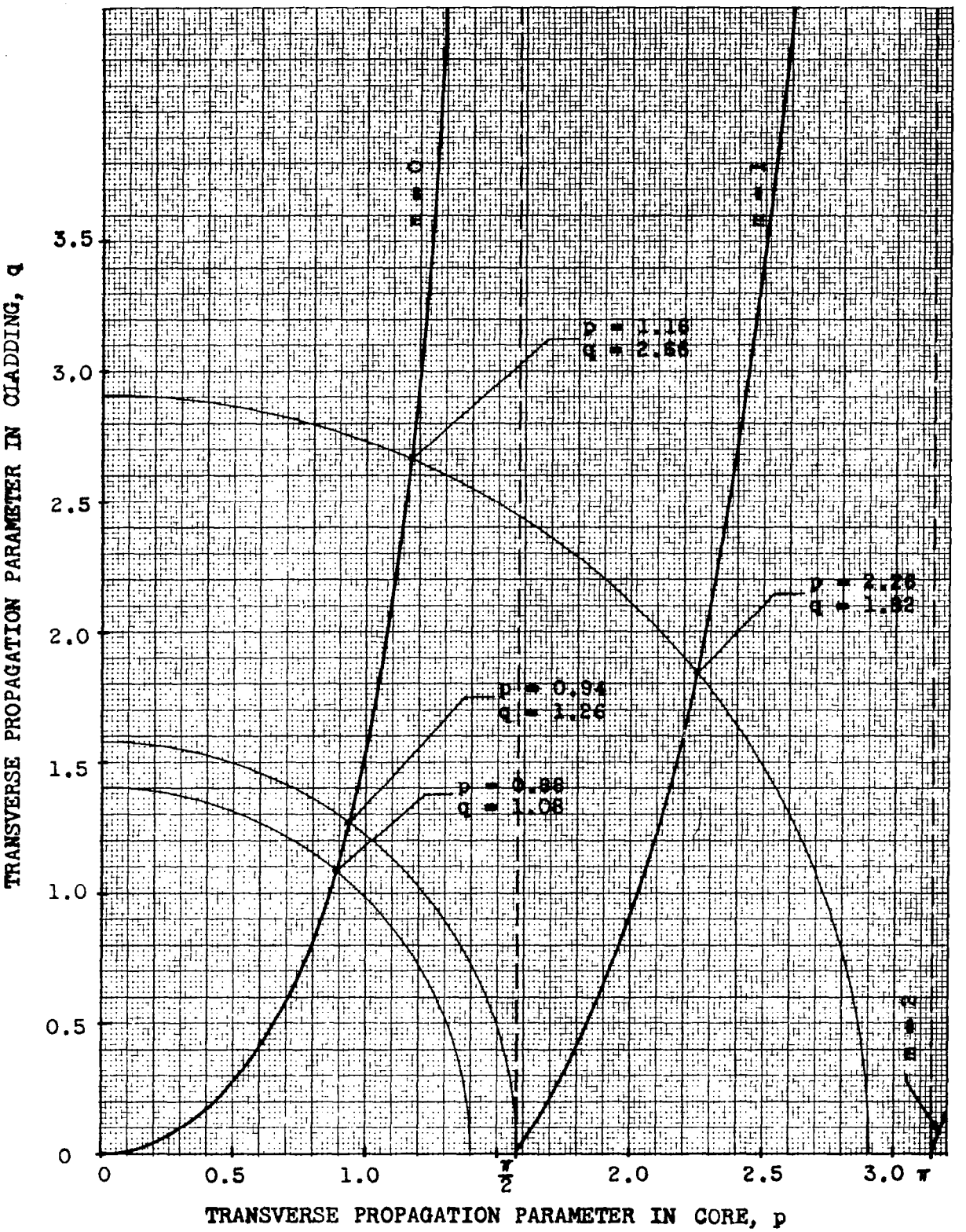

Fig. 37 - Characteristic p vs. q curves for dielectric slab waveguide.

propagation in TM-m and TE-m modes and lower, the curves must intersect in at least m + 1 places (since m = 0 corresponds to the lowest modes). Conversely, if we wish to restrict propagation to only TM-m and TE-m modes and lower, the curves must intersect in only m + 1 places. This requires

$$K_o \frac{d}{2} (k_1 - k_2)^{1/2} < (m + 1) \frac{\pi}{2} , \tag{20}$$

or rewriting in terms of free space wavelength, λ,

$$\frac{d}{\lambda} \sqrt{\Delta k} < (m + 1) \frac{1}{2} . \tag{21}$$

For a single mode guide, therefore, the parameter $(d/\lambda)\sqrt{\Delta k}$ must be less than 1/2.

The field strengths in the waveguide core and cladding are functions of the transverse propagation constants in the respective regions. Therefore, the field distribution can be written in terms of p and q parameters. Expressions for the fields in the core and cladding regions for both TM and TE modes are given in Table III. These expressions are written in terms of the p and q parameters, a wave impedance which depends on the particular field component and a factor, A. A contains a factor A_m, related to the absolute fields in the guide, and the waveguide propagation factor, exp - $K_z z$ exp $j\omega t$, which is the same for all the fields. All of these factors are essentially independent of the waveguide parameters for the case of small Δk, except for the functions of p and q. Therefore, these parameters determine the field distributions almost exclusively. A plot of the transverse fields of the two lowest order modes in slab waveguide is shown in Section III, for several different operating conditions. The values of p and q at these operating points are indicated on the curves of Fig. 37.

The dispersion properties of the waveguide are the variations of propagation constant with frequency and waveguide dimensions. The variation of guide wavelength with free space wavelength is a common way of expressing the dispersion. Guide wavelength is related to the propagation constants as follows:

TM-MODES	TE-MODES
FIELDS IN CORE	
$H_y = A \cos \left(\frac{2px}{d} - \frac{m\pi}{2}\right)$	$E_y = A' \cos \left(\frac{2px}{d} - \frac{m\pi}{2}\right)$
$E_x = -A\, Z_{z_1} \cos \left(\frac{2px}{d} - \frac{m\pi}{2}\right)$	$H_x = A'\, Z_{z_1} \cos \left(\frac{2px}{d} - \frac{m\pi}{2}\right)$
$E_z = -jA\, Z_1 \sin \left(\frac{2px}{d} - \frac{m\pi}{2}\right)$	$H_z = -jA'\, Z_1 \sin \left(\frac{2px}{d} - \frac{m\pi}{2}\right)$
FIELDS IN CLADDING	
$H_y = A \cos b_m \exp - q\left(\frac{x-d/2}{d/2}\right)$	$E_y = A' \cos b_m \exp - q\left(\frac{x-d/2}{d/2}\right)$
$E_x = -A\, Z_{z_2} \cos b_m \exp - q\left(\frac{x-d/2}{d/2}\right)$	$H_x = A'\, Z_{z_2} \cos b_m \exp - q\left(\frac{x-d/2}{d/2}\right)$
$E_z = -jA\, Z_2 \sin b_m \exp - q\left(\frac{x-d/2}{d/2}\right)$	$H_z = -jA'\, Z_2 \cos b_m \exp - q\left(\frac{x-d/2}{d/2}\right)$

$$A = A_m \exp - j K_z z \exp j\omega t$$

$$A' = A'_m \exp - j K_z z \exp j\omega t$$

$$b_m = p - \frac{m\pi}{2}$$

Table III - Expressions for field components in dielectric slab waveguide.

$$\frac{\lambda}{\lambda_g} = \frac{K_z}{K_o} \quad . \tag{22}$$

The factor K_z/K_o can be written in terms of the p and q parameters:

$$\frac{\lambda}{\lambda_g} = \left[\frac{k_2 p^2 + k_1 q^2}{p^2 + q^2}\right]^{1/2} \quad . \tag{23}$$

This expression can be written in many forms to find the variation with particular waveguide parameters. The variation of guide wavelength (λ/λ_g) is plotted as a function of the guide width in wavelengths (d/λ) in Section III of this report.